The genetic and developmental bases of male genital organ size evolution

Joanna Frances Donnelly Hagen

Thesis submitted in partial fulfilment of the requirements of the award of

Doctor of Philosophy at Oxford Brookes University

March 2019

Acknowledgments

There are many people that helped keep me sane (ish?) over the past few years.

First of all, thank you to my family. Mum, you are the kindest most bonkers lady in the world that has helped me through many-a-tearful phonecall - I couldn't have done it without you. Dad, look at what Bobo did! Both of you have been a constant source of support, and inspire me to work my hardest every day. Sisters – thank you for pretending to be interested and for being there for me always. Bet you never thought "Moany old Jo" would write a PhD thesis, even if it is on something as wacky as male genital evolution. I hate you both. Thank you to my grandad, who could always cheer me up during a visit with his kind words of encouragement and life wisdom.

Sami, your unconditional love and support helped me through the tough times, and made me enjoy the good times even more. You have always done your best to understand what I was going through and done everything you could to help me. Most of all, you've always been "kindly".

McGregor lab and Co – thank you for your support throughout the PhD, particularly Alex, Anna and Brittany for their emotional guidance and extremely mature intellectual advice. Thankyou Pedro and Franzi for all your invaluable help throughout, you guys are my lab idols! Thanks to Kentaro, who was always quick to reply to my annoying emails and started the bases for this project so well, that it was destined for greatness!

Thank you to Flybase, garlic bread, true crime podcasts, Sci hub, wine, Purple Turtle, Harry Potter, Clancy, snake bite, Coronation St, gin and tonic, various types of cheeses and all my friends in Belper.

Lastly, thank you to Dani and Alistair. There have been times when I would quite like to strangle both of you, but at the end of the day, I couldn't have asked for more enthusiastic and inspiring supervisors. Thank you for giving me the

opportunity to become a (semi) independent researcher, I've loved (almost) every second.

Abstract

Male genital structures are among the most rapidly evolving morphological traits and are often the only features that can distinguish closely related species. *D. simulans* and *D. mauritiana*, for example, only diverged from their last common ancestor 240 thousand years ago, but are strikingly different in their external genital morphology. The claspers and posterior lobes, for example, are very different in both size and shape between these species. Both of these organs have important roles in copulation. Therefore, this process of rapid morphological evolution is thought to be driven by sexual selection and may reinforce the separation of species. However, little is known about the genetic basis for diversification of male genital organs. In order to unravel the genetic bases for clasper and posterior lobe size evolution, we performed high-resolution introgression mapping to resolve candidate regions previously predicted on the left arm of the third chromosome. Gene expression analysis and genetic manipulation of these regions has reduced the number of potential candidate genes, and revealed novel genes involved in genitalia development. Using these results, I propose a gene regulatory network underlying clasper development. The reciprocal hemizygosity test showed that *tartan* (*trn*), underlies clasper size evolution between these species. *Trn* is a Leucine Rich Repeat transmembrane protein, and is the first gene identified underlying genital organ size differences between species. Moreover, expression analysis of *trn* implies cis-regulatory evolution, and likely candidate *trn* enhancer has been identified. Therefore, this thesis provides insights into the cis-regulation of phenotypic divergence, and given that *trn* functions as a cell affinity molecule, this may represent a novel mechanism for the developmental regulation of organ size.

Table of contents

1 CHAPTER ONE - INTRODUCTION 1

1.1 Evolutionary developmental biology 1

1.2 Anatomical variation of *Drosophila* external male genitalia 2

1.3 *Drosophila* mating and the function of the external male genitalia 5

1.4 Evolutionary mechanisms driving the divergence of male genital morphology 8

1.5 Identifying the genetic variation underlying male genital divergence 13

1.6 The development of *Drosophila* genitalia 21

1.7 Thesis aims 29

2 CHAPTER TWO - MATERIALS AND METHODS 31

2.1 Mapping causative genomic regions underlying male genitalia size divergence 31

2.1.1 Fly husbandry and genotyping of novel ILs 31

2.1.2 Rearing of novel introgression line males 32

2.1.3 Dissection of the male genitalia 32

2.1.4 Imaging and data collection 33

2.1.5 Statistical analysis 33

2.1.6 Fly husbandry and sample collection 36

2.1.7 Statistical analysis 37

2.2 In situ hybridisation of candidate genes 37

2.2.1 Pupal collection and preparation 37

2.2.2 RNA extraction, cDNA synthesis and Probe synthesis by PCR 38

2.2.3 Hybridisation protocol and imaging 39

2.3 Functional validation and characterisation of *tartan* 39

2.3.1 The generation and phenotyping of trn reciprocal hemizygotes using CRISPR 39

2.3.2 Phenotyping and statistical analysis of trn allelic dominance between D. simulans and D. mauritiana 41

2.4 Candidate *trn* regulatory elements and TF binding site analysis 42

2.4.1 Open chromatin analysis over candidate region C2 42

2.4.2 Fly husbandry, sample preparation and imaging of C2 candidate enhancers 42

2.4.3 Sequence analysis of candidate tartan enhancer mcclaspertrn 43

2.4.4 Identification and TF analysis of mcclaspertrn_peak 44

3. CHAPTER THREE - RESULTS 45

MAPPING THE GENOMIC REGIONS UNDERLYING MALE GENITALIA SIZE EVOLUTION BETWEEN *D. SIMULANS* AND *D. MAURITIANA* 45

3.1 Candidate regions for clasper size also affect clasper bristle number 46

3.1.1 Clasper size and bristle number candidate region C0 49

3.1.2 Clasper size and bristle number candidate region C1 51

3.1.3 Clasper size and bristle number candidate region C2 55

3.2 Posterior lobe size candidate regions 60

3.2.1 Posterior lobe size candidate region P1 62

3.2.2 Posterior lobe size candidate region P2 and P3 64

3.2.3 Candidate posterior lobe region P4 69

3.2.4 Posterior lobe size region P5 72

3.3 Chapter Three - Summary 74

4. CHAPTER FOUR - RESULTS 77

EXPRESSION ANALYSIS OF POSITIONAL CANDIDATE GENES 77

4.1 C0/P1 candidate genes 79

4.2 C1 candidate genes 85

1.1.1. In situ hybridisation of Cpr66D 92

4.3 C2 candidate genes 95

4.3.1 CG11279 and CG34429 in situ hybridisation in D. mauritiana and D. simulans 99

4.3.2 trn in situ hybridisation 100

4.3.3 caps in situ hybridisation 104

4.4 P2 candidate genes 107

4.5 P3 candidate genes 108

4.6 P4 candidate genes 110

4.7 P5 candidate genes 111

4.8 Chapter Four – Summary 113

4.8.1 Surf1 116

4.8.2 sgl 116

4.8.3 Mcm7 117

4.8.4 Cpr66D 118

4.8.5 foi 118

4.8.6 Gug 119

4.8.7 h 120

4.8.8 Trn 120

5. CHAPTER FIVE - RESULTS 123

FUNCTIONAL VALIDATION OF THE LEUCINE-RICH-REPEAT TRANS-MEMBRANE PROTEIN *TRN* IN CLASPER MORPHOLOGICAL DIVERGENCE 123

5.1 Knock-out of *trn* in *D. simulans* and IL 43 using CRISPR 124

5.2 Reciprocal hemizygosity test of *trn* on clasper morphology 125

5.3 *trn* allelic dominance 130

6. CHAPTER SIX - RESULTS 132

THE REGULATION OF *TRN* IN THE DEVELOPING DROSOPHILA MALE GENITALIA 132

6.1 Analysis of *trn* expression in *Drosophila* claspers 133

6.2 ATAC-Sequencing and histone modification profiles reveals candidate regulatory elements in C2 135

6.2.1 Functionally testing regions of C2 using VT-Gal 4 lines 138

***6.3* Sequence variation analysis of *mcclaspertrn* 141**

6.4 Refinement of *mcclaspertrn* 143

6.5 Sequence variation analysis of mcclasper*trn*_peak 143

6.5.1 Transcription factor binding site analysis 145

6.6 Testing the role of *hairy* in *trn* regulation in the developing male genitalia 150

6.7 Conclusion 152

7. CHAPTER SEVEN - GENERAL DISCUSSION 154

1.1. Mapping posterior lobe and clasper size differences between *D. simulans* and *D. mauritiana* 155

7.1 Identifying *trn* 158

1.1.1. Trn's role in development 158

1.1.2. The evolution of trn in clasper development 162

1.2. The gene regulatory network of clasper development 166

1.3. *Trn, sneaky* and the mechanisms driving rapid male genital evolution 170

1.4. Future directions 171

1.4.1. Investigating the developmental impact of gene evolution 171

1.4.2. Investigating the behavioural impact of genital evolution 172

8. CLOSING REMARKS 173

9. BIBLIOGRAPHY 174

Table of Figures

Figure 1. Divergence in external male terminalia in the *D. simulans* clade and its relationship to the outgroup *D. melanogaster*

Figure 2. Quantitative Trait Loci map of clasper morphology between *D. simulans* and *D. mauritiana*

Figure 3. Previously mapped clasper and posterior lobe candidate regions

Figure 4. Integration of sex-determination, homeotic, and patterning genes within the male genital disc

Figure 5. Pupal development of *D. melanogaster* male genitalia

Figure 6. Comparisions of clasper morphology between novel introgression lines and *D. simulans* w^{501}

Figure 7. Genomic mapping of clasper candidate region C0

Figure 8. Genomic mapping of clasper candidate region C1

Figure 9. Genomic mapping of clasper candidate region C2

Figure 10. Comparision of posterior lobe size between novel introgression lines and *D. simulans* w^{501}

Figure 11. Genomic mapping of posterior lobe candidate region P1

Figure 12. Genomic mapping of posterior lobe candidate regions P2 and P3

Figure 13. Genomic mapping of posterior lobe candidate region P4

Figure 14. Genomic mapping of posterior lobe candidate region P5

Figure 15. Improved mapping resolution of clasper and posterior lobe candidate regions

Table 1. Summary of resolved mapping results

Figure 16. RNAi effect of C0/P1 candidate genes on clasper and posterior lobe morphology

Figure 17. RNAi effect of C1 candidate genes on clasper morphology

Figure 18. RNAi effect of C1 candidate genes on posterior lobe morphology

Figure 19. *Cpr66D* in situ hybridisation

Figure 20. RNAi effect of *trn* on clasper morphology

Figure 21. *CG11279* and *CG34429* in situ hybridisation

Figure 22. *trn* in situ hybridisation

Figure 23. *caps* in situ hybridisation

Figure 24. Summary results of gene expression analysis

Figure 25. CRISPR design to knock-out *trn*

Figure 26. Crossing schemes to functionally validate and characterise *trn*'s role in clasper divergence
Figure 27. *trn* reciprocal hemizygosity test results
Figure 28. *trn* allelic dominance
Figure 29. Functional expression domains of *trn* in clasper development
Figure 30. Identification of candidate enhancer elements in C2
Figure 31. Expression of candidate enhancer mcclasper*trn*
Figure 32. Refinement and sequence variation analysis in mcclasper*trn*
Figure 33. Variant nucleotides in mcclasper*trn*_peak
Figure 34. The effect of variant nucleotide #4 on TF binding affinity
Figure 35. The regulation of *trn* by *h* in the developing male genitalia
Figure 36. Outline of possible GRN underlying clasper development
Figure 37. Preliminary insights into clasper development

Supplementary Files

Supplementary File 1. Primer stock list
Supplementary File 2. Novel introgression line break points
Supplementary File 3. Raw phenotypic measurements of introgression lines
Supplementary File 4. Descriptive statistics and comparisions of introgression line phenotype against *D. simulans* w^{501}
Supplementary File 5. Pairwise comparisions between introgression lines
Supplementary File 6. Maximum gene contents in candidate regions
Supplementary File 7. Compiled quantitative expression analysis data set
Supplementary File 8. RNAi screen raw data and summary statistics
Supplementary File 9. Gene expression analysis and RNAi manipulation summary of positional candidate genes
Supplementary File 10. CRISPR primer design
Supplementary File 11. *trn* reciprocal hemizygote and allelic dominance raw data and statistical analysis
Supplementary File 12. mcclasper*trn Drosophila* sequences
Supplementary File 13. ATAC-Seq leg predicted peaks of open chromatin within candidate region C2
Supplementary File 14. Sequence analysis of mcclasper*trn* between Drosophila species
Supplementary File 15. TF binding site analysis in mcclasper*trn*_peak

1 Chapter One - Introduction

1.1 Evolutionary developmental biology

Explaining the diversity of life has always been a fundamental question in biology. In the latter half of the twentieth century, the discovery of Hox genes (Averof, 1997; Carroll, 2008; Gehring, 1985; Grenier et al., 1997; Lewis, 1978), and so-called "master regulator" genes (Dahl et al., 1997; Suga et al., 2010), led to the unprecedented realisation that animals that look nothing alike share a conserved underlying genetic 'toolkit'. As a result, the 1970-1980s saw the beginning of a modern synthesis between developmental and evolutionary disciplines ("Evo-devo"), whereby evolutionary perspectives were applied to developmental processes (Lewis, 1978; Nusslein-Volhard and Wieschaus, 1980).

Evo-devo studies since, have mainly focussed on comparative expression and functional analyses of conserved genes of different lineages of plants and animals, in order to elucidate ancestral features of the regulation of their development (Holland et al., 2017; Jiggins et al., 2017; Shubin et al., 2009; Tokita et al., 2017; Tucker, 2017). However, in order to properly understand the mechanism of phenotypic change, the underlying genetic variation must first be identified (e.g. how many genetic changes underlie phenotypic differences),

what kind of differences are they (coding or regulatory, epistatic or additive) and which types of genes are affected (biased towards master regulators or not) (Nunes et al., 2013). Once the genetic variation has been identified, we can then learn more of the evolutionary forces that may have driven, spread and maintained these changes throughout populations (e.g. through sexual selection, stabilising selection, directional selection) and potentially provide new insights into the development of the focal traits.

Historically, male genital morphology has been of interest to evo-devo biologists, since their rapid evolution has been widely documented across many animal groups; including insects, artiodactyls, bats, rodents, primates, molluscs, fishes, rays, snakes, lizards, nematodes, flatworms, crustaceans, mites and aves (Eberhard, 1985). Charles Darwin himself, is said to have spent eight years studying the extraordinary diversity of male barnacle genitalia. In *Drosophila*, attempts to understand the genetic and developmental mechanisms underlying rapid evolution of male genitalia started more than three decades ago (Coyne, 1983).

1.2 Anatomical variation of *Drosophila* external male genitalia

Classically used in species identification, the male periphallic organs of *Drosophila* (also known as the external male genitalia), vary greatly in morphology. Since *D. mauritiana*, *D. simulans* and *D. sechellia* only diverged from their last common ancestor less than 240 thousand years ago (Garrigan et al.,

2012; Nunes et al., 2010), differences in the size and shape of the posterior lobes and claspers are thought to have evolved very rapidly (Fig 1a).

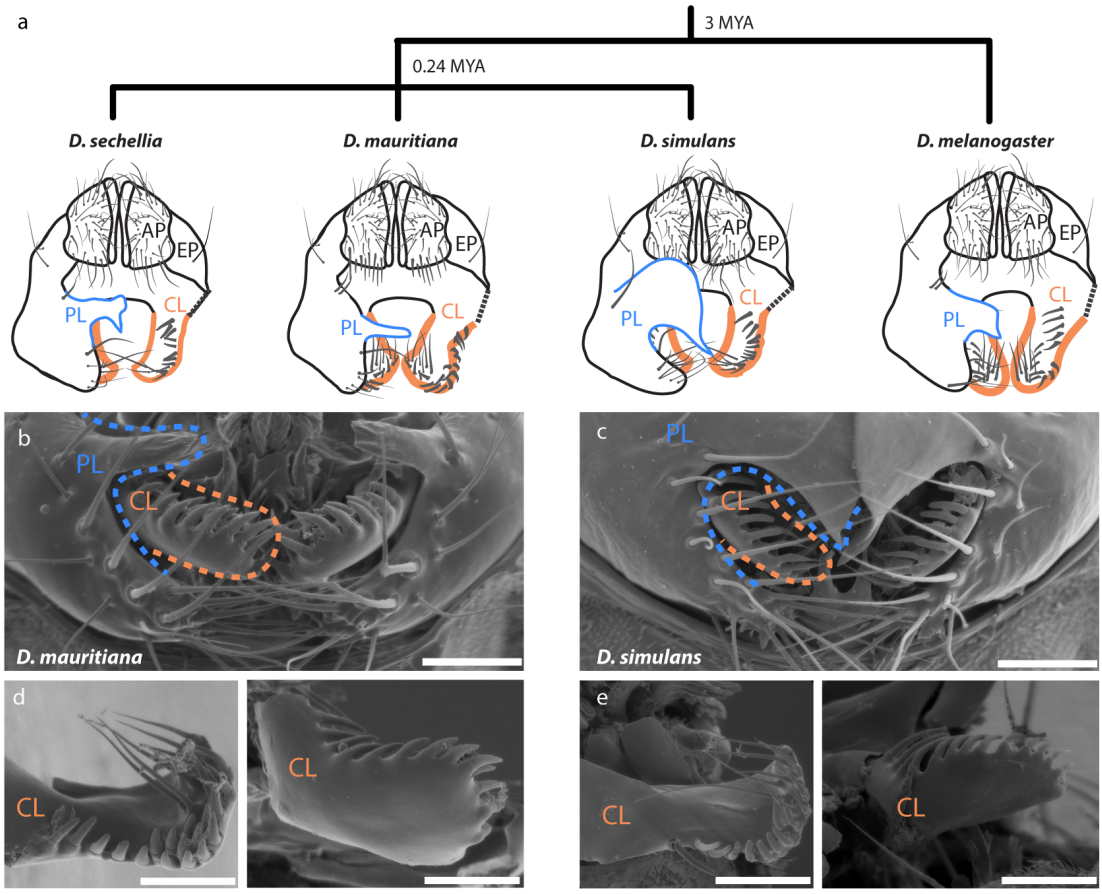


Figure 1. Divergence in external male terminalia in the *D. simulans* clade and its relationship to the outgroup *D. melanogaster*. Adapted from (Hagen et al., 2018). **(a)** Schematic representation of the male analia and genitalia (posterior view). Posterior lobes (outlined in blue) are illustrated as dissected away on the right-hand-side, in order to facilitate visualization of the claspers (outlined in orange), which are typically covered by the posterior lobes. While the shape and size of the posterior lobes is species-specific, the claspers and anal plates are very similar between *D. simulans and D. sechellia*, which are smaller and have less bristles than those of *D. mauritiana* and *D. melanogaster. D. mauritiana* also contain a third more, and thicker clasper bristles than those of the other three species (Tanaka et al., 2015; True et al., 1997; Tsacas and David, 1974). **(b** and **c)** Scanning electron micrographs of the position of the claspers under the lobes in *D. mauritiana* and *D. simulans*, respectively. **(d** and **e)** the morphology of the claspers from anterior view (left) and lateral view (right) in *D. mauritiana* and *D. simulans*, respectively. Scale bars show 50 um in all cases. Posterior lobes (PL), claspers

(CL), anal plates (AP) and epandrium (EP).

The posterior lobes are a *D. melanogaster* subgroup specific novelty (Jagadeeshan and Singh, 2006). In *D. mauritiana,* they are small, thin finger-like projections (on average 11.22 ($x10^3mm^2$), Supplementary File 4a), in comparison to the much larger, helmet shaped lobe of *D. simulans* (on average 1.54 ($x10^3mm^2$), Supplementary File 4a) (Fig 1a). *D. melanogaster*, contain intermediate sized lobes, which are trapezoid shaped, whilst *D. sechellia* lobes are also intermediate and resemble "boots" (Fig 1a). Whilst the differences in genital size between species are very striking, it is important to note that there is some variation within species (though the extremes of these differences do not overlap with the differences detected between species (Hackett et al., 2016; McNeil et al., 2011)). Therefore, the posterior lobes are considered to be the most reliable character in distinguishing *D. melanogaster*-subgroup species (Ashburner, 1989).

The claspers lie underneath the posterior lobes (Fig 1b and 1c), and are over twice as large in *D. mauritiana* (on average 3.38 ($x10^3mm^2$) Supplementary File 4a) compared to *D. simulans*(on average 1.41 ($x10^3mm^2$) Supplementary File 4a), with a third more bristles (on average 24 versus 18.5, respectively (Supplementary File 4a) (Fig 1a, 1d – 1e)(Tanaka et al., 2015; True et al., 1997). The morphology of these bristles also differs between the species, with *D. mauritiana* bristles being generally shorter and thicker than *D. simulans* (Fig 1a, 1d – 1e) (Tanaka et al., 2015; True et al., 1997). *D. sechellia* male claspers are very similar morphology to that of *D. simulans*, whilst the clasper morphology of

D. melanogaster appears to be an intermediate between *D. mauritiana*, and *D. simulans*/*D. sechellia* (Fig 1a).

1.3 *Drosophila* mating and the function of the external male genitalia

Sex in *Drosophila* is made up of a complex combination of behaviours that involve many parts of male and female *Drosophila* anatomy. Beginning with courtship, males tap the females with their forstarsi (T1 tibia)(Manning, 1959), scissor their wings, perform rowing motions (whereby one wing extends and arches, and then alternates to the opposing wing (Cowling, 1981)), and vibrate their wings to perform a song (Ding et al., 2016; Routtu et al., 2007). These behaviours vary between species (Greenspan and Ferveur, 2000; Ding et al., 2016) and are thought to contribute to pre-copulatory success (e.g. mate acceptance) and post-copulatory success (e.g. sperm storage, insemination frequency, number of offspring sired) of males during mating (Robertson, 1983; Price et al., 2001; Yassin and Orgogozo, 2013).

Studies suggest the morphology of the lobes could contribute to both pre- and post-copulatory processes. Genetic manipulation of lobe morphology in conspecific *D. melanogaster* mating pairs has been shown to affect the amount of sperm transferred, the number of eggs deposited by the female, and the percentage of progeny sired under competitive conditions (Frazee and Masly, 2015). Therefore, lobe morphology appears to influence male post-copulatory

success partly by influencing female behaviour. However, it could be that genetic manipulation of genes involved in lobe development pleiotropically affected other genetic factors contributing to these copulatory traits, and other studies in *D. simulans* did not link lobe morphology to post-copulatory success, but surprisingly found evidence for a role in pre-copulatory mechanisms (LeVasseur-Viens et al., 2015). In this study, males with manipulated lobes failed more frequently in copulation compared to un-manipulated males. However, this study used crude microdissection laser techniques to modify the posterior lobes of *D. simulans,* and so it remains unclear as to whether this affect is due to the severe injury inflicted onto males, or the role of the lobes.

In contrast, the mechanical role of the lobes in facilitating genital coupling is more tangible. Curled inward at rest, the posterior lobes evert outwards during copulation and insert at the intersegmental membrane between female abdominal tergites VII-VIII (Kamimura and Mitsumoto, 2011; Robertson, 1983; Robertson, 1988; Yassin and Orgogozo, 2013). In some species such as *D. simulans* and *D. sechellia,* the lobes insert in the intersegmental membrane but not in others, such as *D. melanogaster* (Bertin and Fairbairn, 2007).

The claspers are also known to have a mechanical role during copulation, as they have been shown to open medially, "clasp" and open the oviscapt valves of the female (Kamimura and Mitsumoto, 2011; Mattei et al., 2015). The sensory bristles of the clasper intermesh with the ovisensilla on the ventral side of the female oviscapt in all species except *D. sechellia* in the *D. melanogaster* subgroup

(Kamimura and Mitsumoto, 2011; Mattei et al., 2015), but also do in more distantly related species such as *D. saltans* and *D. willistoni* (Eberhard, 2004a).

Although intermeshing of the clasper bristles with the ovensilla (peg-like bristles on the female genitalia) is a widely conserved process, the role of the bristles varies between species (Acebes et al., 2003; Chen and Baker, 1997; Tsacas and David, 1974). Bristles which are long, thin, and distally located on the claspers of *D. melanogaster* have been shown to have a role in proprioception and correct positioning of the male during copulation; as ablation of these bristles on one of the claspers results in asymmetrical male mating position towards the contralateral side (Acebes et al., 2003). Interestingly, this asymmetry only affects posture, and had no effect on latency or duration (Acebes et al., 2003). However, ablation of the same type of bristle in *D. simulans* and *D. sechellia* does not affect mating posture or copulation success; suggesting that morphologically similar bristles are not homologous or functionally equivalent between species (Acebes et al., 2003).

Once the male is securely mounted by the external genitalia, the organs of the internal genitalia sequentially unfold, opening the female reproductive tract as they do so to allow the adeagus to reach to the proximal ends of the paired oviscapts, where the sperm is transmitted (Kamimura and Mitsumoto, 2011).

1.4 Evolutionary mechanisms driving the divergence of male genital morphology

The cause of rapid male genital divergence is debated in three main theories; the Pleiotropy Hypothesis (Mayr, 1966), the Lock and Key Hypothesis (Dufour, 1844), and the Sexual Selection Hypothesis (Eberhard 1985).

The Pleiotropy Hypothesis, suggests that rapid male genital divergence is a by-product of shared genetic elements underlying genital development, and other morphological traits undergoing high levels of selection pressure (Mayr, 1966). Therefore, as species accumulate selected morphological changes, they also gather neutral changes in the male genitalia as a secondary effect (Mayr, 1966). However, due to lack of supportive experimental evidence the pleiotropy hypothesis is not considered the most likely explanation (Liu et al., 1996; Song, 2009).

The Lock and Key Hypothesis, unlike the Pleiotropy Hypothesis, considers the morphology of the male genitalia to be a key factor in driving their rapid evolution (Dufour, 1844). The "lock" (female genitalia) is thought to exert selective pressure on the "key's" morphology (male genitalia); driving morphological evolution to ensure the latter adopts a complementary form. Presumably, therefore, males and females of the same species should contain morphologically compatible genitals. Until recently, however, the female

genitalia were largely understudied, and those that did regarded the female genitalia as relatively simple and not thought likely to have co-evolved alongside the divergent male genitalia (Jagadeeshan and Singh, 2006; Eberhard, 2004b). Moreover, in 1927, Richards, and more recently Shapiro and Porter (1989), argued that pre-copulatory isolation mechanisms (such as the behavioural differences previously described) are likely to pre-date such mechanisms, which would render the lock and key barrier redundant (Richards, 1927; Shapiro & Porter, 1989).

However, recent studies have shown that multiple *Drosophila* female genital structures, such as the vaginal shields, oviscapt furrows and oviscapt pouches, co-evolve with the male phallic hooks and spines (Yassin and Orgogozo, 2013), adeagus, and posterior lobes, respectively (Kamimura and Mitsumoto, 2011; Robertson, 1988; Yassin and Orgogozo, 2013). It is been proposed that the co-evolution of posterior lobes and their female insertion points within species is thought to reinforce reproductive isolation between species (Cobb et al., 1988; Coyne, 1989; Jagadeeshan and Singh, 2006; Price et al., 2001; Robertson, 1988; Robertson, 2013; Robertson, 1983; Frazee and Masly, 2015; Kamimura and Mitsumoto, 2011; LeVasseur-Viens et al., 2015). For example, small-lobed species males (e.g. *D. mauritiana* and *D. sechellia*) mate relatively comfortably with large-pouch species females (e.g. *D. simulans*) whilst crosses in the opposing direction often fail. Therefore, the lobe morphology could undergo heavy selection pressures to ensure compatible mating within species, as well as preventing incompatible mating between species.

However, in the case of the clasper bristles, and the female structure with which they intermesh, there is no evidence for lock and key co-evolution (Eberhard and Ramirez, 2004; Kamimura and Mitsumoto, 2011; Eberhard, 2004a). Therefore, it is unlikely that female selective pressure within species can explain the species-specific arrangement of this divergent organ.

However, the Sensory Lock and Key Hypothesis (De Wilde, 1964; Eberhard, 1992) bypasses such contradictions. Instead of females possessing morphologically compatible genitals to males (as in the classical Lock an Key Hypothesis), they are instead proposed to recognise the correct male genital morphology to make behavioural decisions which affect male reproductive success post-copulation (such as selectively storing sperm, releasing eggs and fertilising them with the sperm of males with specific genital morphology (De Wilde, 1964; Eberhard, 1992)). Therefore, in contrast to the classical Lock and Key Hypothesis, the sensory adaptation implies that male genital organs are under selection due to their role in influencing female reproductive decisions.

Similarly, in the Sexual Selection Hypothesis, the theory of "cryptic female choice" predicts females have a preference for a particular male genital morphology, and use this to conditionally dictate post-coupling processes (such as those described above) after mating with more than one male (Eberhard, 2010). Females who selectively reproduce with males of specific genital morphology will give rise to male progeny with similar genitalia, and through

Fisherian selection, drive the evolution of that genital morphology within species (as in the "Sexy Sons Hypothesis") (House et al., 2013). Evidence for this theory include the observation that across many insects, male genitalia (and not other parts of the male anatomy) has diverged more extensively in polyandrous species (e.g. those whose females mate more than once per reproductive attempt), than species with monogamous systems (House et al., 2013; Arnqvist, 1998). This implies that females enforce post-copulatory sexual selection on male genital morphology and consequently drive their rapid evolution.

Similarly to the Lock and Key Hypothesis, cryptic female choice could also drive male genital evolution by preventing costly interspecific mating but through post-copulatory mechanisms (Frazee and Masly, 2015; Price et al., 2001). For example, conspecific mating between *D. simulans* pairs and heterospecific *D. simulans* males and *D. mauritiana* females pairs results in the same amount of sperm transfer (Price et al., 2001). However, females of the latter pair only store 40% of sperm compared to the first. If females use male genital morphology to make reproductive decisions such as these, (e.g. a proposed mechanism of posterior lobe function (Frazee and Masly, 2015) – see previous section), differences in male genital morphology and female preference will be selected on; thereby driving their evolution.

The expulsion of male sperm can also occur within conspecific crosses, and is an example of sexual conflict; as the females have evolved mechanisms to increase their own fitness, despite being costly to males (House et al., 2013).

The reproductive interests of males and females are barely ever identical (Eberhard, 1985), and this leads to males and females successively evolving morphological traits to ensure the fitness of their individual sex (as in the Red Queen Hypothesis) (Brennan et al 2007, Hosken and Stockley 2004, Simmons and Garcia-Gonzalez 2011). Therefore, in the context of the male genitalia, complex traits could have arisn quickly to improve a male's likelihood of insemination and to regain reproductive control (Kamimura, 2007). Sperm itself, as well as allowing insemination, contains seminal fluid proteins able to increase egg-laying rate and decrease receptivity of females to future mating (Poiani, 2005).

In some *Drosophila* species such as *D. eugracilis*, copulatory wounds inflicted on the female by the male external genitalia have been shown to transfer this seminal fluid (not sperm); therefore bypassing the post-copulatory control mechanisms of the female (Kamimura and Mitsumoto, 2011). In the *D. melanogaster* group, copulatory wounds frequently occur, and their location and frequency differ between species (Kamimura and Mitsumoto, 2011b). These wounds often correlate with the contact point of the male posterior lobes and claspers (Kamimura and Mitsumoto, 2011), and in females often contain sclerotized patches (Kamimura, 2007; Yassin and Orgogozo, 2013).

Why would reducing the fitness of females drive male genital divergence? Studies have suggested that if the damage to the female is culminative throughout multiple mating attempts, females would be less receptive to future

mating; thereby increasing the fitness of the harmful male (Johnstone and Keller, 2000). Alternatively, it was proposed that males could benefit from inflicting wounds to females during copulation; because injured females that recognise their fecundity might be affected could increase their investment to their current reproduction (Crudgington and Siva-Jothy, 2000). However, in the case of the *D. melanogaster* group, it is unclear how these copulatory wounds increase male fitness, and could be a mere by-product of the mechanics of sex (Kamimura and Mitsumoto, 2011; House et al., 2013).

1.5 Identifying the genetic variation underlying male genital divergence

Identification and subsequent manipulation of the loci underlying the rapid divergence of male genital morphology would allow us to test the validity of the above theorems, without the interference of other confounding species-specific differences.

Previously, it was generally accepted that phenotypic differences are predominantly caused by gene regulatory changes (Carroll, 2008; Jacob and Monad, 1961; Jacob, 1977; Stern 2000; King and Wilson, 1975) and especially by enhancer sequence turnover (Carroll, 2008; Lynch and Wagner, 2008). Evolution, as Jacob described in 1977, acts as a "tinkerer", creating subtle changes in gene regulation to generate morphological diversity. This is perhaps

counterintuitive, since in organisms such as *Drosophila*, only 3% of the genome is predicted to be cis-regulatory in function (Alonso and Wilkins, 2005). The key reason why mutations occur and are retained in regulatory elements is thought to be due to selection pressure; since the modularity of gene regulatory regions bypass the widespread disadvantageous affects of mutations in the protein-coding elements of genes (Carroll, 2008; Lynch and Wagner, 2008).

However, some studies also argue there is a lack of evidence to support such assumptions (Hoekstra and Coyne, 2007), since only 22% of the mutations documented for morphological variation so far occur in cis-regulatory regions (Stern and Orgogonzo 2008). Examples include mutations linked to variation in wing pigmentation (Arnoult et al., 2013; Gompel et al., 2005; Prud'homme et al., 2006), skeletal changes (Guerreiro et al., 2013; Indjeian et al., 2016; O'Brown et al., 2015), trichome patterning (Frankel et al., 2011; McGregor et al., 2007; Stern and Frankel, 2013; Sucena and Stern, 2000; Kittelmann et al., 2018) and the co-evolution of copulatory organs (Nagy et al., 2018).

However, the number of these cases is rapidly increasing (ref stern and orgogonzo 2008), and their relative under-representation could be due the difficulty in identifying the regulatory elements of genes, which can lie up to 100 kilobases away from their core promoters (Hoekstra and Coyne, 2007).

Another challenge to scientist attempting to identify the genetic variation underlying morphological variation - whether it be regulatory or not – is empirically proving which mutations are causative. One method most widely accepted for these purposes is the reciprocal hemizygosity test (Stern, 2014). The test involves the comparison of animals that are genetically identical except for the species- (or strain-) specific functioning allele of the gene in question. Therefore, if a change in phenotype is observed in the expected direction, mutations in that allele are regarded as causative.

To functionally test which genes underlie the rapid diversification of male genitalia between *Drosophila*, we must first identify possible candidate genes. Quantitative Trait Loci Mapping (QTL) allows for large regions of the genome to be associated with differences in a specified trait, but often only reaches a resolution of hundreds of candidate genes (Liu et al., 1996; Macdonald and Goldstein, 1999; True et al., 1997; Zeng et al., 2000). Therefore, these studies are most powerful when combined with techniques that allow for fine-scale resolution, such as introgression mapping (Tanaka et al., 2015). Introgression mapping involves the backcrossing of inter-species F1 females, to one of (or both of) the parental strains for 'n' generations. This allows for the generation of a panel of "introgression lines" (ILs) that contain homogenous genetic background of one species, apart from small regions of introgressed DNA from the alternative species. These regions may contain the causative loci underlying phenotypic differences, and can be detected by comparing the morphology of the lines. Both of these mapping techniques rely on the availability of species

which are phenotypically divergent but are able to produce fertile progeny; as is the case in crosses between the three species of the *D. simulans* species clade (Lachaise, 1986),

Indeed, several research groups have already attempted to map differences in male genitalia between these species. Most mapping studies have focused on the evolution of posterior lobe size and shape (Coyne et al., 1991; Laurie et al., 1997; Liu et al., 1996; Macdonald and Goldstein, 1999; Masly et al., 2011; Zeng et al., 2000). The major finding of these studies was that posterior lobe divergence has a very polygenic basis, with the number of QTL ranging from a minimum of 8 to 19, mapped across every major chromosome (Coyne et al., 1991; Laurie et al., 1997; Liu et al., 1996; Macdonald and Goldstein, 1999; Masly et al., 2011; Zeng et al., 2000). Consistently in these studies, more QTL map to the left arm of the third chromosome than any other part of the genome. In addition, all loci were found to affect posterior lobes in the same direction of the parental difference (e.g. for example, exchanging *D. simulans* alleles for *D. mauritiana* alleles during introgression analysis gives rise to smaller lobes, a more *D. mauritiana* -like phenotype), suggesting strong directional selection acting on this trait (Zeng et al., 2000, Macdonald and Goldstein, 1999a). However, so far none of the genes underlying posterior lobe divergence have been identified.

To date, only two QTL maps have been generated to identify loci underlying clasper morphological differences (Tanaka et al., 2015; True et al.,

1997) (Fig 1). Both True et al (1997) and Tanaka et al (2015) predicted peaks on the left arm of the third chromosome (3L) underlying clasper bristle number differences between the species, and Tanaka et al (2015) also identified a major peak on the X chromosome (Fig 2). Tanaka et al (2015) also mapped differences in clasper size (known to positively correlate to clasper bristle number (Tanaka et al., 2015)), and found one QTL peak on the second chromosome, and one peaks on either arm of the third chromosome (Fig 2). The peak on 3L overlapped across both studies (indicated by the orange bar in Fig 2).

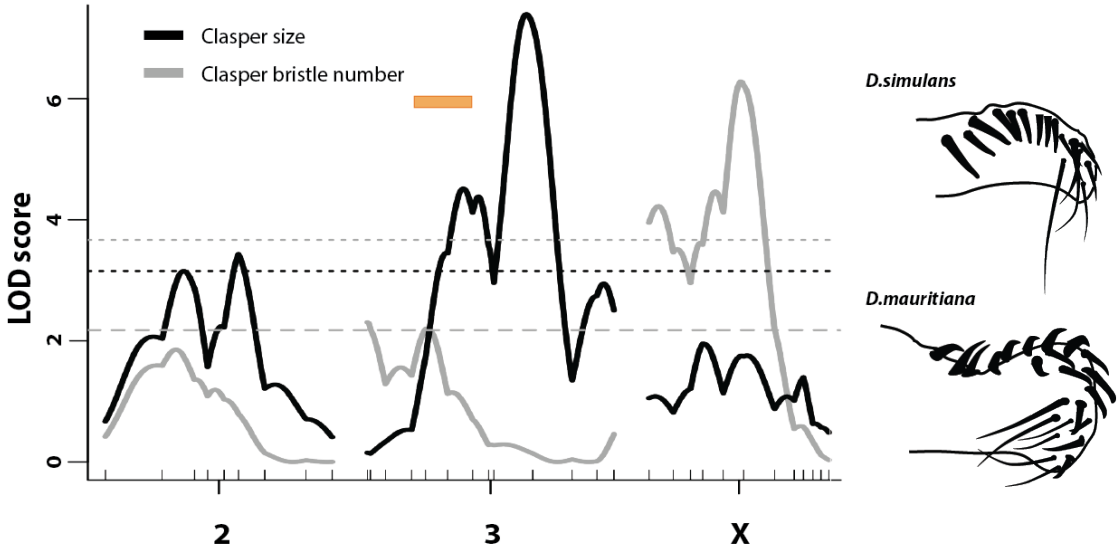


Figure 2. Quantitative Trait Loci map of clasper morphology between *D. simulans* and *D. mauritiana* (adapted from Tanaka et al. 2015). LOD score along the Y-axis indicates result from HK regression analysis for clasper size (black line) and clasper bristle number (grey line) for chromosomal regions (X-axis). The position of genetic markers is shown above the X-axis. Dotted lines indicate a 0.5% significance threshold for clasper size (black) and bristle number (grey) (Tanaka et al., 2015). The orange bar indicates the region of 3L that contains significant peaks for both mapped traits. *D. simulans* and *D. mauritiana* clasper morphology and clasper bristle number is illustrated on the right-hand side.

By using this QTL map to guide an introgression mapping approach between *D. mauritiana D1* and *D. simulans* w^{501}, Tanaka et al (2015) was able to

fine scale map regions underlying clasper divergence on 3L to reduce the number of potential candidate genes (orange bars, Fig 3). ILs which contained introgressed *D. mauritiana* DNA on 3L in an otherwise *D. simulans* w^{501} genetic background were generated and maintained (Tanaka et al., 2015) using the visible P-element marker (*P*[lac-w^{+}]) "D1" (True et al., 1996) indicated by the red arrow in Fig 3. By comparing the effect each introgressed region has on clasper morphology, Tanaka et al (2015) identified multiple regions underlying clasper (C) differences between these two species (Fig 3).

Clasper candidate region "C1" is a 446.5 kb region that was isolated due to the observation that all IL with *D. mauritiana* DNA in this region have significantly larger claspers, with more bristles, than *D. simulans* w^{501}. At the highest resolution, C1 is defined by the boundaries of introgressed DNA in D23.42 and D21.43e (Fig 3) (Tanaka et al., 2015), and is predicted to contain loci able to explain 8% of the differences in clasper size, and 13% of the differences in clasper bristle number between the species. In *D. melanogaster*, this region contains 52 annotated protein-coding genes, all of which are considered "positional candidate genes" – i.e. any one or more of these genes could underlie clasper differences between the species.

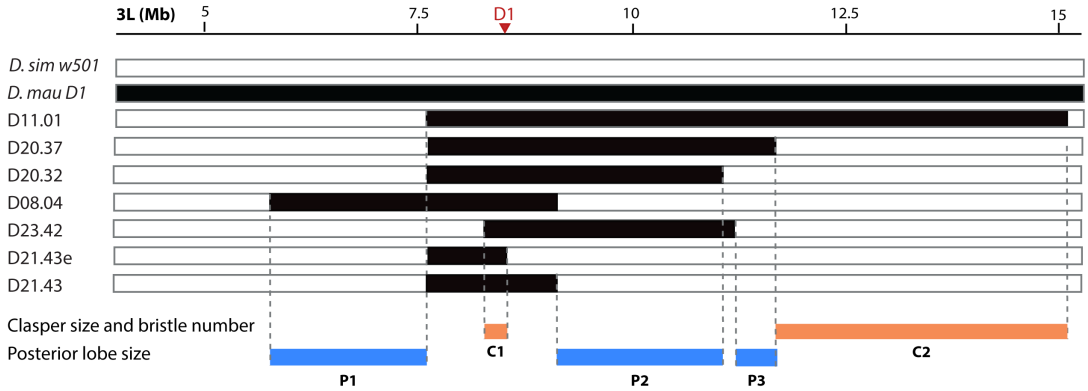


Figure 3. Introgression lines generated on 3L and the resolution of clasper divergence candidate regions adapted from Tanaka et al (2015). Black bars indicated *D. mauritiana* DNA and white bars indicate *D. simulans* DNA. Previously predicted clasper candidate regions (C1 and C2) and posterior lobe candidate regions (P1, P3 and P3) are indicated by orange bars and blue bars, respectively. Note, none of the clasper and posterior lobe predicted regions overlap (Tanaka et al., 2015). The position of visible marker "D1" on 3L is indicated by the red triangle.

Tanaka et al (2015) found that IL D11.01 (Fig 3), exhibited significantly larger claspers than all other introgression lines containing C1, which suggested an additional region that contributes to clasper divergence. This region is referred to as "C2", and the boundaries of this region are defined by the 3.49 Mb difference in breakpoints between D11.01 and D20.37 (Fig 3). Region C2 contribute 16% of differences in clasper area, and 20% of differences in clasper bristle number between *D. simulans* and *D. mauritiana,* respectively (Tanaka et al., 2015). At the resolution achieved by Tanaka et al., (2015), this region contains 312 annotated protein-coding genes in *D. melanogaster*.

As previously discussed, many QTL mapping studies of posterior lobe size and shape differences in the *D. melanogaster* species complex have

predicted peaks on 3L (Liu et al., 1996c; Macdonald and Goldstein, 1999b; Masly et al., 2011a; True et al., 1997a; Zeng et al., 2000). Therefore, to determine whether or not the peak on 3L predicted for clasper morphology also contributes to posterior lobe divergence, Tanaka et al (2015) also compared posterior lobe size between the ILs outlined in Fig 3 and *D. simulans*.

The only introgressed *D. mauritiana* DNA that did not significantly decrease the size of the posterior lobes compared to *D. simulans* w^{501} was that in ILs D21.43 and D21.43e (Fig 3). Based on this observation, and by comparing how much each line affected the size of the lobes, Tanaka et al (2015) was able to map three posterior lobe candidate regions to this part of 3L (P1, P2 and P3). Candidate region P1 was mapped between the left-hand breakpoints of ILs D08.04 and D11.01, P2 between the right-hand breakpoints of ILs D21.43 and D20.32, and P3 between the right-hand breakpoints of ILs D23.43 and D20.37 (Fig 3). These regions span 1.8 Mb, 1.9 Mb and 562 kb respectively, and (assuming the variation in P1 - P3 contribute additively to the phenotypic differences in lobe size), explain 9%, 6% and 7% of differences in lobe sized between the species, respectively. However, these candidate regions still contain a total of 494 positional candidate genes, with the smallest region P3 still containing as many as 78 (annotated in *D. melanogaster*) (Tanaka et al., 2015).

1.6 The development of *Drosophila* genitalia

Since previous studies have not been able to identify the genes underlying male genital organ size divergence, it is unclear which developmental processes they differentially affect between species. Presumably, genetic variation could alter genital development at any number of stages, and so I will now review some of the main processes underway during male genital development.

The genitalia, like many adult *Drosophila* structures, are derived from imaginal discs. However, unlike other imaginal discs, the genital disc is unpaired, sexually dimorphic, and develops at a medial position at the posterior end of the fly. Both male and female genital discs are formed from the ventral cells of abdominal segments A8, A9 and A10 of the larva (Epper, 1983; Nöthiger, 1977; Schupbach et al., 1978). In males, A9 is also formed from cells derived from the mesoderm, as a result of FGF signalling between these cells and the male genital primordium (Ahmad and Baker, 2002).

The abdominal segments are described as being differentially "repressed" between the sexes; with the "repressed" primordia growing more slowly than the dominant, resulting in dimorphic genital disc sizes between males and females (Epper & Nöthiger, 1982). In females, abdominal segment 8 develop into the internal and external genitalia, but being "repressed" in males, remains as an abdominal segment. In contrast, cells of the A9 segment gives rise

to the male genitalia in males, but develop into the paraovaria in females. In both sexes, A10 becomes the analia and hindgut, which are also sexually dimorphic (Keisman, Christiansen, & Baker, 2001).

The ability of male and female genitalia to develop from the same pools of cells, and yet form such phenotypically different organs, is thought to be derived from a combinatorial effect of differentially transcribed homeotic genes, and sex-determination genes (Keisman and Baker, 2001; Sanchez and Guerrero, 2001; Estrada et al., 2003; Estrada and Sanchez-Herrero, 2001; Burtis and Baker, 1989).

Sexually dimorphic expression of *Double sex (Dsx)* occurs due to differences in the X: autosome chromosome ratio between the sexes. In females, this ratio leads to the expression of *Sex lethal* (*Sxl*), which in turn leads to the expression of transformer (*tra*) (Burtis and Baker, 1989). Tra, along with Tra-2, causes female-specific splicing of Dsx (generating Dsx^F), which regulates a downstream cascade of sex determination genes (Burtis and Baker, 1989; Nothiger and Steinmann-Zwicky, 1987; Baker and Ridge, 1980). In males, where *Sxl* is not activated, Tra protein is also absent, and therefore the male isoform of Dsx^M is produced (see black outline of male genital disc in Fig 4) (Schutt and Nothiger, 2000). Therefore, throughout A8 – A10, Dsx^F is found in females, and Dsx^M in males (black lines Fig 4). In both sexes, disruption of Dsx^F or Dsx^M, (in females and males respectively), results in the development of hermaphrodites (Hildreth, 1965).

Rather than differing between the sexes, expression of homeotic gene *Abdominal-B* (*Abd-B*) differs between abdominal segments (Fig 4) (Casares et al., 1997). In A8, only the 'm' transcript of *Abd-B* is expressed (and only the 'M' Abd-B protein produced). In contrast, in A9, the *Abd-B* transcript 'r' is expressed (and only Abd-B 'R' protein produced) (Casares et al., 1997) (Fig 4). The absence of 'M' or 'R' protein can cause homeotic mutations (such as the genitalia being replaced with a leg or a distal antennae (Estrada and Sanchez-Herrero, 2001)), and ectopic expression in the head results in the development of ectopic genitalia (in either sex) (Kuhn et al., 1993; Postlethwait et al., 1972). Therefore, *Abd-B* is considered both necessary and sufficient for genital development in both sexes.

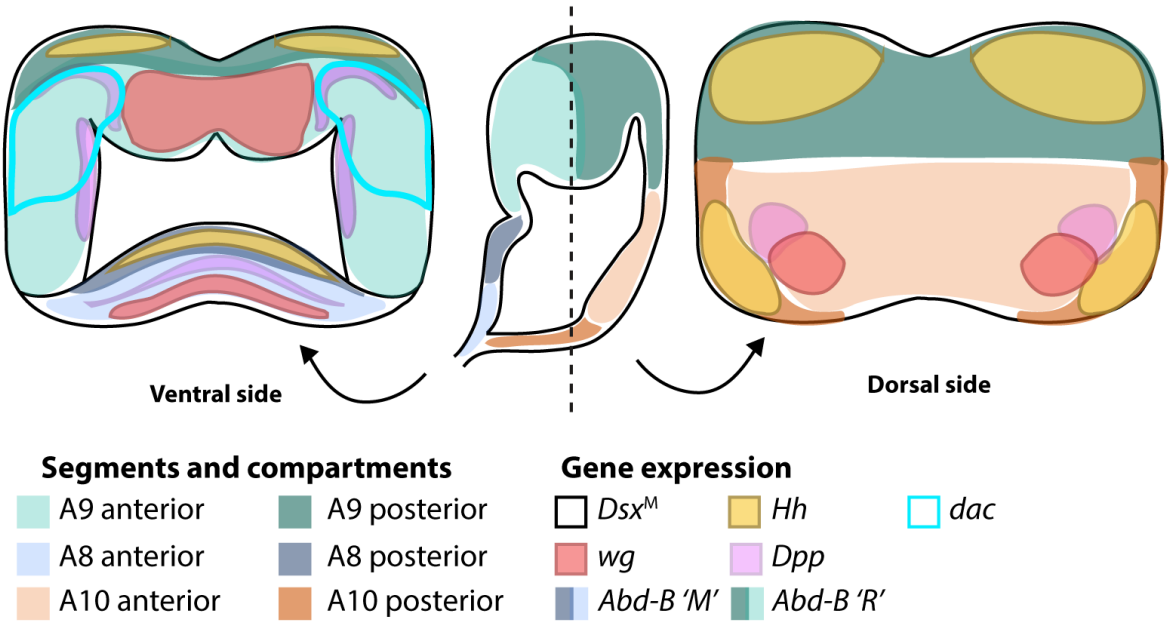


Figure 4. Integration of sex-determination, homeotic, and patterning genes in the male genital disc. Anterior and posterior

compartments are indicated by dark and light shades respectively, for A8 (blue), A9 (green) and A10 (orange) segments. Note, "anterior" and "posterior" compartments of the disc refers to the origin of the cells in the segments of the embryo (Gorfinkiel et al., 2003). Abd-B 'M' transcript is exclusively found in the A8 segment, whilst Abd-B 'R' transcript is in A9. Hh (yellow) is expressed in the posterior compartments of the segments (darker shades), which induces Dpp and Wg expression in the anterior compartments in complementary domains. Dsx^M is expressed in all segments of the male disc (black outline). Dsx^M renders wg repressive towards dac, and Dpp enhancive in A9. Expression patterns are based on findings of (Schutt and Nothiger, 2000; Casares et al., 1997; Estrada and Sanchez-Herrero, 2001; Keisman and Baker, 2001; Keisman et al., 2001; Sanchez and Guerrero, 2001).

Despite these differences in sex determination and homeotic transcription between male and female genital discs (and moreover imaginal discs in general), *wingless* (*wg*) and *decapentaplegic* (*dpp*) interact antagonistically and are expressed in complementary patterns at 'organizing regions' in both sexes (see red and pink shading, Fig 4) (Blackman et al., 1991; Casares et al., 1997; Chen and Baker, 1997; Freeland and Kuhn, 1996; Sanchez and Guerrero, 2001; Keisman and Baker, 2001). The interaction between these genes at organising regions defines the compartmental boundaries of each disc, where downstream patterning genes are activated (Blackman et al., 1991; Casares et al., 1997; Chen and Baker, 1997; Freeland and Kuhn, 1996; Sanchez

and Guerrero, 2001; Keisman and Baker, 2001), and often give rise to the morphological boundaries of the mature organ (Mirth and Akam, 2002).

The expression of *wg* and *dpp* is set up by *hedgehog (hh)* (Fig 4, yellow shading), which is expressed posterior to the AP boundary of each segment of the genital disc as a result of a negative interaction between transcription factors *cubitus interruptus (ci)* (expressed in the anterior), and *engrailed (en)* (expressed in the posterior, not shown in Fig 4) (Eaton and Kornberg, 1990; Kornberg et al., 1985; Garcia-Bellido, 1973; Morata and Lawrence, 1975; Diaz-Benjumea and Cohen, 1995).

Functioning downstream of Wg and Dpp is the sexual differentiation transcriptional co-factor *Dachshund (dac)* (shown in bright blue line, Fig 4 (Keisman et al., 2001)). In female genitalia, *dac* directly regulates the development of the spermitheca and paraovia ducts in females, and in males regulates the size of the claspers and the number of clasper bristles (Keisman et al., 2001; Christiansen et al., 2002). *Dac* is expressed in a pattern that is highly sexually dimorphic, due to differences in *Dsx* processing between males and females (Keisman et al., 2001). Dsx^F renders Wg enhancive, and Dpp repressive, towards *dac* in females. However, in males, Dsx^M facilitates the opposite (repression of *dac* by Wg, and activation of *dac* by Dpp (Keisman et al., 2001; Sanchez and Guerrero, 2001)). This gives rise to the overlapping expression of *dac* within the *dpp* domain in the A9 male genital disc, without encroaching on the expression domain of *wg* (Fig 4).

In the female genital disc, the combination of Wg activation of *dac*, and the Abd-B 'M' protein in A8, leads to activation of developmental factors required for female genital formation (Estrada et al., 2003; Estrada and Sanchez-Herrero, 2001; Keisman and Baker, 2001; Keisman et al., 2001; Sanchez and Guerrero, 2001). Male A8 also contains Abd-B 'M' protein, but due to the activity of Dsx^M in males, Wg represses *dac*. These sexually dimorphic "identity" inputs result in male A8 developing into an abdominal segment (see Fig 5). In female abdominal segment 9, Wg activates *dac* (due to Dsx^F), but Abd-B 'R' is expressed. Because of this combination, A9 develops into the paraovaria in females. In contrast, in male abdominal segment 9, Abd-B 'R' is present, and the repression of *dac* by Wg in parts of the disc controls the cascade of male genital differentiation, such as regulating the size and bristles of the claspers (Estrada et al., 2003; Estrada and Sanchez-Herrero, 2001; Keisman et al., 2001; Sanchez and Guerrero, 2001). Therefore, the combination of sex determination and homeotic genes, not only coordinates the differentiation of sex-specific structures (such as the claspers), but also pattern the genital disc by mediating the response of cells to key developmental pathways such Wg and Dpp.

Unfortunately, the activity of these factors during pupal development of the male genitalia is unknown. This is surprising, since it is during this stage (mainly over the first 50 hours after puparium formation (hr APF)), that major morphogenesis of the segments of the imaginal disc occurs (Fig 5).

During the first 4 hrs of puparium formation, the A8 segment of the disc is the first to evert, unfolding posteriorly (Fig 5) (Chatterjee et al., 2011; Keisman et al., 2001) (n.b. this segment contains the "repressed" female primordia in males, and will develop into an abdominal segment). Between 4 – 16 hrs, A10 everts upwards, developing the anal plate primordia (see AP in Fig 5). After this initial eversion, the AP primordia slowly develop in shape until 46 – 50 hr APF, when these structures appear to fully differentiate (including anal plate bristles etc., Fig 5) (Hagen et al., 2018; Glassford et al., 2015; Chatterjee et al., 2011; Keisman et al., 2001). In A9, a ridge begins to form between the developing clasper and lateral plate primordia between 30 – 34 hr APF (orange line, see CL and LP in Fig 5). This separation develops, and the increase in size until 46 hr APF, and then (as with the anal plate primordia), between 46 – 50 hr APF the claspers appear to fully differentiate (Hagen et al., 2018; Glassford et al., 2015). Between 42 hr - 50 hr APF, the posterior lobe first presents as a ridge and slowly develops into a fully outgrown lobe extending over the claspers (see blue line, PL in Fig 5) (Hagen et al., 2018; Glassford et al., 2015; Chatterjee et al., 2011; Keisman et al., 2001). Although I have coloured these compartments based on the described fate maps of the genital disc (Chatterjee et al., 2011; Epper, 1981; Keisman and Baker, 2001; Keisman et al., 2001), it is not known how (or if) these compartments are maintained during pupal metamorphosis.

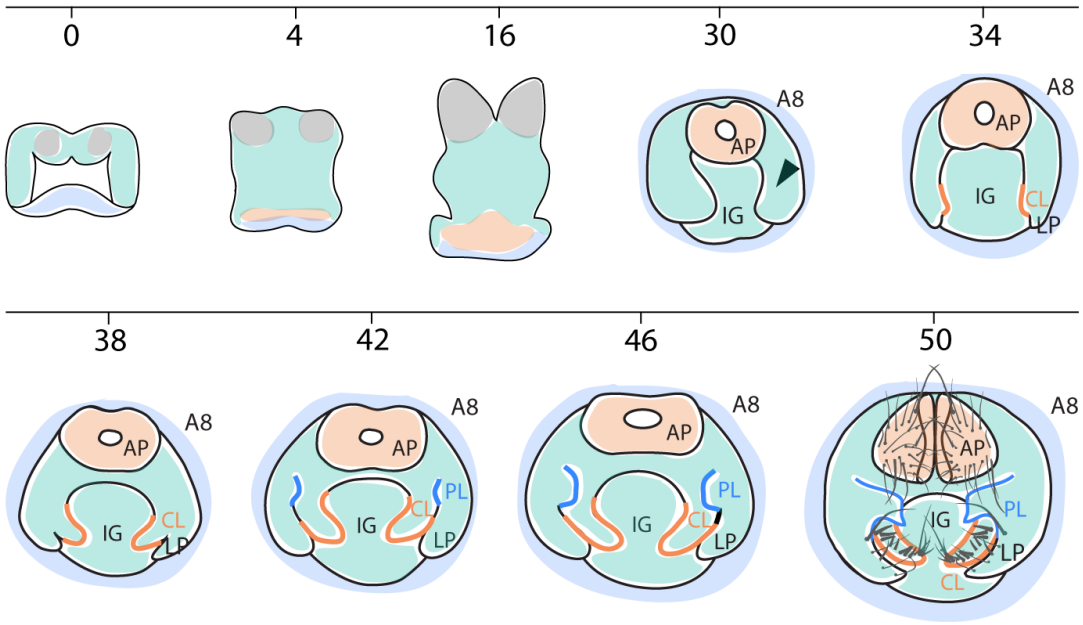


Figure 5. Schematic drawing of pupal development of *D. melanogaster* male genitalia between 0 – 50 hr APF, Based on previously described morphogenesis described (Hagen et al., 2018; Glassford et al., 2015; Chatterjee et al., 2011; Keisman and Baker, 2001; Keisman et al., 2001). Numbers indicate hr APF and upwards points dorsally. Colours correlate to cells derived from derived from A8 (blue), A9 (green) and A10 (orange) segments. Orange and blue highlight the development of the claspers (CL) and posterior lobes (PL), respectively. Grey indicates cells that will metamorphose out of the tissue to form the vas deferens and accessory glands (Chatterjee et al., 2011). A8 = abdominal segment 8, AP = anal plates, LP = lateral plates, PL = posterior lobes, CL = claspers.

1.7 Thesis aims

1. To improve the current mapping resolution (Tanaka et al., 2015) of clasper and posterior lobe evolution between *D. simulans* and *D. mauritiana* on the left arm of the third chromosome by:
    - Generating novel IL
    - Phenotyping and genotyping novel IL

2. To narrow down the number of positional candidate genes by:
    - Analysing which positional candidate genes are expressed during male genital development using gene expression datasets
    - Identifying which expressed, positional candidates have a role in genital development using RNAi gene knockdown in *D. melanogaster*
    - Examining which candidate genes are spatially and temporally expressed in a pattern consistent with a role in either clasper or posterior lobe evolution

3. To functionally validate promising candidate genes underlying genital differences between *D. simulans* and *D. mauritiana* by:
    - Generating and phenotyping reciprocal hemizygotes

4. To investigate the role of regulatory evolution on genital divergence
    - Examining the cis-regulatory landscape in candidate regions
    - Identifying and characterising candidate enhancers of genes underlying genital diversification
    - Analysing sequence variation in candidate enhancers between *Drosophila* species
    - Conducting transcription factor binding site analysis over variant loci

2 Chapter Two - Materials and methods

2.1 Mapping causative genomic regions underlying male genitalia size divergence

2.1.1 Fly husbandry and genotyping of novel ILs

We generated new recombinants from IL D11.01 and D08.04 (Tanaka et al., 2015), which contain *D. mauritiana* w^- DNA in the genomic location 3L: 7527144..15084689 Mb and 3L: 5911371..9167745 Mb (R2.02 *D. simulans*) respectively. Introgressed *D. mauritiana* DNA in IL D11.01 encompasses the candidate regions C1, C2, P2 and P3 whilst introgressed DNA in IL D08.04 contains candidate region P1 and C1 (Tanaka et al., 2015). To increase the resolution of these regions, we backcrossed virgin D11.01/*D. simulans* w^{501} heterozygous females, and virgin D08.04/*D. simulans* w^{501} heterozygous females to *D. simulans* w^{501} males. Novel recombinants were detected by selecting loss of the visible marker D1 (True et al., 1996; Tanaka et al., 2015) (indicated in Fig 3), restriction fragment length polymorphisms (RFLPs) and sequencing markers (see Supplementary File 1 for primers used). Novel introgression lines (Supplementary File 2) were then maintained as homozygous stocks.

2.1.2 Rearing of novel introgression line males

To minimize environmental variation in body size, male genitalia were phenotyped on males that had developed in controlled growth conditions. All males were progeny of 10 females and five males that were transferred every 48 hours, and allowed to develop at 25ºC in a 12 hours light - 12 hours dark cycle incubator unless otherwise stated. All adult males were allowed to mature on a standard cornmeal diet at 25 ºC for at least three days before collecting in 70% EtOH.

2.1.3 Dissection of the male genitalia

Where possible, two duplicates or three replicates of the IL were phenotyped alongside each other. Replicates and duplicates defined as ILs derived from the same recombination event (and therefore contain the same introgressed region of *D. mauritiana* DNA). The abdominal tip and T1 leg was dissected away for each fly in 70% EtOH, and transferred to Hoyer's dissection medium to dissolve the fatty tissue. Using entomological pins, the posterior lobes were dissected away from the claspers and anal plates. The claspers, posterior lobes and T1 tibia were mounted for at least 32 males for each line in Hoyer's medium for imaging.

2.1.4 Imaging and data collection

Images were taken using a Zeiss Axioplan light microscope at X250 magnification for the claspers and lobes and X160 for the T1 tibia, using a DFC300 camera. Clasper area, posterior lobe size and tibia length were measured manually using ImageJ (Schneider et al., 2012), and bristle number was recorded for each clasper. T1 tibia length was used as a proxy for body size, in order to confirm consistency in rearing conditions and to ensure genital differences are not a result of general differences in size. Most introgression lines showed no significant difference in T1 tibia length compared to *D. simulans* w^{501} (Supplementary File 4f), and since genitalia are hypoallometric (Coyne et al. 1991; Liu et al. 1996; Macdonald and Goldstein 1999; Eberhard 2009; Shingleton et al 2009; Masly et al 2011), the phenotypic data was not corrected for body size.

2.1.5 Statistical analysis

Phenotypic measurements and descriptive statistics for each introgression line are shown in Supplementary File 3 and 4a respectively. First, I tested for normality on the data generated from each introgression line using a Shapiro-Wilk test (Supplementary File 4b, non-normally distributed data shaded in purple). In general, most phenotypic measurements yielded normally

distributed data for each line, except for clasper bristle number, which was often non-normal in distribution (Supplementary File 4b).

Since many of my novel introgressed regions are represented by multiple lines, I first tested for significant differences between IL replicates / duplicates (see above for definition of replicates / duplicates).

If replicates were non-normally distributed (mostly clasper bristle number measurements), I conducted a Kruskal-Wallis test, followed by a Pairwise Wilcox test. Replicate ILs that contained normally distributed data were compared using an ANOVA followed by a Tukey's test. For introgressed regions represented by duplicate pairs that were non-normally distributed, I conducted a Pairwise Wilcox test, or for those that were normally distributed phenotypes were compared using a Welch Two-Sample t-test.

If the replicate/duplicate lines were not significantly different from each other, they were considered equivalent and the phenotypic measurements were pooled together (See Supplementary File 4b), replicate/duplicate that could not be merged are highlighted in blue for each trait, and were omitted from downstream mapping analysis, as reliable conclusions could not be drawn.

To assess the effect of the introgressed region, these pooled values were first compared against the parental w^{501} *D. simulans* line. For traits which yielded mostly normally distributed data (clasper size, posterior lobe, tibia

measurements), this was achieved using an ANOVA followed by a Dunnetts test. For those that appear mostly non-normal in distribution (clasper bristle number), a Kruskal-Wallis Dunn's test was performed. If the genital phenotype of an introgression line is significantly different from that of *D. simulans* w^{501}, there must be at least one locus in the introgressed region affecting the divergence of the trait. The lines, which contain the smallest amount of introgressed *D. mauritiana* DNA still able to significantly affect genital phenotype compared to *D. simulans*, were then compared against all overlapping introgression lines, in order to identify any differences in genital phenotype. For overlapping lines containing normally distributed phenotypic data, I conducted an ANOVA, whilst those with non-normally distributed data were compared using a Kruskal-Wallis test.

If there were no significant differences between lines overlapping with the smallest introgressed region of affect, then the minimal shared region of overlap can be used to define the newly resolved candidate region. If significant differences exist between the lines with the smallest introgressed region with an affect and the overlapping lines, this implies the existence of multiple causative loci. In order to determine where these loci can be mapped at the highest resolution, I conducted pairwise comparisons between these lines. For normally distributed data, lines were compared using a Tukey's test, whilst those with non-normally distributed data using a Pairwise Wilcox test. All statistics were conducted in RStudio (Team, 2015).

After determining the location of the resolved candidate regions, the phenotypic effect size of each region was calculated. By effect size, I refer to the proportion of phenotypic difference in clasper size between *D. simulans* and *D. mauritiana* the causative loci can explain. This value was calculated as a percentage, based on the average phenotype of ILs containing introgressed *D. mauritiana* DNA over each candidate region.

2.1.6 Fly husbandry and sample collection

Based on my gene expression analysis (GEA), or if the candidate region has a managble number of positional candidates, the developmental role of genes were tested using RNAi screen in *D. melanogaster*. UAS-RNAi lines for these genes were ordered from both Vienna *Drosophila* RNAi centre and TRiP lines from Bloomington stock centre (See Supplementary File 8b for stock numbers). UAS males of our candidate genes were crossed to NP6333–Gal4 ("NP6333") driver virgins (P{GawB}Pen^{NP6333}) (Chatterjee et al., 2011). NP6333 carries the transgene UAS-Dicer-2 P{UAS-Dcr-2.D}, and drives expression in the leg, wing and genital discs (Stieper et al., 2008). RNAi knockdown was conducted at either 25°C or 28°C (Supplementary File 8b), with identical rearing conditions, dissection and imaging method as described above. At least 15 males were measured for NP6333–Gal4 control, UAS control and RNAi knock-down lines. This screen was a joint endeavour between myself, K Tanaka, C Mendes and undergraduate students S Sankey, E White, S Williams and L Hill.

2.1.7 Statistical analysis

To assess the role of a gene in genitalia development, we compared the phenotype of genital structures of gene knock-downs against the respective NP6333 driver controls using a Dunnetts test. If gene knock-down phenotype differed significantly from the NP6333 driver control, I then assessed whether or not this significant effect is a result of genetic background (e.g. an effect of the UAS-parental phenotype), or reflects a role of the gene in genital development. To do this, I compared all three experimental males using an ANOVA. If this gave significant results, I then analysed where these differences arise using a Tukey's test, and only concluded genes have a developmental role in the genitalia if the RNAi knockdown males are significantly different in phenotype compared to both controls.

2.2 In situ hybridisation of candidate genes

2.2.1 Pupal collection and preparation

Staged male pupae, which had been incubated at 25°C, were flash-frozen on a metal heat block cooled to -80°C. The posterior third of the pupae were cut off and fixed in 4% paraformaldehyde (Sigma Aldrich)/PBT (Tween20 Sigma Aldrich) for 30 minutes, and washed in methanol and stored at -20'C. Before the *in situ*, the vitellin membranes were peeled away in ice-cold methanol.

2.2.2 RNA extraction, cDNA synthesis and Probe synthesis by PCR

Total RNA was extracted from *D. mauritiana* D1 and *D. simulans* w^{501} at a range of developmental time-points using Trizol extraction. A Quantitect Reverse Transcription Kit (Qiagen) was used to synthesize cDNA, in which gene-specific fragments were amplified separately for each species. Primers for *Cpr66D, Caps, tartan, CG11279* and *CG34429* were designed using Primer3 (http://primer3.ut.ee) with the addition of T7 linker sequences added to the 5' end of each primer. To FWD primers (sense) and REV primers (antisense) we added ggccgcgg and cccggggc respectively. Primers are as follows; *trn* (514bp) ATCGAGGAGCTGAATCTGGG and TCCAGGTTACCATTGTCGCT; *CG11279* (458bp) CATCTCGAAGTCGGTCAACA and AGGGTCACCTGACCATCAAT and *CG34429* (393bp) GGCTTTGGTATACCTGCAGAA and TGAGCAGGATGTGAAGCACT and *Caps* (520 bp) CCGGGAGAACTAACCTTCCA and CTTCATCCAGGCTGCTCAAC. Probes were labelled with 10x DIG labelling mix (Roche Diagnostics) and T7 RNA polymerase (Roche Diagnostics). Purple/dark blue staining was detected using alkaline phosphatase-conjugated anti-DIG antibody FAB fragments (Roche Diagnostics) and Nitro Blue tetrazolium/5-bromo-4-chloro-3-indolyl-phosphate NBT/BCIP (Roche Diagnostics).

2.2.3 Hybridisation protocol and imaging

In situ hybridizations were based on the Carroll lab "*Drosophila* abdominal in situ" protocol, which can be found at http://carroll.molbio.wisc.edu/methods.html with some modifications. For *D. simulans* and *D. melanogaster* in situ's, the time of fixation in steps 6 and 11 were adjusted to avoid excessive damage to the samples whilst still allowing the probe to penetrate. Samples were twice rinsed with glycine in order to inactivate the proteinase K digestion in step 8. For *D. mauritiana,* samples were incubated in hyb overnight, whilst in *D. simulans* and *D. melanogaster* this step was not necessary. The secondary structures of all probes were denatured by heating to 85°C for three minutes before transferring onto ice for 2 minutes. Samples were incubated with the probes overnight, and hybridised to pre-absorbed anti-DIG antibody for 1.5 hours to avoid background staining. Samples were then mounted in 80% glycerol and imaged using a Zeiss Axiozoom V16. Images were then prepared in Adobe Illustrator C6.

2.3 Functional validation and characterisation of *tartan*

2.3.1 The generation and phenotyping of trn reciprocal hemizygotes using CRISPR

We generated a double-stranded cut 121 bp into the first coding exon of *trn*, resulting in a frameshift mutation. For CRISPR primer design, see

Supplementary File 10. The cut was mediated by pCFD3 gRNA plasmid and pHD-DsRed-attp donor plasmid co-injected by The University of Cambridge Department of Genetics Fly Facility at 0.1ug/ul and 0.5ug/ul respectively, into *D. simulans* w^{501} and IL43, which endogenously express Cas9 from the X chromosome. These strains were generated by introgressing the X chromosome from *y w* p{nos-Cas9, w^{+}} in pBac{3XP3::EYFP,attp} sim 1087, which was kindly provided by David Stern (Stern et al., 2017). The cut site of two transgenic stocks were verified from each of the injected strains (see Chapter Five, Fig 25).

Transgenic *D. simulans* w^{501} and IL43 males heterozygous for the mutation were then crossed to non-injected IL43 and *D. simulans* w^{501} virgins respectively (Fig 26a). These crosses were amplified and the F1 males carrying the mutation (hemizygous for *trn* allele) were phenotyped for clasper size and bristle number as described previously (raw data and descriptive statistics can be found in Supplementary Files 11a and 11b).

In order to assess the effect of *trn* reciprocal hemizygotes to clasper phenotype, we first tested for normality and then conducted an ANOVA of clasper size and bristle number (Supplementary File 1c). If significant differences difference were detected, a Tukey's test was used to determine where these differences occur.

2.3.2 Phenotyping and statistical analysis of trn allelic dominance between D. simulans and D. mauritiana

D. simulans w^{501} males were crossed to IL 43 females (the smallest IL containing *D. mauritiana trn* alleles) to generate flies heterozygous for *trn*. Heterozygous males, *D. simulans* w^{501} males and IL 43 males were reared and clasper area measured (as described above, raw data and descriptive statistics can be found in Supplementary Files 11a and 11b). In RStudio (Team, 2015), I compared absolute differences in clasper size between IL 43 and heterozygous males, against the absolute differences between *D. simulans* w^{501} and heterozygous males using a Wilcox Rank Sum Test (Supplementary File 12), with the significance of the W statistic being evaluated by random permutation of trait values ($\alpha \leq 0.05$). If these datasets do not exhibit the same deviation in clasper size, one of these species-specific *trn* alleles is dominant over the other. I determined which is dominant by identifying which of the two comparisons gave rise to the smallest amount of difference (e.g. was most similar to the heterozygous clasper size phenotype).

2.4 Candidate *trn* regulatory elements and TF binding site analysis

2.4.1 Open chromatin analysis over candidate region C2

In order to predict the location of regulatory elements in C2, I utilised existing ATAC-Seq data generated by Kittlemann et al., (2018) from *D. melanogaster* OregonR T2 legs at 20 hr - 28 hr APF (Fig 2a) (see Supplementary File 13 for a full list of peaks and their co-ordinates in C2). By aligning these ATAC-Seq data against *D. melanogaster* R6.24, I then analysed which of the predicted peaks are also annotated in histone modification profiles of S2 and BG3 *Drosophila* cell lines (Flybase, (Kharchenko et al., 2011)). I then annotated which peaks likely overlap with promoter regions, and which contain candidate intronic or intergenic enhancers.

2.4.2 Fly husbandry, sample preparation and imaging of C2 candidate enhancers

In order to assess whether or not any of the candidate enhancer elements outlined above could potentially regulate *trn* in the male genitalia, I utilized *D. melanogaster* VT-Gal4 enhancer trap lines (VT030021 (#214361) and VT030010 (#210150) crossed to UAS-Stinger GFP (nuclear bound). The ability of these non-coding regions to drive expression in the developing genitalia was then assessed by dissection in PBS, 20-minute fixation in 4% PFA and DAPI stained at a range of stages. Images of the male genitalia were then acquired

using a confocal microscope at X40 objective, and stacks were projected using standard deviation Z-project in ImageJ software. The ability of the candidate regions to drive in other parts of the fly was then assessed using a Zeiss Axiozoom V16. Images were then prepared in Adobe Illustrator C6.

2.4.3 Sequence analysis of candidate tartan enhancer mcclaspertrn

The sequence of *mcclaspertrn* was compared between three *D. simulans* sequences (*D. simulans* 2.02 reference genomes from Flybase and generated from Popoolation DB (Pandey et al., 2011), *D. simulans* w^{501} lab strain (primers can be found in Supplementary File 1), three *D. mauritiana* sequences (reference genome *TAM16, D. mauritiana* SRA000000, and lab strain *D. mauritiana* D1), as well as *D. melanogaster* R6.24 and *D. sechellia* R1.03 (both from Flybase). Using these sequences, I determined variant nucleotides between *D. simulans* and *D. mauritiana,* and analysed to presence of these sites amongst the other species of the *D. melanogaster* subgroup. All alignments were performed in Benchling ((2018), from https://benchling.com). In order to determine which of these sites are polymorphic in *D. simulans* and *D. mauritiana* , I utilised an online resource developed by Alex Payne (Oxford Brookes University), built from the Popoolation database (Pandey et al., 2011). This resource extracts polymorphic sites in *D. simulans* and *D. mauritiana* strains, so that non-fixed differences could be detected.

2.4.4 Identification and TF analysis of mcclaspertrn_peak

The boundaries of mcclasper*trn*_peak was determined by comparing the region of overlap between the ATAC-Seq (Kittlemann et al., 2018) and S2 / BG3 histone modification profiles (Kharchenko et al., 2011) in mcclasper*trn*. The effect of variant nucleotides in mcclasper*trn*_peak between *D. simulans* and *D. mauritiana* on TF binding site affinity was assessed using the online resource Jasper (Khan et al., 2018). TF binding sites were only considered at the 70% sequence match threshold, and TF's whose binding affinity changed by < 5% due to variant nucleotides between species was recorded.

3 Chapter Three - Results

Mapping the genomic regions underlying male genitalia size evolution between *D. simulans* and *D. mauritiana*

As mentioned in the introduction, previous mapping efforts have identified several regions underlying male genital evolution between *D. simulans* and *D. mauritiana* on the left arm of the third chromosome (Tanaka et al., 2015). However, while some regions are already quite small and amenable to functional validation (e.g. C1 only contains 52 annotated genes in *D. melanogaster*), most regions are large (e.g. C2 contains 312 genes), and requires further work to narrow down the list of positional candidate genes (Tanaka et al., 2015). In order to increase the mapping resolution of the candidate regions previously identified in Tanaka et al (2015) (Introduction, Fig 3), we generated new introgression lines (ILs) in the genomic region between 3L: 5911371-15084689 Mb (Supplementary File 2, Fig 6b) by backcrossing IL D08.04 and D11.01 (Tanaka et al. 2015, Fig 3) to the parental w^{501} *D. simulans* strain (see Methods for details).

In order to determine which introgressed *D. mauritiana* DNA is able to affect clasper and/or posterior lobe morphological traits, I first compared each novel IL against the parental *D. simulans* w^{501} strain (see Supplementary File 2

for raw phenotypic data and Supplementary file 3 for details of these comparisons). Since the background genome of each IL is identical to that of *D. simulans* w^{501} (Tanaka et al., 2015), this analysis directly tests which regions of introgressed *D. mauritiana DNA* contains variation able to affect genital morphology. The term "minimal IL" is used to describe ILs, which contain the smallest amount of DNA able to affect genital morphology, and therefore contains at least one causative loci. The genital morphology of the minimal IL can then be compared against other lines that overlap in their introgressed DNA, either to refine the candidate region in the minimal IL, or to identify other regions not contained by the minimal IL (see Methods for details).

3.1 Candidate regions for clasper size also affect clasper bristle number

Out of the 18 new IL*s* generated, only 7 had no affect on clasper morphology compared to *D. simulans* w^{501} (see grey bars, Fig 6b). Therefore, the regions 3L: 12277961 - 12911597 and 3L:14402074 - 15084689 were excluded from our map. All lines with an effect on clasper size (Dunnett's test, $p < 0.05$), also affected clasper bristle number (Dunn's test, $p < 0.05$ (clasper bristle number) (bars containing orange, Fig 6b and Supplementary File 4c and 4d respectively). This corroborates findings by Tanaka et al (2015), who consistently mapped regions underlying clasper size and bristle number differences to the same genomic locations.

Four minimal IL were identified across this region of 3L (orange shaded bars, Fig 6b). Three of these (D21.43e, 43 and 16.14) overlap with genomic areas previously predicted to be candidate regions underlying clasper size and bristle number variation (C1 and C2, Fig 6a and 6b), whilst one (IL 6) does not overlap with any previously predicted clasper candidate regions (left-most orange bar, Fig 6a and 6b)

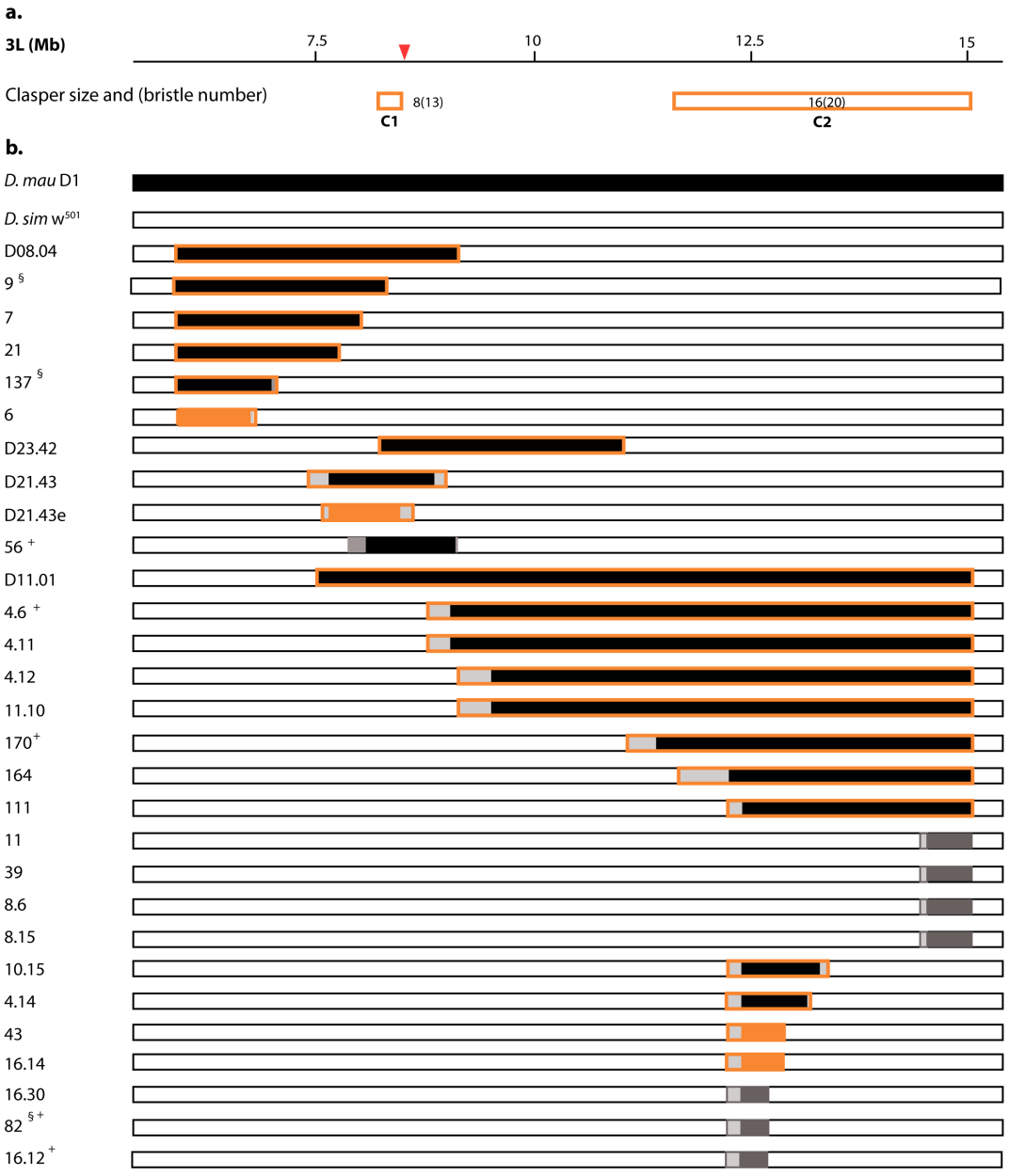


Figure 6. Comparision of novel IL clasper size and bristle number against *D. simulans* w^{501}. (a) Current mapping resolution determined by Tanaka et al., (2015) for both clasper size and bristle number divergence (orange shade bars). Candidate region names are described below each bar, with effect sizes labelled for each region (rounded to the nearest whole number). Position along 3L is indicted in Megabases (Mb), with the P element insertion "D1" shown as a red triangle (see Methods). (b) Novel introgression lines generated between *D. simulans* and *D. mauritiana* on chromosome 3L and their effect on clasper size and clasper bristle number phenotype compared to *D. simulans* w^{501}. Lines that were omitted from statistical analysis due to significant differences between duplicates are labelled with § for clasper size and + for clasper bristle number (Supplementary File 4b). Black bars with orange outlines indicate lines whose clasper size and bristle number are significantly different from *D. simulans* w^{501} (Dunnetts test, $p < 0.05$ (clasper size), Dunn's test, $p < 0.05$ (clasper

bristle number) Supplementary File 4c and 4d), and orange bars indicate minimal IL. Grey bars indicate lines not significantly different from *D. simulans* w^{501} in clasper size (Dunnetts test, $p > 0.05$ (clasper size), Dunn's test, $p > 0.05$ (clasper bristle number), Supplementary File 4c and 4d). Black bars indicate *D. mauritiana* DNA, white bars indicate *D. simulans* DNA, and light grey boxes outline regions of unknown break points (See Supplementary File 4 for introgressed region breakpoint mapping).

3.1.1 Clasper size and bristle number candidate region C0

Minimal IL 6 contains introgressed *D. mauritiana* DNA that generates significantly different sized claspers (Fig 6b, Dunnetts test, $p < 0.001$, Supplementary File 4c), and number of bristles (Fig 6b, Dunn's test, $p < 0.01$, Supplementary File 4d), compared to *D. simulans* w^{501} (Fig 6b). As can be seen in Fig 7a and 7b, *D. mauritiana* alleles in this region significantly increase the size of the claspers and the number of bristles. However, minimal IL 6 does not overlap with any other previously predicted clasper size or clasper bristle number candidate regions (Fig 6a and 6b), and so could represent a novel clasper candidate region "C0".

The introgressed *D. mauritiana* DNA contained by ILs D08.04, 9, 7, 21 and 137 overlap with that of minimal IL 6 (Fig 7c), and also contain significantly more bristles (orange outline Fig 15b and Fig 11b, Dunn's test, $p < 0.01$) and larger claspers (orange outline Fig 15b and Fig 11a, Dunnetts test, $p < 0.001$) compared to *D. simulans* w^{501}. In order to determine whether this effect on clasper morphology is solely attributed to C0, and not due to additional causative regions in the right-hand breakpoints in which these lines differ (Fig

7c), I compared clasper size and bristle number of these lines against minimal IL 6. This indicated no significant differences in clasper size (grey line Fig 7a, Tukey's test, $p > 0.05$) or bristle number (grey line Fig 7b, Wilcoxon rank sum test, $p > 0.05$) between any of these lines and IL 6 (Supplementary file 5a and 5b). Therefore, I conclude that the only causative clasper size and bristle number region detected in these ILs is C0, which is defined by the boundaries of minimal IL 6 (Fig 7c).

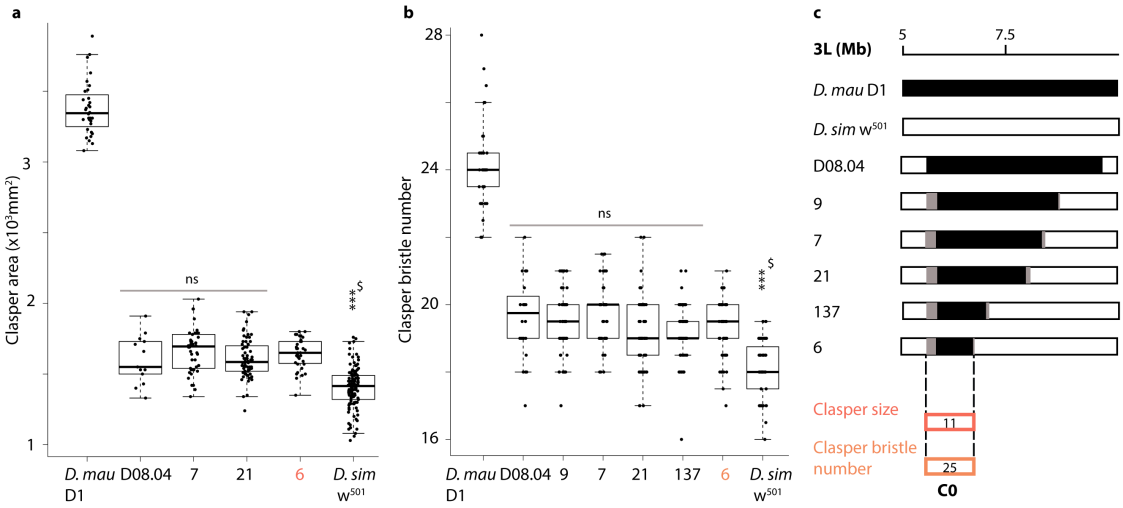


Figure 7. Mapping and phenotypic effect of C0 on clasper size and bristle number – comparisons between IL 6 and overlapping ILs. (a) IL 6 males have significantly larger claspers than *D. simulans w*^{501} ($ Dunnetts test, $p < 0.001$), but the same sized claspers as all overlapping ILs (IL D08.04, 7 and 21, Tukey's test, $p > 0.05$). (b) IL 6 males have significantly more clasper bristles than *D. simulans w*^{501} ($ Dunn's test, $p < 0.001$), but the same number of clasper bristles as all overlapping ILs (IL D08.04, 0, 7, 21, 137, Wilcoxon rank sum test, $p > 0.05$). Asterisks indicate significant comparisions in each statistical test where $p < 0.001$ *** and $p > 0.05$ = "ns" (Supplementary File 4c, 4d, 5a and 5b). Boxes indicate the range, upper and lower quartiles and median for each sample. (c) Genomic mapping of C0. Based on statistical analysis (a & b), I determine candidate region C0 to lie in the boundaries of IL 6. Percentage effect size for clasper size (dark orange) and clasper bristle number (light orange) divergence is indicated for C0 and has been rounded to the nearest whole number.

Black bars indicate *D. mauritiana* DNA, white bars indicate *D. simulans* DNA, and grey boxes outline regions of unknown break points.

Therefore, C0 lies between max (min) 3L: 5903109..6852222 (3L: 6136507..6806943) (Fig 7c). At the current resolution, this region spans 949 kb - 670 kb, and contains 99 - 35 protein-coding genes (Supplementary File 6a). Based on the phenotypic effect of lines determined to contain C0 only (see above), I calculate that C0 is able to explain 10.8% of clasper size differences, and 24.8% of clasper bristle number differences between *D. simulans* and *D. mauritiana* (Fig 7c, Table 1).

3.1.2 Clasper size and bristle number candidate region C1

IL 9 is the only novel line that contains introgressed DNA that breaks within candidate region C1 (Tanaka et al., 2015), but unfortunately was omitted from mapping analysis due to consistent significant differences arising between IL 9 duplicates (Supplementary File 4b). Instead, I use this opportunity to re-analyse ILs to confirm the location of C1 (Tanaka et al, 2015).

Minimal IL D21.43e overlaps with previously predicted candidate region C1 (Fig 6a and 6b, Tanaka et al., 2015), and contains larger sized claspers (Fig 8a, Dunnetts test, $p < 0.001$, Supplementary File 4c), and more bristles (Fig 8b, Dunn's test, $p < 0.001$, Supplementary File 4d) than *D. simulans* w^{501}.

In order to attempt to improve the resolution of C1, I compared the clasper morphology of all other lines that contain introgressed *D. mauritiana* DNA that overlaps with that of minimal IL D21.43e (IL D08.04, 7, 21, D23.42, D21.43, IL 56 and D11.01) (Fig 8a).

The only significant comparison detected was between minimal IL D21.43e and IL D11.01 for both clasper size (Fig 8a, Tukey's test, $p < 0.001$), and bristle number (Fig 8b, Wilcoxon rank sum test, $p < 0.001$). This indicates, as was previously predicted (Tanaka et al., 2015), an additional clasper candidate region "C2" lies between the right-hand boundaries of D21.43e and D11.01 (Fig 8c).

Since the minimal IL containing C1 is not significantly different in clasper size (Fig 8a, Tukey's test, $p > 0.05$) or bristle number (Fig 8b, Wilcoxon rank sum test, $p > 0.05$) compared to D08.04, 7, 21, D23.42, D21.43 and IL 56, C1 can be refined to the region of *D. mauritiana* DNA shared by all of these lines (Fig 8c).

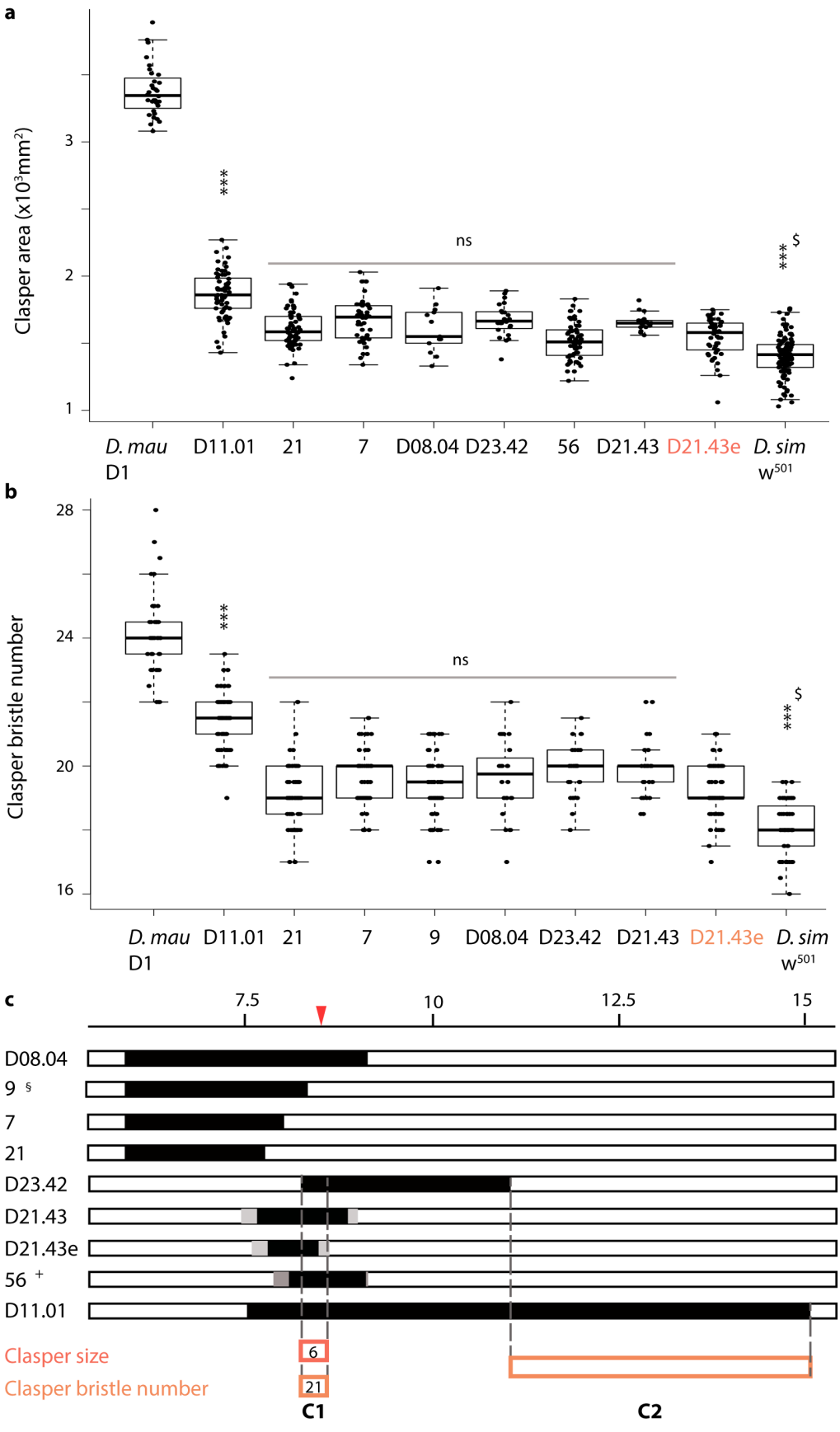

a
Clasper area (x10³mm²)
3
2
1
***
ns
***
$
D. mau D1
D11.01
21
7
D08.04
D23.42
56
D21.43
D21.43e
D. sim w501
b
Clasper bristle number
28
24
20
16
***
ns
***
$
D. mau D1
D11.01
21
7
9
D08.04
D23.42
D21.43
D21.43e
D. sim w501
c
7.5
10
12.5
15
D08.04
9 §
7
21
D23.42
D21.43
D21.43e
56 +
D11.01
Clasper size
Clasper bristle number
6
21
C1
C2

Figure 8. Mapping and phenotypic effect of C1 on clasper size (a) and bristle number (b) – compairison between D21.43e (highlighted in orange) and overlapping ILs. IL D21.43e contains larger claspers (a) and more brisles (b) than *D. simulans* w^{501} ($ Dunnetts test $p < 0.001$ for clasper size, and Dunn's test for clasper bristle number). D21.43e contains the same size claspers (a) (Tukey's test, $p > 0.05$) and bristle numbers (b) (Wilcoxon rank sum test, $p > 0.05$) as IL 21, 7, D08.04, D23.42, 56, D21.43 and 9 (9 included in bristle number analysis only). This indicates candidate region C1 lies in the region of overlap between these lines (Fig 8c). IL D11.01 contain significantly larger claspers (a) (Tukey's test, $p < 0.001$), and signficiantly more bristles (b) (Wilcoxon rank sum test, $p < 0.001$) than D21.43e. This indicates the presence of candidate region C2 between the right-hand break points of D23.42 and D11.01 (Fig 8c). Asterisks indicate significance, where $p < 0.001$ *** and $p > 0.05$ = "ns" in both statistical tests. (c) Genomic mapping of clasper size and bristle number candidate region C1. C1 is mapped between the overlapping region of IL D23.42, D21.43, D21.43e, which at the smallest resolution is between the left-hand break point of D23.42 and the right-hand break point of D21.43e. C2 is provisionally mapped, to lie between the right-hand boundaries of IL D23.42 and D11.01. Black bars indicate *D. mauritiana* DNA, white bars indicate *D. simulans* DNA, and grey boxes outline regions of unknown break points. Percentage effect size for clasper size (dark orange) and clasper bristle number (light orange) divergence is indicated for C1 is inidcated and has been rounded to the nearest whole number.

Therefore, IL D08.04 contains introgressed *D. mauritiana* DNA over both C0 and C1 clasper candidate regions, as overlaps entirely with the introgressed *D. mauritiana* DNA of D21.43e (Fig 6b) and IL 6 (Fig 7c). Despite this, IL D08.04 is not significantly different in clasper size or bristle number compared to IL 6 (C0, see above), or IL D21.43e (C1) (Tukey's test, $p > 0.05$, Supplementary File 5a and Wilcoxon rank sum test, $p > 0.05$, Supplementary File 5b), indicating that loci in C0 and C1 do not act additively towards clasper morphology. Therefore, although some of the lines containing C0 also contain potentially useful break points for refining C1 (e.g. IL 9, 7, 21), we are unable to utilise these for defining C1 boundaries (as the effects of C1 and C0 cannot be distinguished).

Instead, I have mapped candidate region C1 to the overlapping region contained by ILs thought to contain C1 only (minimal IL D21.43e, D21.43, D23.42 and 56 (IL 56 used in clasper size analysis only, Supplementary file 4b)). The smallest overlapping region of these lines lies between the left-most break point of IL D23.42 and the right-most break point of D21.43e (Fig 8c). Therefore, C1 has been mapped to the same genomic location as previous studies (Tanaka et al 2015); to a region between 3L: 8253548..8699816 (446kb max) and 3L: 8257826..8556334 (299 kb min). According to my phenotypic analysis, C1 contains variation accounting for 6% of clasper size differences, and 21% of clasper bristle number differences between the species (versus the previously predicted 8% and 13% for clasper size and bristle number respectively, Tanaka et al 2015). C1 therefore contains 39 - 57 protein coding genes in *D. melanogaster R6.24* (Table 1, Supplementary File 6b).

3.1.3 Clasper size and bristle number candidate region C2

Previously, candidate region C2 was mapped between the boundaries of D20.37 and D11.01 (a region of 3.49 Mb, between 3L: 11597867..15084689, Fig 3). By comparing clasper size of novel ILs to *D. simulans* w^{501}, I have identified two minimal IL that overlap with this region (43 and 16.14, Fig 6b, Supplementary File 4c and 4d).

As can be seen in Supplementary File 2 and Fig 6b, the introgressed *D. mauritiana* DNA within these two minimal IL lies in the same boundaries (up to current resolution), and this region is also contained by many other ILs (IL D11.01, 4.6, 4.11, 4.12, 11.10, 170, 164, 111, 10.14, 4.14, 16.30 and 16.12).

A comparison between these two minimal ILs and these other lines revealed many interesting results (Supplementary File 5a and 5b). The significant affect of clasper size and bristle number detected in the two minimal ILs lines is likely attributed to the same causative loci, as these lines are not significantly different in clasper size (Tukey's test, $p > 0.05$) or clasper bristle number (Wilcoxon rank sum test, $p > 0.05$). Therefore, candidate region "C2" can be provisionally mapped to their region of overlap, between 3L: 12277961..12911531.

However, as previously mentioned, the region between 3L: 12277961-12911597 can be excluded from our map, since IL 16.30 and 16.12 are not significantly different in clasper size or bristle number compared to *D. simulans* w^{501} (Fig 6b). Moreover, my analysis indicates that both minimal ILs contain significantly larger claspers (Tukey's test, $p < 0.001$, Fig 9a), and also significantly more bristles (Wilcoxon rank sum test, $p < 0.001$, Fig 9b), than these lines. Since the minimal ILs only differ from IL 16.30 and 16.12 in the right-hand break point (Fig 9d), candidate region C2 can be refined to this region max (min) 3L: 12734279..12911597 (3L: 12737959.. 12911531), region of 178 – 173

kb, and contains between 8 and 9 protein – coding genes (Supplementary File 6c).

In order to identify any other clasper candidate regions in the remainder of this area on 3L, I analyzed the remaining pairwise comparisons of clasper size and bristle number between the minimal ILs and the other overlapping lines (IL D11.01, 4.6, 4.11, 4.12, 11.10, 170, 164, 111, 10.14 and 4.14 - which as can be seen in Fig 6b, are all significantly different in clasper morphology compared to *D. simulans* w^{501}).

Consistently, D11.01 was significantly different from the minimal IL for both clasper traits; containing significantly larger claspers (Fig 9a, Tukey's test, $p < 0.001$, Supplementary File 5a) and more bristle number (Fig 9b, Wilcoxon rank sum test, $p < 0.001$, Supplementary File 5b). This is likely due to the affect of variation in C1, for which D11.01 is the only one of these lines that contains *D. mauritiana* alleles (Fig 8c). This analysis illustrates that (in contrast to my observations between IL C1 and C0), the causative loci within C1 and C2 appear to interact additively to regulate clasper morphology.

In contrast to clasper size analysis however, IL 164 and 10.15 are different in clasper bristle number compared to the minimal IL (Fig 9b, Wilcoxon rank sum test, Supplementary File 5b). This is curious, since IL 164 shares most of it's introgressed region with IL 111, 11.10 and 4.12 (only differing with these lines on the left-hand break point (Fig 9d)), but these three

ILs contain the same number of clasper bristles at the minimal ILs (Fig 9b, Wilcoxon rank sum test, $p > 0.05$, Supplementary File 5b). In order to test for additional candidate regions in the left-hand break point (which might explain how IL 164 contains more bristles than the minimal ILs 43 and 16.14), I compared clasper bristle number phenotype between these lines. This analysis did not give rise to significant differences in clasper bristle number (Wilcoxon rank sum test, $p > 0.05$, Supplementary File 5b); and therefore, I cannot predict any additional candidate regions in IL164.

Similarly, IL 111 and 4.14 only differ in introgressed DNA compared to IL 10.15 on the right-hand break-point (Fig 9d) (and these lines contain the same number of bristles as IL 43 and 16.14 (Fig 9b)). Comparison of clasper bristle number between IL 111, 4.14 and IL 10.15 gave rise to no significant differences (Wilcoxon rank sum test, $p > 0.05$, Supplementary File 5b), which therefore negates the possibility of additional candidate regions within the right-hand break point of IL 10.15.

Since I am unable to detect any other clasper candidate regions in the remainder of 3L contained by these lines, I predict these lines only contain candidate region C2 (except for D11.01). Based on the affect of these lines, I calculate C2 accounts for 16.4% of differences in clasper size, and 33.5% of differences in clasper bristle number between *D. simulans* and *D. mauritiana* (Fig 9d) (Supplementary File 5c & Table 1).

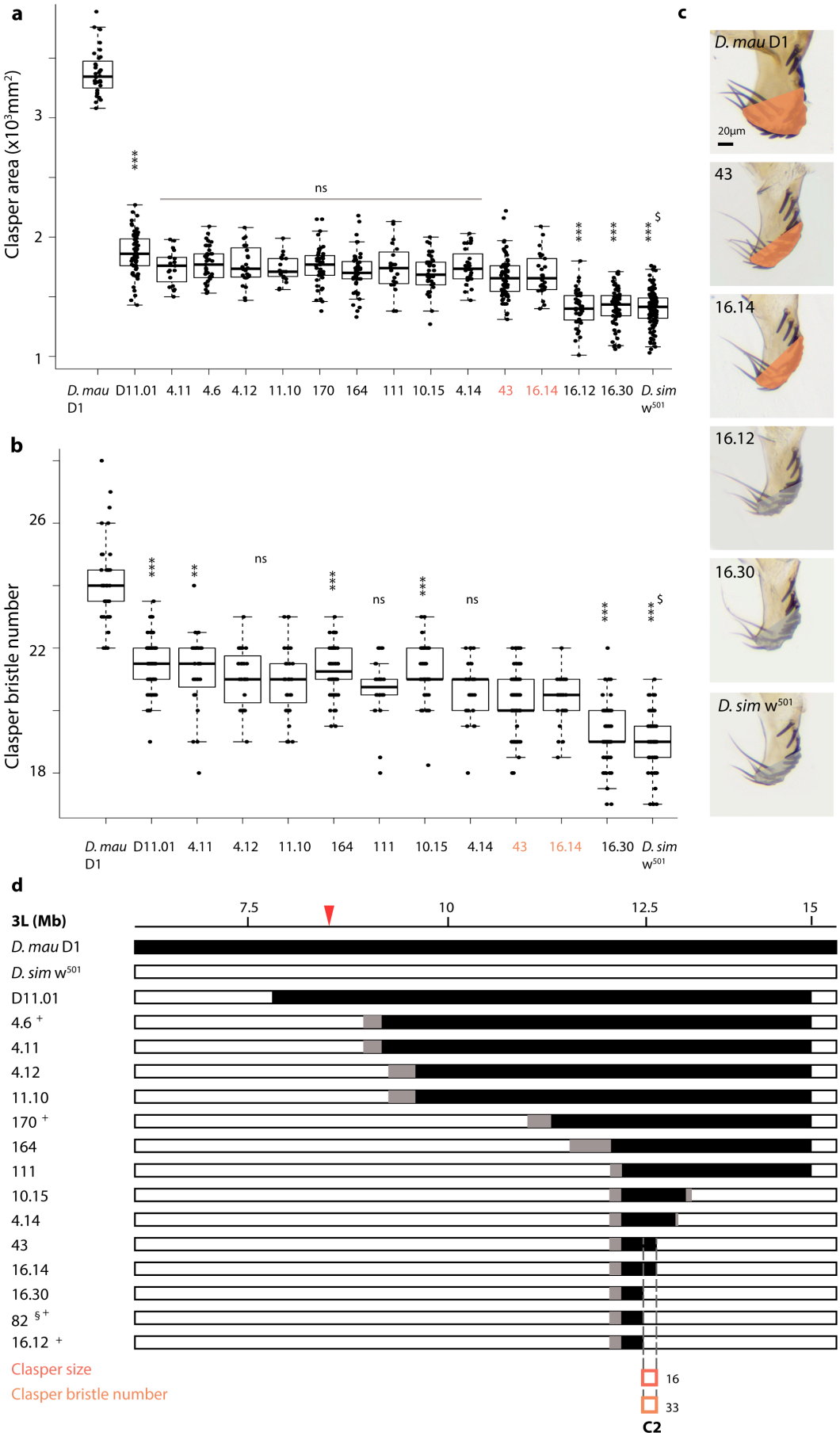

a
Clasper area (x10³mm²)
3
2
1
***
ns
***
***
***
$
D. mau D1
D11.01
4.11
4.6
4.12
11.10
170
164
111
10.15
4.14
43
16.14
16.12
16.30
D. sim w501
b
Clasper bristle number
26
22
18
***
**
ns
***
ns
***
ns
***
***
$
D. mau D1
D11.01
4.11
4.12
11.10
164
111
10.15
4.14
43
16.14
16.30
D. sim w501
c
D. mau D1
20µm
43
16.14
16.12
16.30
D. sim w501
d
3L (Mb)
7.5
10
12.5
15
D. mau D1
D. sim w501
D11.01
4.6 +
4.11
4.12
11.10
170 +
164
111
10.15
4.14
43
16.14
16.30
82 §+
16.12 +
Clasper size
Clasper bristle number
16
33
C2

Figure 9. Mapping and phenotypic effect of C2 - comparision of IL 16.14 and 43 against overlapping ILs. **(a)** IL D11.01 males have signficantly larger claspers than ILs 43 and 16.14 (Tukey's test $p < 0.001$), whilst IL 16.12, 16.30 and *D. simulans* $w^{501\$}$ have significantly smaller claspers (Tukey's test $p < 0.001$ and Dunnetts test$^{\$}$ $p < 0.001$) (Supplementary File 4c and 5a). No other overlapping ILs are significantly different in clasper size compared to IL 16.14 and 43 (see ns, Tukey's test $p > 0.05$). **(b)** IL D11.01 males have signficantly more clasper bristles than ILs 43 and 16.14 (Wilcoxon rank sum test $p < 0.001$), whilst IL 16.12, 16.30 and *D. simulans* $w^{501\$}$ have significantly fewer clasper bristles (Wilcoxon rank sum test, $p < 0.001$ and Dunn's test$^{\$}$ $p < 0.001$) (Supplementary File 4d and 5b). IL 164, 10.15 and 4.11 (in the case of IL 43 only) also contain significantly more bristles than IL 16.14 and 43, although no additional clasper bristle region was mapped here (Fig 9c). Boxes indicate the range, upper and lower quartiles and median for each sample. $^{\$}$ indicates Dunnetts test (clasper size) or Dunn's test (clasper bristle number) comparisions between 16.14 and 43 against *D. simulans* w^{501}, with all other comparisions derived from Tukey's pairwise analysis (clasper size) or Wilcoxon rank sum test (clasper bristle number). Asterisks indicate significance, where $p <$ 0.001 ***, $p < 0.01$** and $p > 0.05$ = "ns" in both statistical tests. **(c)** Images of the affect of variation in C2 on clasper morphology (shading indicates area measured). **(d)** Genomic mapping of C2. Black bars indicate *D. mauritiana* DNA, white bars indicate *D. simulans* DNA, and grey boxes outline regions of unknown break points. Percentage effect size for clasper size (dark orange) and clasper bristle number (light orange) divergence is indicated for C2 is inidcated and has been rounded to the nearest whole number.

3.2 Posterior lobe size candidate regions

Similarly to the analysis conducted on clasper size and bristle number phenotype of novel ILs (Fig 6b), I compared posterior lobe area measurements of each novel IL against *D. simulans* w^{501} (Fig 10b, Supplementary File 4e). This analysis indicated that most introgressed *D. mauritiana* DNA is able to significantly alter posterior lobe size compared to *D. simulans* w^{501} (blue bars or blue outlined bars in Fig 10b (Dunnetts test, $p < 0.05$, Supplementary File 4e), except that contained by IL D21.43, D21.43e and 8.15 (dark grey bars Fig 10b, Dunnetts test, $p > 0.05$, Supplementary File 4e)). This therefore allows the

regions between 3L: 7441137..9055135 and 3L: 14402074..15084689 to be excluded from our mapping. As with the clasper phenotypic analysis, minimal IL able to affect posterior lobe size were identified (shaded blue bars, Fig 10b).

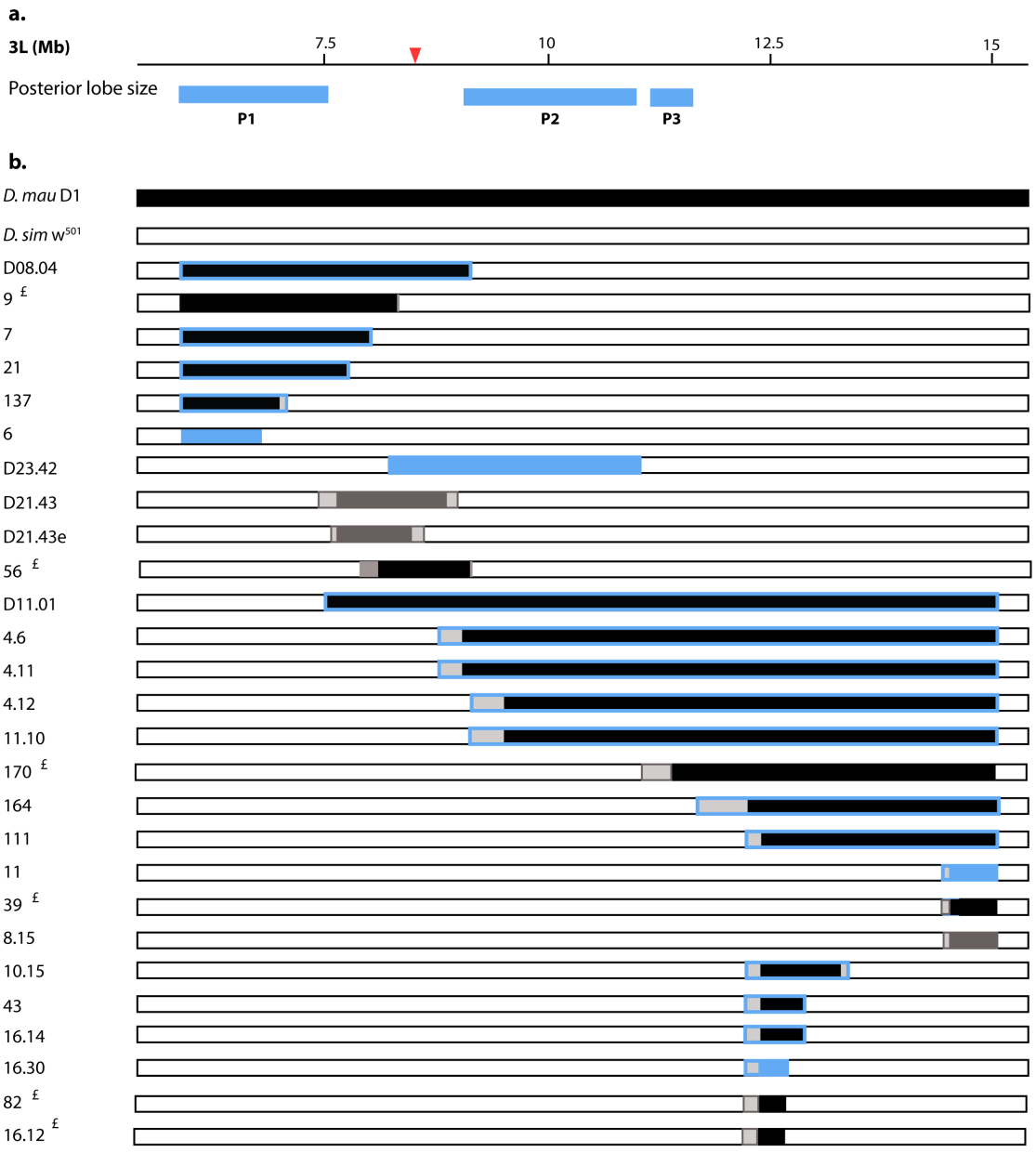


Figure 10. Comparision of novel IL posterior lobe size against *D. simulans w*^{501} (a) Current mapping resolution determined by Tanaka et al (2015) for posterior lobe size (blue bars) divergence. Candidate region names are described below each bar. Position along 3L is indicted in Megabases (Mb), with the P element insertion "D1" shown as a red triangle (see Methods). (b) Novel

introgression lines generated and their affect on posterior lobe size phenotype compared to *D. simulans* w^{501}. £ indicates lines that were ommitted from posetrior lobe analysis, due to significant differences between duplicates (Supplementary File 5b). Black bars with blue outlines indicate lines whose posterior lobe size are significantly different from *D. simulans* w^{501} (Dunnetts test, $p < 0.05$, Supplementary File 5e). Blue shaded bars indicate the ILs that contain the smallest, non-overlapping introgressed regions that significantly affect posterior lobe size compared to *D. simulans* w^{501} (Dunnetts test, $p < 0.05$, Supplementary File 5e). Grey bars indicate lines that do not significantly differ from *D. simulans* w^{501} in posterior lobe size (Dunnetts test, $p > 0.05$, Supplementary File 5e). Black bars indicate *D. mauritiana* DNA, white bars indicate *D. simulans* DNA, and light grey boxes outline regions of unknown break points (See Supplementary File 5 for breakpoint mapping).

3.2.1 Posterior lobe size candidate region P1

One of these minimal IL, IL 6, lies within previously predicted posterior lobe candidate region "P1" (Fig 10a and 10b) (which was mapped between 3L: 5911371..7527144, a region of 1.8 Mb). This IL contains 949 kb of introgressed *D. mauritiana* DNA (between 3L: 5911371..6852222 (Supplementary File 2)), with 35 – 99 protein-coding genes (Supplementary File 5a), and allows for substantial reduction of the size of P1.

Many other ILs with significantly different posterior lobes compared to *D. simulans* w^{501} also contain *D. mauritiana* DNA over this refined P1 region (IL D08.04, 7, 21 and 137, Fig 10b). However, it appears variation in P1 is able to explain all of these effects (as are the same in size as minimal IL 6, Fig 11a, Tukey's test, $p > 0.05$), except for that detected in D08.04, which has smaller posterior lobes compared to minimal IL 6 (Fig 11a, Tukey's test, $p < 0.001$). Since these lines only differ in their right-hand break point of introgressed DNA

(Supplementary File 2), this suggests that IL D08.04 contains an additional candidate region P2 in the right-hand region (Fig 11b). Refinement of candidate region P2 will continue in the section below. Interestingly therefore, P1 and P2 appear to interact additively towards posterior lobe phenotype.

Based on the phenotypic effect of lines containing P1 only (IL 6, 137, 21 and 7), I calculate that this region explains 3.7% of posterior lobe size differences between *D. simulans* and *D. mauritiana (*Table 1).

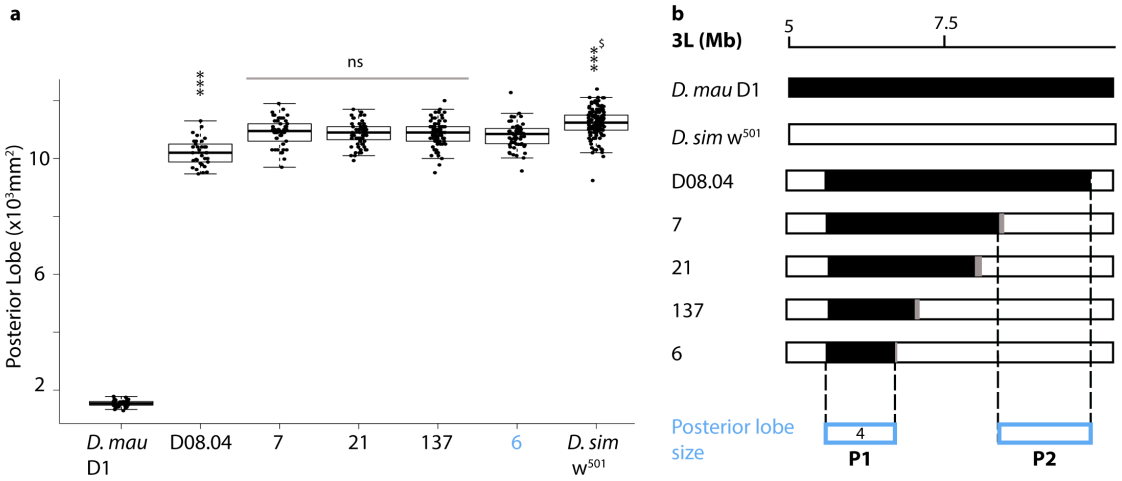


Figure 11. Mapping and phenotypic effect of posterior lobe size candidate region P1 – comparison between IL 6 (highlighted in blue in (a)) and overlapping ILs. (a) IL 6 contains significantly smaller posetrior lobes compared to *D. simulans w*^{501} ($ Dunnetts test, $p < 0.001$). All overlapping ILs, except D08.04, contain the same sized posterior lobes as IL 6 (Tukey's test, $p > 0.05$). IL D08.04 contain signficantly smaller lobes than IL 6 (Tukey's test, $p < 0.001$). This analysis indicates IL 6, 137, 21, 7 and D08.04 share candidate region P1, but D08.04 also contains additional region P2 (see (b)). Asterisks indicate significance, where $p < 0.001$ *** and $p > 0.05$ = "ns" in both statistical tests. Boxes indicate the range, upper and lower quartiles and median for each sample. (b) Genomic mapping of P1 and provisional mapping of P2. Candidate region P1 can be mapped between the left and right hand boundaries of IL 6. Candidate region P2 is provisionally mapped between the right-hand boundaries of IL 7 and D08.04. Black bars indicate *D. mauritiana* DNA, white bars indicate *D.*

simulans DNA, and grey boxes outline regions of unknown break points. Percentage effect size for P1 on posterior lobe size is indicated and has been rounded to the nearest whole number.

3.2.2 Posterior lobe size candidate region P2 and P3

Minimal IL D23.42 overlaps with the previous mapped candidate region P2 (Tanaka et al., 2015, Fig 10a and 10b), and contains variation that confers significantly smaller claspers compared to *D. simulans* w^{501} (Fig 12a, $^{\$}$Dunnetts test, $p < 0.001$). This line spans the region between 3L: 8253548..11084746, a region of 2.8 Mb (Tanaka et al., 2015).

However, as previously described, a substantial part of this region can be excluded (between 3L: 7441137..8903265), since neither D21.43 or D21.43e contain variation that changes the size of the lobes compared to *D. simulans* w^{501} (grey bars, Fig 10b). Therefore, P2 can be provisionally reduced to the region between 3L: 8903265.. 11084746 (2 Mb) (between the right-most breakpoints of IL D21.43 and D23.42).

Many IL that are significantly different in posterior lobe size compared to *D. simulans* w^{501} also contain introgressed DNA that breaks in, or overlaps with this region (see blue outlines, IL D08.04, 7, D11.01, 4.6, 4.11, 4.12, 11.10 Fig 10b). In order to potentially refine candidate region P2 using these different breakpoints (or alternatively identify other posterior lobe regions), I compared

the posterior lobe size of minimal IL D23.42 against all these IL, as well as D21.43 and D21.43e (Fig 12a).

Both IL D08.04 and 11.10 are statistically the same as the minimal IL D23.42 in posterior lobe size (Fig 12a, Tukey's test, $p > 0.05$). In contrast, IL's D21.43, D21.43e, D11.01, 4.6, 4.11, 4.12 and 7 are not (Fig 12a, Tukey's test, $p < 0.001$). Based on these results, we could assume that there are regions of *D. mauritiana* DNA shared with the minimal IL D23.42, D08.04 and IL 11.10, but not with D21.43, D21.43e, D11.01, 4.6, 4.11, 4.12 or 7. However, as can be seen in Fig 12b, no such genomic region exists. In order to explain these results, I conclude there must be more than one causative loci in this region of 3L, and that these loci not shared by all the IL. Therefore, the provisionally mapped P2 (between 3L: 8903265.. 11084746) probably contains both "P2" and "P3", and will now be referred to as "provisional P2/P3".

During P1 mapping, I detected differences in posterior lobe size between IL D08.04 and 7 (with D08.04 containing smaller lobes, as can be seen in Fig 11a). The region of difference in *D. mauritiana* DNA between these lines (3L: 8096301..9167745), overlaps with provisional P2/P3, between 3L: 8903265.. 9167745. Moreover, comparison between IL D11.01 and IL 4.6, 4.11 (which only differ between 3L: 7527144..9092982), indicated significant differences between these lines (with D11.01 containing smaller lobes, Fig 12a, Tukey's test, $p < 0.001$), and this region overlaps with provisional P2/P3 between 3L: 8903265.. 9092982.

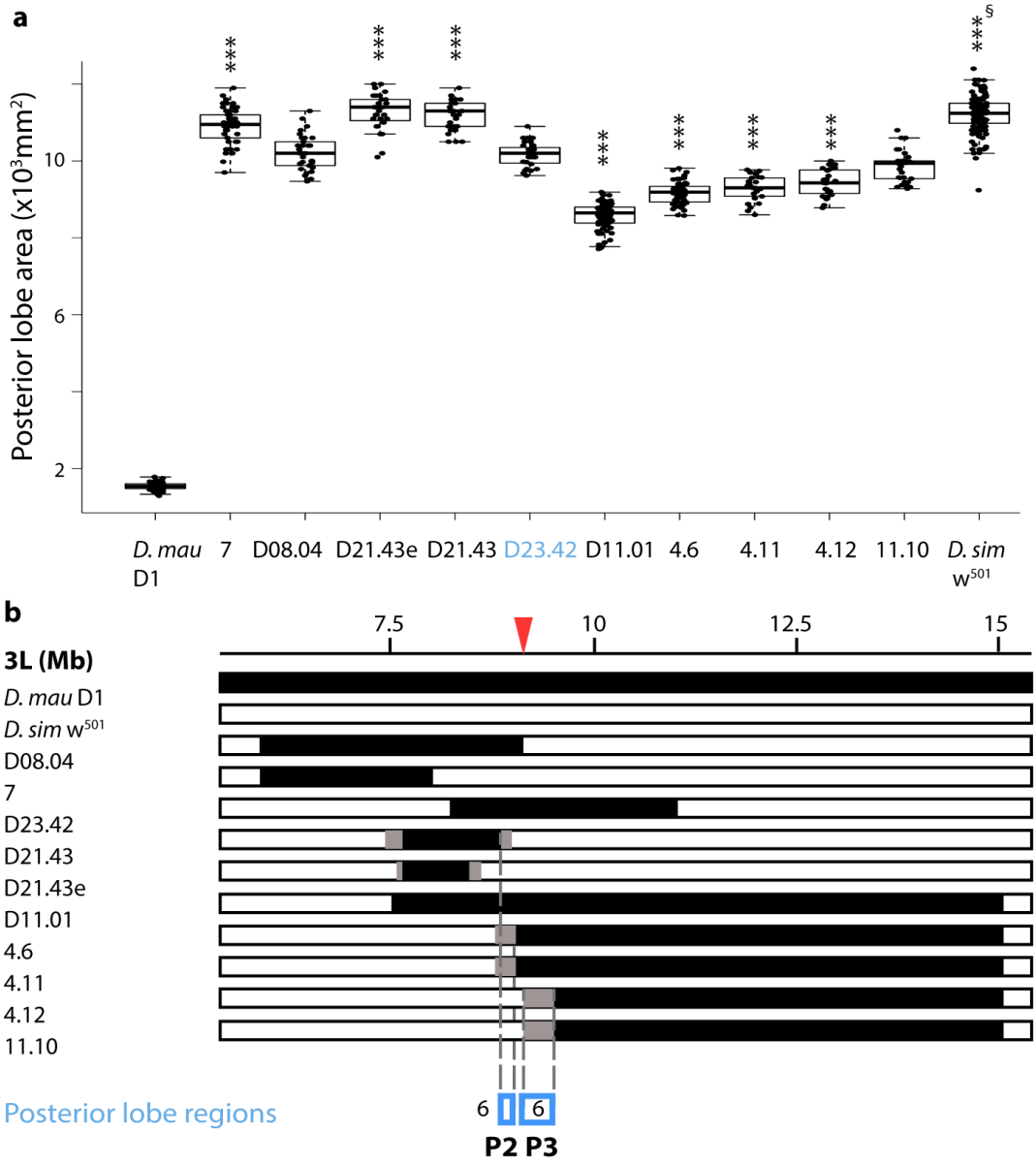


Figure 12. Mapping and phenotypic effect of candidate regions P2 and P3 – pairwise comparisions. (a) Pairwise comparisions between posterior lobe size of IL D23.42 (blue text) and overlapping ILs.D23.42 contain significantly smaller lobes than *D. simulans w*^{501} ($^{\$}$ Dunnetts test, $p < 0.001$). IL 7, D21.43e and D21.43 contain significantly larger size posterior lobes than D23.42 (Tukey's test, $p < 0.001$), whilst IL D11.01, 4.6, 4.11, 4.12 contain significantly smaller lobes (Tukey's test, $p < 0.001$). Asterisks indicates significant comparisions, where $p < 0.001$ *** and $p > 0.05$ = ns. (b) Genomic mapping of P2 and P3. Candidate region P2 can be mapped between the right-most boundary of IL D21.43 and the left-most boundary of IL 4.6 and 4.11 (based on pairwise comparisions desribed in the main text), but note differences in posterior lobe size between IL D08.04 and 7, D11.01 and 4.6/4.11, and lack of posterior lobe size effect compared to *D. simulans w*^{501} of D21.43. Candidate region P3 can be mapped between the left-hand break-points of 4.12 and 11.10 (as these

lines differ from eachother, Fig 12a and main text). Black bars indicate *D. mauritiana* DNA, white bars indicate *D. simulans* DNA, and grey boxes outline regions of unknown break points. Percentage effect size for P2 and P3 (blue boxes) on posterior lobe size is indicated and has been rounded to the nearest whole number.

The common introgressed region highlighted by these comparisons, and within provisional P2/P3, lies between max (min) 3L:8093265.. 9158500 (3L: 9055135..9092982) (between the right-most break point of D21.43 and the left-most break point of IL 4.11 and 4.6 (Fig 12b)). As a result, I have resolved candidate region P2 from 1.95 Mb to 190 kb (max), and due to an overlap in the potential break points of lines used to define P2, this region contains between 0 and 7 protein-coding genes (Supplementary File 5d), and explains 6% of differences in posterior lobe size between the species.

The remainder of the provisional P2/P3 not implicated in the mapping of P2 spans 3L: 9167745.. 11084746 (between the left-most breakpoints of IL 4.6 and 4.11 and the right-most break point of IL D23.42). This will now be referred to as "provisional P3", and is likely to contain variation able to explain 5% of the differences in posterior lobe size between the species (since P2 only accounts for 6% of the 11% total variance captured by minimal IL D23.42 (Supplementary File 4e)).

Interestingly, IL 4.12 and 11.10 contain *D. mauritiana* DNA that recombined within provisional P3, and only differ compared to IL 4.6 and 4.11

on this left-hand break point (Fig 12b). Comparisons between these lines indicated that IL 11.10 contains significantly larger posterior lobes compared to both IL 4.6 and 4.11 (Tukey's test, $p < 0.001$), but IL 4.12 is statistically the same (Tukey's test, $p > 0.05$) (see IL 4.6, 4.11, 4.12 and 11.10 in Fig 12a, Supplementary File 5c). This indicates that IL 4.12 and 11.10 break differently within the provisional P3 region, but because at the current mapping resolution these lines contain the same spans of *D. mauritiana* DNA (Supplementary File 2), it is difficult to decipher where.

However, comparisons between IL 4.12 and 11.10 against the next downstream IL (IL 164, Fig 10b), revealed that whilst IL 4.12 contains significantly smaller lobes than IL 164 (Tukey's test, $p < 0.001$), 11.10 does not (Tukey's test $p > 0.05$, Supplementary File 5c). Together, these comparisons suggest that the *D. mauritiana* DNA within IL 4.12 breaks further upstream (to the left) of IL 11.10, and that IL 4.12 contains *D. mauritiana* alleles over candidate region "P3" (Fig 12b). However, confusingly, IL 4.12 and IL 11.10 indicates these lines do not actually differ significantly in posterior lobe size measurements themselves (Tukey's test, $p = 0.09$, Supplementary File 5c).

Despite these contradictory results, I conservatively map an additional candidate region "P3" to the potential right-hand break point of IL 4.12 and IL 11 (Fig 12b). P3 lies between max (min) 3L: 9178292..9572682 (3L: 9178946..9571715), a region between 394 – 392 kb (Table 1). At the current resolution, P3 contains between 66 – 67 protein-coding genes (Supplementary

File 6e). Additional genetic markers and sequencing of these lines is required to determine where IL 4.12 and IL 11.10 break differently.

Interestingly, I calculate posterior lobe candidate region P3 to underlie 5.9% of posterior lobe size differences between the species (Fig 12b, Table 1), which has captured all of the expected effect based on the total effect size of minimal IL D23.42 (see above).

3.2.3 Candidate posterior lobe region P4

There are now no unexplored areas of the previously mapped P2 and P3 candidate regions (Tanaka et al., 2010). However, as can be seen in Fig 10b, there are an additional two minimal IL (IL 16.30 and IL 11) not yet analysed.

Introgressed *D. mauritiana* DNA in minimal IL 16.30 significantly reduced posterior lobe size compared to *D. simulans* (Fig 13a, $^{\$}$Dunnetts test, $p < 0.001$). Since there are no IL that contain *D. mauritiana* DNA that breaks in the region in order to resolve it, I map posterior lobe region "P4" in the boundaries of IL 16.30; between max (min) 3L: 12277961..12737959 (3L: 12419849..12734279) (Fig13c, Table 1), spanning between 460 – 312 kb, and contains between 52 – 49 protein coding genes (Supplementary File 6f).

As can be seen in Fig 10b, all the IL that contain *D. mauritiana* alleles over P4 (D11.01, 4.12, 4.11, 4.6, 10.10, 4.14, 43 and 16.14), are also significantly

different in posterior lobe size compared to *D. simulans* w^{501} (blue outlines in Fig 10b, Dunnetts test, $p < 0.001$). Some of these lines are already known to contain additional posterior lobe regions (e.g. P2 in D11.01 and P3 in D11.01, 4.6, 4.11 and 4.12, Fig 12b). In order to test whether or not the remaining lines that significantly differ in posterior lobe size, (IL 11.10, 164, 111, 10.10, 4.14, 43, 16.14), do so as a result of solely containing candidate region P4, I compared posterior lobe size of these lines against IL 16.30.

This analysis revealed that whilst IL 16.30 contains the same sized posterior lobes as IL 10.15, 43, 4.14 and 16.14 (Fig 13a, Tukey's test, $p > 0.05$), IL 11.10, 164 and 111 contain significantly smaller sized posterior lobes (Fig 13a, Tukey's test, $p < 0.001$). This indicates that whilst IL 10.15, 43 and 16.14 share candidate region P4, and contain no other posterior lobe size region (Fig 13b), ILs 11.10, 164 and 11, appear to contain an additional region "P5" (Fig 13b). Based on this analysis, P5 can be provisionally mapped between 3L: 13393862..15084689 (1.7 Mb)(Fig 13c).

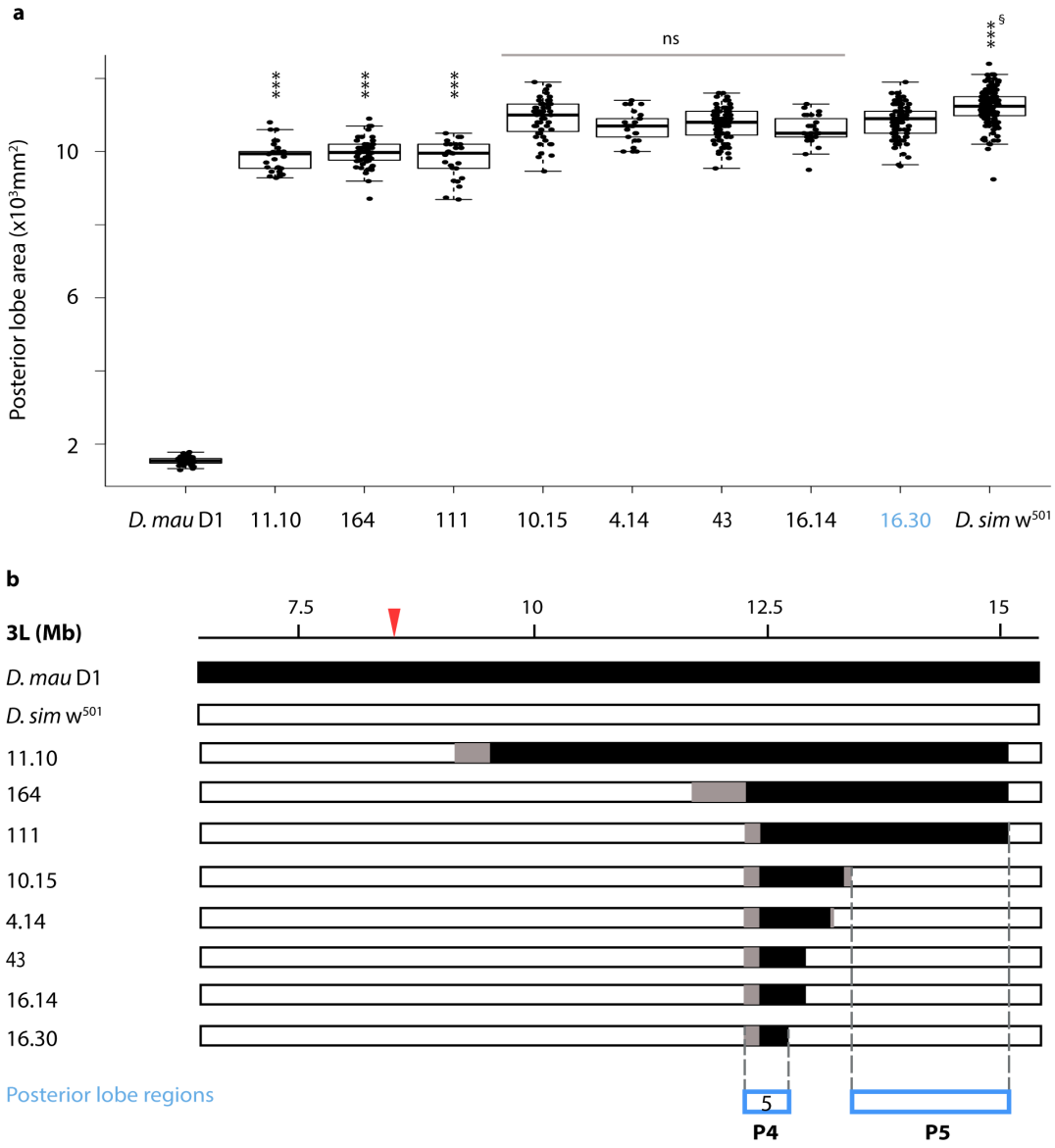


Figure 13. Mapping and phenotypic effect of P4 on posterior lobe size. (a) Pairwise comparisions between IL 16.30 and overlapping ILs. IL 16.30 has significantly smaller posterior lobes compared to *D. simulans w*^{501} ($ Dunnets test, $p < 0.001$). IL 10.15, 4.14, 43 and 16.14 contain the same sized posterior lobes as IL 16.30 (Tukey's test, $p > 0.05$). IL 11.10, 164 and 111 contain signficantly smaller posterior lobes than IL 16.30 (Tukey's test, $p < 0.001$). Asterisks indicates significant comparisions, where $p < 0.001$ *** and $p > 0.05$ = ns (Supplementary File 5c). Boxes indicate the range, upper and lower quartiles and median for each sample. (b) Genomic mapping mapping of the P4 region, and possible candidate region P5. Candidate region P4 is §defined by the boundaries of IL 16.30, whilst candidate region P5 can be provisionally mapped to the region between the right-hand break points of IL 111 and 10.15. Black bars indicate *D. mauritiana* DNA, white bars indicate *D. simulans* DNA, and grey boxes outline regions of unknown break points.

Percentage effect size explained by P4 in posterior size divergence is indicated and has been rounded to the nearest whole number.

Based on the effect size of ILs determined to exclusively contain posterior lobe candidate region P4 (IL 10.15, 43, 16.14 and 16.30), I calculate P4 is able to contribute to 4.7% of posterior lobe differences between the species (Table 1).

3.2.4 Posterior lobe size region P5

Minimal IL 11, and IL 8.15 contain introgressed *D. mauritiana DNA* that overlaps with the provisionally mapped P5. These IL contain the same region of introgressed DNA (up to our current resolution) (Supplementary File 2), but despite this, minimal IL 11 contains posterior lobes which was significantly different in size compared to *D. simulans* w^{501} (blue bar, Fig 14b), whilst IL 8.15 does not ("ns", Fig 14b). Even more curiously however, introgressed *D. mauritiana* DNA in IL 11 results in the generation of posterior lobes significantly larger than those of *D. simulans* (Dunnetts test, $p < 0.001$); implying that variation contained by IL 11 is able to affect posterior lobe size in the opposite to the expected direction (e.g. *D. mauritiana* DNA conferring larger posterior lobes).

However, direct analysis of IL 11 and IL 8.15 indicates these lines are not significantly different in posterior lobe size compared to each other (Tukey's test, $p > 0.05$, Fig 10b). Because of these contradictory results, and the unusual

nature of P5, I am unable to reliably map posterior lobe region P5 between these lines.

Instead, I compared posterior lobe phenotype between lines that provisionally map P5 (IL 11.10, 164 and 111) against these lines. As can be seen in Fig 14b, these lines contain significantly smaller lobes than both IL 11 and 8.15 (Tukey's test, $p < 0.001$, Supplementary File 5c); indicating the loss of a posterior lobe candidate region by the latter (Fig 14b).

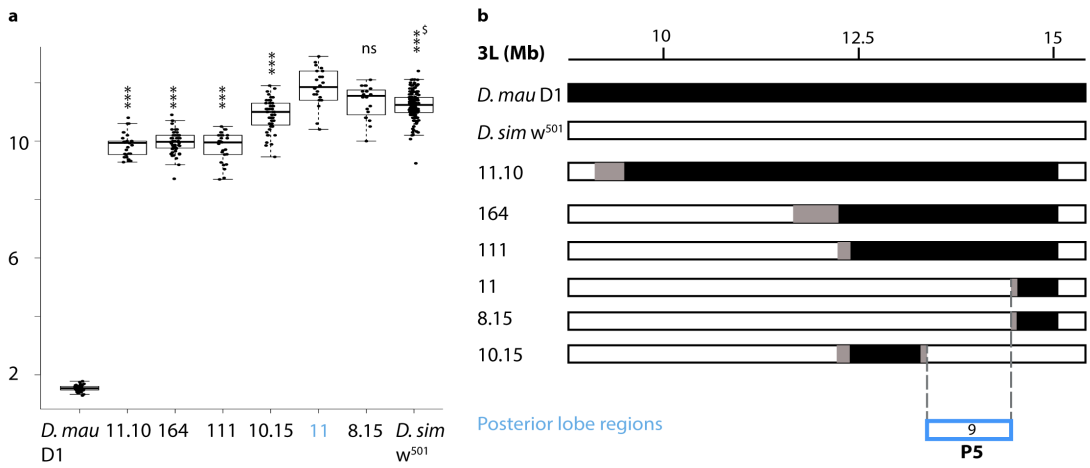


Figure 14. Mapping and phenotypic effect of P5 on posterior lobe size. (a) Pairwise comparisions between IL 11 and overlapping ILs (IL 10.15 included to show phenotypic effect of variation in P4). IL 11 has significantly larger posterior lobes compared to *D. simulans* w^{501} ($ Dunnets test, $p < 0.001$). However, IL 11 and 8.15 are not signficiantly different from eachother and contain the same introgressed region (upto current resolution, Supplementary File 2) (Tukey's test, $p > 0.05$). IL 11.10, 164 and 111 contain signficantly smaller posterior lobes than IL 11 (Tukey's test, $p < 0.001$) (and IL 8.15). However, this is not soley due to the phenotypic effct of candidate region P4, as these lines are also signficianalty smaller then IL10.15 (Tukey's test, $p < 0.001$, Supplementary File 5c) Asterisks indicates significant comparisions, where $p < 0.001$ *** and $p > 0.05$ = ns (Supplementary File 5c). Boxes indicate the range, upper and lower quartiles and median for each sample. (b) Genomic mapping mapping of the P5 region. Candidate region P5 is defined by the right-most boundary of IL 10.15, and the left-most regions of IL 8.15 / IL 11. Black bars indicate *D.*

mauritiana DNA, white bars indicate *D. simulans* DNA, and grey boxes outline regions of unknown break points. Percentage effect size explained by P5 in posterior size divergence is indicated and has been rounded to the nearest whole number.

Based on this analysis, P5 can be mapped in the span of introgressed *D. mauritiana* DNA shared by IL 11.10, 164, 111, but not shared by IL 10.15 (Fig 13b), IL 8.15 and IL 11 (Fig 14b). Therefore P5 lies between max (min) 3L: 13393862.. 14532063 (3L: 13430267.. 14402074), and spans a region between 1.14 Mb – 972 kb (Fig 14b, Table 1). This region contains 91 – 78 candidate genes and contains variation able to explain 9% of posterior lobe size differences between species.

3.3 Chapter Three - Summary

By comparing the clasper bristle number, clasper size and posterior lobe size between a panel of novel and previously generated (Tanaka et al 2015) ILs spanning ~ 10 Mb on 3L, I have been able to identify multiple causative regions for the evolution of these traits between *D. simulans* and *D. mauritiana* (Fig 15b). Identifying these regions involved refinement of three candidate regions (C2, P1 and P2), discovery of four novel causative regions (C0, P3, P4, P5), and confirmation of one region to the same mapping resolution as previous studies (C1, Tanaka et al., 2015) (Fig 15a and 15b).

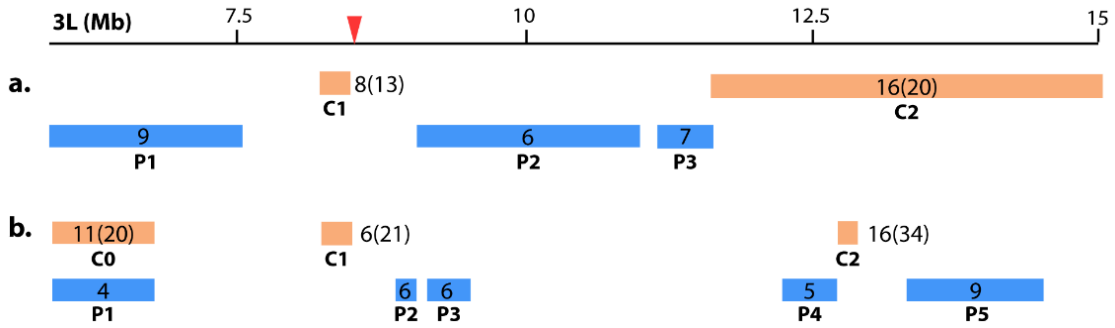


Figure 15. Refinement of mapped regions underlying genital divergence. Candidate regions underlying posterior lobe size (blue) and clasper size/ clasper bristle number (orange) are shown at Tanaka et al (2015) resolution **(a),** and current resolution based on novel introgressions **(b).** Effect size is indicated for each region (clasper bristle effect size in brackets), and have been rounded to the nearest whole number. The resolution of P1, and C2 has been resolved, P2 and P3 has been re-mapped, and three novel regions underlying have been revealed (C0, P4 and P5).

In doing so, I have collectively identified loci explaining 33% of clasper size differences, and 75% of difference in clasper bristle number between the species (Fig 15 and Table 1). In total, C0 – C2 contain 165 positional candidate genes (maximum), (annotated in *D. melanogaster* R6.24, Supplementary Files 6a – 6c, Table 1). Together, P regions account for 30% of differences in posterior lobe size between the species, and at the current resolution, contain 316 positional candidate genes (Supplementary Files 6d – 6g, Table 1).

Candidate Region	Phenotypic effect size %			Location on 3L *D. sim* R2.02 max (min)		Region size	Gene # max (min) *D. mel* ortho
	Clasper area	Clasper bristle #	Posterior lobe size	LHS	RHS	max (min) kb	
C0	10.8	19.9		5903109(6136507)	6852222(6806943)	949,113 (670,436)	99(35)
C1	6.0	21.0		8253548(8257826)	8699816(8556334)	446,268 (298,508)	57 (39)
C2	16.4	33.5		12734279(12737959)	12911597(12911531)	178,189 (173,697)	9(8)
P1			3.7	5903109(6136507)	6852222(6806943)	949,113 (670,436)	99(35)
P2			6.0	8903265(9055135)	9158500(9092982)	190, 279	7(0)
P3			5.9	9178292(9178946)	9572682(9571715)	394,390 (392,769)	67(66)
P4			4.7	12277961(12419849)	12737959(12734279)	459,998 (311,741)	52(49)
P5			9.0	13393862(13430267)	14532063(14402074)	1,138,201 (971, 807)	91(78)

Table 1. Summary of candidate regions for each mapped trait. The effect size is calculated as a percentage of the difference in phenotype between the parental strains. The size and location of each region (In *D. simulans* R2.02), and the number of *D. melanogaster* protein coding orthologous (r6.24) is indicated. CL = clasper, CLB = clasper bristle number, PL = posterior lobe effect sizes.

Table 1 summarizes the resolution and effect sizes of each mapped region (Table 1). Although some of these regions have reached a manageable resolution for conducting gene expression analysis (GEA) (Chapter Four), some ILs require the generation of more genetic markers to resolve the potential break points (namely C0/P1, C1, P2 and P5 - note large difference in potential candidate gene number in maximum breakpoints versus to minimum breakpoints in Table 1). For regions such as P3 and P5, the generation of novel introgression lines (e.g. that introduced *D. simulans* DNA in the left-hand side of 4.6 / 4.11 and in the middle of IL 111), may be necessary to reach the resolution required to identify causative genes.

Nonetheless, in Chapter Four I will conduct GEA to narrow down the candidate genes in these regions at their current resolution.

4 Chapter Four - Results

Expression analysis of positional candidate genes

In the previous chapter, I defined candidate regions that contain variation contributing to differences in posterior lobe size, clasper size and clasper bristle number between *D. simulans* and *D. mauritiana.* Whilst some of these candidate regions contain as few as nine protein-coding genes (C2), others contain up to 99 genes (C0/P1) (see Chapter Three, Table 1). In this chapter, I used gene expression analysis (GEA) to narrow down the number of candidate genes likely to have evolved. The term "evolved gene" is used specifically to refer to genes underlying diversification of the concerned male genital trait (as all genes are the product of evolution).

I first analysed RNA-Seq data (generated by Kentaro Tanaka and described in Hagen et al., 2018), from developing terminalia of *D. simulans* and *D. mauritiana* at two different time points (30 hr after puparium formation (APF) and 50 hr APF) (Supplementary File 7). During this time window, *Drosophila* male genitalia metamorphose from a disc-like tissue into those that resemble the adult morphology (e.g. see illustration in Fig 22a). Positional candidate genes not expressed (< 1 rpkm) at any point during this window were

excluded from further analysis. I also used the RNA-Seq data to identify genes differentially expressed between *D. simulans* and *D. mauritiana* during pupa stages (Hagen et al., 2018), and cross-referenced these to a dataset of differentially expressed genes between *D. mauritiana* and *D. sechellia* genital discs (Masly et al. 2011) (Supplementary File 7). Note, posterior lobe size differs between all three of these *D. simulans* subgroup species (Fig 1), and although the claspers of *D. simulans* and *D. sechellia* are quite similar (Fig 1), *D. mauritiana and D. sechellia* are morphologically divergent. Since genes could potentially underlie genital differences between many different species, differentially expressed genes in both comparisons (and with the same species bias, such as e.g. consistently upregulated in species with a specific sized lobe) were prioritised for downstream analysis.

Based on these analyses, a selection of promising candidate genes, or alternatively all the genes in a candidate region (if the number of genes was manageable), were then genetically manipulated using RNAi knockdown in *D. melanogaster* (see Supplementary File 8a for raw data, 8b for summary statistics). Supplementary File 8 also contains RNAi results for genes that are not currently in the candidate regions, since the resolution of these regions progressed during the screen. In Supplementary File 9, the expression analysis from both data sets (Hagen et al., 2018; Masly et al., 2011) and RNAi result of each gene still in candidate regions can be found.

Finally, I used *in situ* hybridisation (ISH) to evaluate whether or not candidate genes are expressed in a pattern consistent with a role in the development of the claspers, posterior lobes or both, and analysed any spatial and temporal expression pattern differences between the species. These disparities could represent how the gene in question could have evolved to affect genital organ size between *Drosophila* species. If transcripts could be detected at an "early" (30 – 34 hr APF) pupal stage or a late pupal stage (46 – 50 hr APF) (see Methods), I proceeded to test stages of development at a higher temporal resolution.

4.1 C0/P1 candidate genes

In the previous chapter, I showed candidate region C0/P1 contains variation contributing to the evolution of all three mapped traits (3.7% of posterior lobe size, 10.8% of clasper size and 19.9% of clasper bristle number differences between *D. simulans* and *D. mauritiana*). The maximum size of this region is 949 kb, and contains 99 protein-coding genes (with *D. melanogaster* orthologs) (Table 1).

According to the RNA-Seq analysis of *D. simulans* and *D. mauritiana* pupal terminalia, only 64 of these 99 genes are expressed (at either 30 hr or 50 hr APF, Supplementary File 9). Of these genes, only 40 are differentially expressed between these species (at either of the pupal stages), and only 16 are

differentially expressed between *D. sechellia* and *D. mauritiana* genital discs (Supplementary File 9).

So far, of the genes shown to be differentially expressed in at least one of the datasets, only six have been tested for clasper bristle number phenotype during RNAi knock-down. Five of these knock-downs contained the same number of clasper bristles as the NP6333 driver control (Dunnett's test, $p > 0.05$, see Supplementary File 9a*, ventral veins lacking (vvl), ImpL3, CG10064, CG9953* and *Surf1),* whilst knock-down of *sugarless (sgl)*, gave rise to significant differences (Dunnett's test, $p < 0.001$, Supplementary File 8b). This did not appear to be purely an effect of the genetic background (e.g. an inherited trait from the UAS-*sgl* control), since although UAS-*sgl* contained significantly fewer bristles than the NP6333 control (Fig 16a orange asterisks, ANOVA $F(2, 36) = 101.7$, $p < 0.001$, followed by a Tukey's test $p < 0.001$), *sgl* knock-down contains fewer bristles still (black line and black asterisks, Fig 16a, Tukey's test $p < 0.001$). Therefore, although part of the clasper bristle number effect of *sgl* knock-down is likely attributed to genetic background, it also reflects a significant effect of gene knock-down on clasper morphology. Compared to the average phenotype of the parental strains, *sgl* knock-down generates claspers with 15.7% fewer bristles (Supplementary File 8b).

The developmental role of *sgl* seems to be specific to the claspers, as *sgl* knock-down does not affect posterior lobe size compared to the NP6333 control (Dunnett's test, $p > 0.05$, Supplementary File 8b). Therefore, *sgl* represents a

clasper developmental candidate in "C0" of C0/P1, and is not able to explain the posterior lobe effect of "P1". According to K. Tanaka's RNA-Seq data, *sgl* is not differentially expressed between *D. simulans* and *D. mauritiana* terminalia, at either 30 hr APF or at 50 hr APF ($p > 0.05$, Supplementary File 9), but is significantly upregulated in *D. sechellia* genital discs ($p < 0.01$, Supplementary File 9).

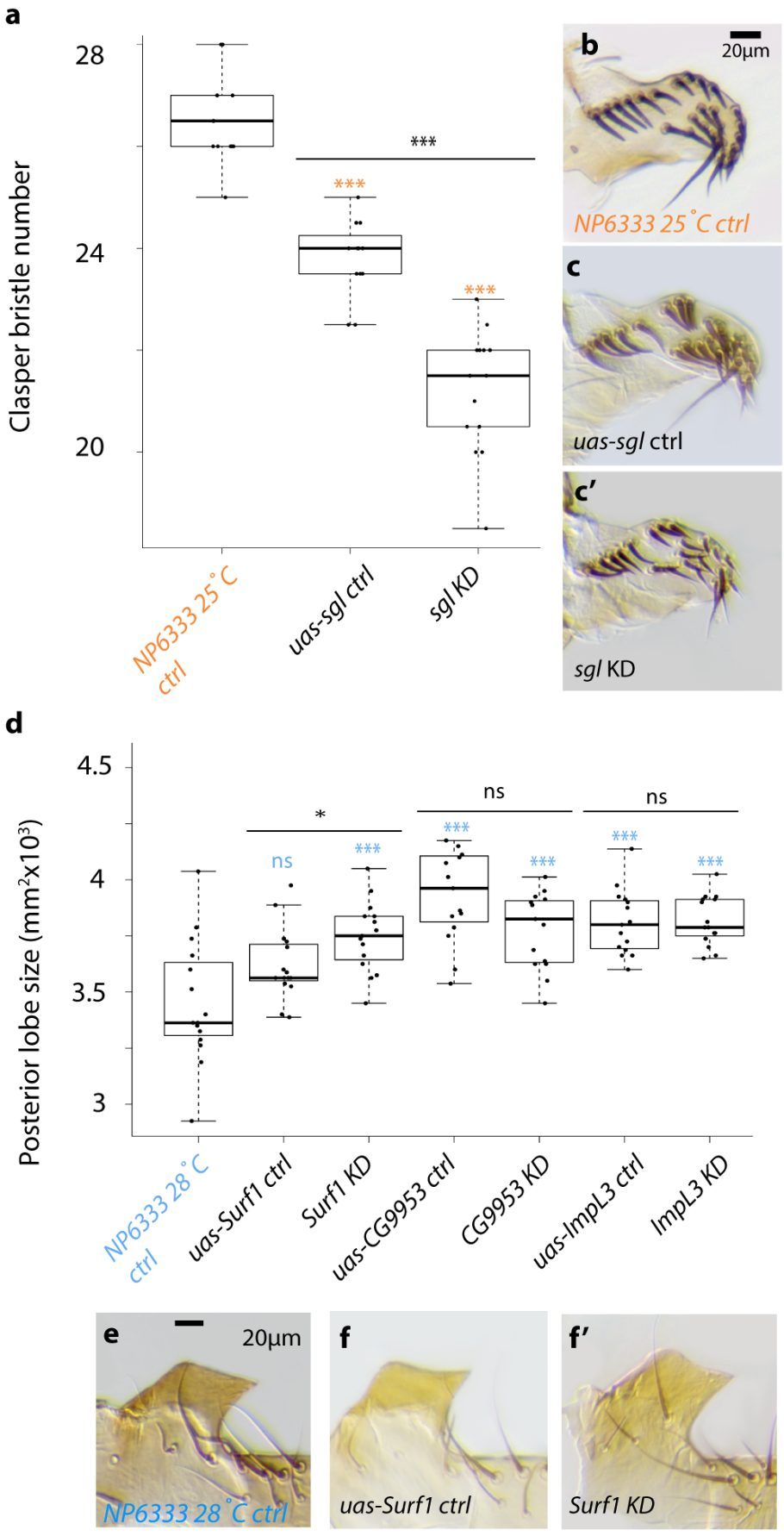

a
Clasper bristle number
28
24
20
***
***
***
NP6333 25˚C ctrl
uas-sgl ctrl
sgl KD
b
20µm
NP6333 25˚C ctrl
c
uas-sgl ctrl
c'
sgl KD
d
Posterior lobe size (mm²x10³)
4.5
4
3.5
3
*
ns
ns
ns
***
NP6333 28˚C ctrl
uas-Surf1 ctrl
Surf1 KD
uas-CG9953 ctrl
CG9953 KD
uas-ImpL3 ctrl
ImpL3 KD
e
20µm
NP6333 28˚C ctrl
f
uas-Surf1 ctrl
f'
Surf1 KD

Figure 16. Clasper and posterior lobe developmental candidates in candidate region C0/P1. **(a)** C0 candidate gene *sgl* knock-down results in signficantly less clasper bristles compared to both UAS-*sgl* control (black asterisks, $p < 0.001$) and NP6333 driver control (orange asterisks, $p < 0.001$). **(b – c')** morphological affect of *sgl* knock-down on clasper morphology. **(d)** P1 candidate gene *Surf1* knock-down results in signficantly larger posterior lobes compared to both UAS-*Surf1* control (black asterisks, $p < 0.05$) and NP6333 driver control (blue asterisks, $p < 0.001$) (Supplementary File 8b). Knock-down of *CG5593* and *ImpL3* results in significantly larger lobes compared to NP6333 drive control (blue asterisks, $p < 0.001$), but not compared to UAS- controls (black "ns", $p > 0.05$). (Supplementary File 8b). Asterisks indicate significant differences detected during Tukey's test pairwise comparisons, where $p < 0.001$ *** and $p > 0.05$ = "ns" (see in text for ANOVA results, Supplementary File 8b).Colors link comparisons between NP6333 driver controls against UAS-controls / gene knock-downs, whilst comparisons between UAS- controls and knock-downs are indicated by black lines and black asterisks. Boxes indicate the range, upper and lower quartiles and median for each sample. KD = knock-down, ctrl = control. (e – f') morphological affect of *Surf1* knock-down on posteiror lobe morphology. For ANOVA results see main text.

Since C0/P1 contains variation contributing to both clasper size and posterior lobe size differences, we also measured posterior lobe size for all six knocked-down genes mentioned above, as well as an additional candidate gene *SP1173* (clasper bristle number phenotype not recorded for this gene unfortunately). Four of these yielded no significant effect on posterior lobes size compared to the NP6333 driver control during RNAi knock-down (Dunnetts test, $p > 0.05$, *vvl, SP1173, CG10064, sgl*, Supplementary File 8b and 3a). However, *ImpL3, Surfeit1* (*Surf1) and CG9953* knock-down significantly affected posterior lobe size compared to NP6333 driver control (Dunnetts test, $p < 0.001$ in all cases, Supplementary File 8a). As can be see in Fig 16d, knock-down of each gene resulted in the development of significantly larger lobes compared to the NP6333 control (blue asterisks, 1d).

In the case of *Surf1,* this knock-down effect appears to truly reflect a role of *Surf1* in posterior lobe development; as UAS-*Surf1* and NP6333 control are not different from each other in lobe size ("ns" in Fig 16d, ANOVA $F(2, 42) = 7.7$, $p < 0.01$, followed by a Tukey's test $p > 0.05$), whilst *Surf1* knock-down generates larger posterior lobes than both controls (see blue asterisks, and black line/ black asterisks, Fig 16d – 16f'). This corroborates my GEA of *Surf1;* being consistently upregulated in species with smaller posterior lobes (and larger claspers, as described above) in both datasets (Supplementary File 9). *Surf1* knock-down results in the production of 5.2% larger posterior lobes compared to the average parental phenotype (Supplementary File 8b). Similarly, *Surf1's* role seems to be exclusive to posterior lobe development; inflicting no effect on clasper bristle phenotype (Dunnett's test, $p > 0.05$, see Supplementary File 9a).

In contrast to Surf1, the initial significance detected between the posterior lobes of *CG9953* and *ImpL3* knock-downs against NP6333 is purely a result of genetic background; as the UAS-controls are significantly different in posterior lobe size compared to knock down NP6333 (ANOVA $F(2, 42) = 17.8$, $p < 0.001$, followed by a Tukey's test $p < 0.001$ (*ImpL3*)), and (ANOVA $F(2, 42) = 16.9$, $p < 0.001$, followed by a Tukey's test $p < 0.001$ (*CG9953*)), but the gene knock-downs are the same as the UAS-controls (Tukey's test $p > 0.05$ in both cases). Therefore, *Surf1* is the only P1 gene identified so far with a role in posterior lobe development.

Based on my GEA, the next genes I would recommend testing using RNAi would be *CG10289*, which is consistently upregulated in species with smaller posterior lobes, and larger claspers (*D. mauritiana* , Supplementary File 9). I would also be interested to test the function of *Best2, SP1173* and *loj* in the development of the claspers and lobes (apart from *SP1173,* which as mentioned above, has no effect on lobe development). All three of these genes are differentially expressed between species throughout both data sets, though they appear to be dynamically expressed (and do not correlate with species or a particular genital morphology) (Supplementary File 9).

4.2 C1 candidate genes

At the current resolution, C1 has a maximum size of 446 kb and underlies 6% of clasper size and 21% of clasper bristle number differences between the species. This region contains 57 protein-coding genes (in *D. melanogaster*), with 40 of these genes being expressed in either *D. simulans* or *D. mauritiana* developing terminalia (Supplementary File 9). In total, 29 genes are differentially expressed between *D. simulans* and *D. mauritiana* pupal terminalia, and only eight are differentially expressed between *D. mauritiana* and *D. sechellia* genital discs (Supplementary File 9).

Of the C1 genes, we have tested the effect of RNAi knockdown on clasper bristle number for 30 (Supplementary File 9) (note, some of these are not

differentially expressed in either data set, but were tested regardless in an attempt to saturate the region). Twenty-one of these knock-downs resulted in the development of claspers with statistically the same number of bristles compared to the NP6333-Gal4 control (Dunnetts test, $p > 0.05$, Supplementary File 8b and 8a). In contrast, knock-down of *hairy* (*h*), *Cuticular protein 66D* (*Cpr66D), Grunge* (*Gug*), *CG5989, CG13305, Minichromosome maintenance 7 (Mcm7), division abnormally delayed (dally*) and *prm* significantly affected the number of clasper bristles compared to NP6333 driver controls (Fig 17a, Supplementary File 8a). As can be seen in Fig 17a, knock-down of *h* and *Cpr66D* results in the development of significantly more bristles compared to the NP6333 driver control, whilst knock-down of all other genes results in the production of fewer bristles (*Gug*, *CG5989, CG13305, Mcm7, dally* and *prm*) (see dark and light orange asterisks in Fig 17a).

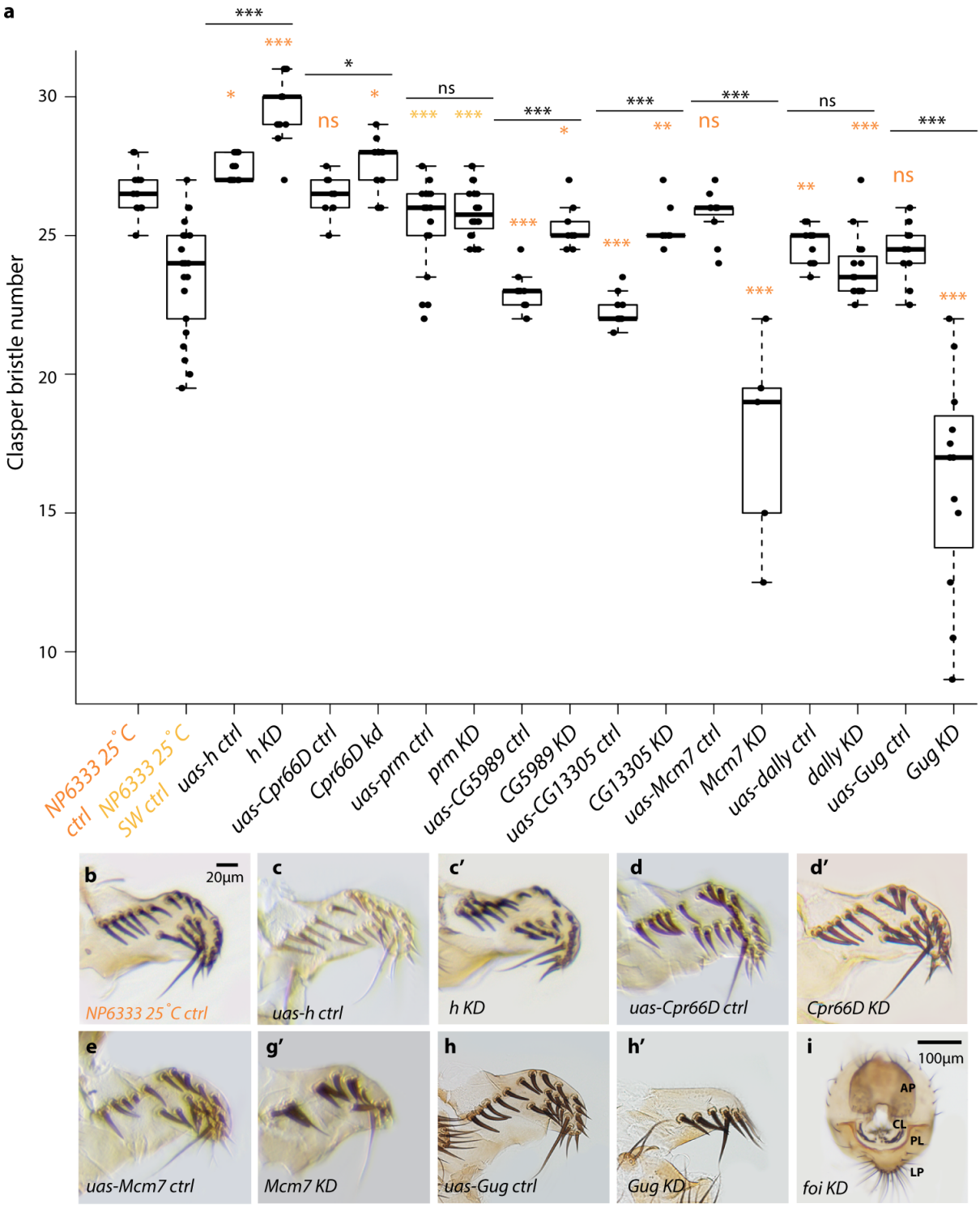


Figure 17. Clasper developmental candidates in candidate region C1. (a) C1 candidate genes *h* and *Cpr66D* knock-down results in signficantly more clasper bristles compared to NP6333 25'C driver control (Tukey's test $p < 0.001$ and $p < 0.05$ respectively, dark orange asterisks) and UAS-controls (Tukey's test $p < 0.001$, $p < 0.05$ respectively, black lines and black asterisks). Knock down

of *prm* and *dally* resulted in signficantly fewer clasper bristles compared to NP6333 25'C SW driver control (light orange asterisks) and NP6333 25'C driver control (dark orange asterisks) respectively ($p < 0.001$ in both cases). However, neither of these knock-downs were signficiantly different in clasper bristle number compared to UAS- controls (see black lines and "ns", $p > 0.05$). Knock down of *CG5989* and *CG13305* also resulted in signficantly fewer clasper bristles compared to 25'C driver control (dark orange asterisks, $p < 0.05$ and $p < 0.01$ respectively). However, knock down of these genes results in signficantly more bristles than UAS- controls ($p < 0.001$ in both cases, black lines and black asterisks). Knock-down phenotype may therefore be an intermediate between parental controls. Knock-down of *Mcm7* and *Gug* however results in the production of claspers with fewer bristles than both the NP6333 25'C driver control ($p < 0.001$ in both cases dark orange asterisks), and UAS- controls ($p < 0.001$ in both cases, black lines and black asterisks). Asterisks indicate significant differences detected during Tukey's test pairwise comparisons, where $p < 0.001$ *** and $p > 0.05$ = "ns" (Supplementary File 8b), for ANOVA results see main text. Colors link comparisons between NP6333 driver controls against UAS- controls / gene knock-downs, whilst comparisons between UAS- controls and knock-downs are indicated by black lines and black asterisks. Boxes indicate the range, upper and lower quartiles and median for each sample. KD = knock-down, ctrl = control. **(b – i)** morphological affect of C1 developmental candidate gene knock-down on clasper morphology.

Further analysis of gene knock-down phenotype indicated that only *Cpr66D* (ANOVA $F(2, 39) = 7.4$, $p < 0.01$), *h* (ANOVA $F(2, 25) = 46.7$, $p < 0.001$)), *Mcm7* (ANOVA $F(2, 26) = 54.5$, $p < 0.001$)) and *Gug* (ANOVA $F(2, 34) = 66.11$, $p < 0.001$)) significantly affected clasper bristle number compared to both UAS- and NP6333 controls (Tukey's test, $p < 0.001$ for all genes except *Cpr66D*, in which $p < 0.05$, Fig 17a).

Compared to the average of the parental phenotypes, *Cpr66D* and *h* knock-down resulted in the production of claspers with 4.3% and 11.8% more bristles, respectively (Supplementary File 8b), and therefore these genes appear to have a repressive role in the formation of clasper bristles. In contrast, *Gug* and

Mcm7 appear to positively regulate bristle formation, as knock down of these genes resulted in the production of 63% and 32.7% fewer bristles, respectively (Supplementary File 8b). Moreover, clasper shape is clearly affected in both of these knock-downs; with claspers appearing significantly smaller and malformed compared to both controls (Fig 17e – 17h').

Although knock-down of *CG5989* (ANOVA $F(2, 27) = 38.8$, $p < 0.001$) and *CG13305* (ANOVA $F(2, 27) = 59.1$, $p < 0.001$) significantly changed clasper bristle number compared to both parental controls (Fig 17a, Tukey's test, $p < 0.01$ in both cases), upon closer inspection, I realized that their knock-down phenotype is intermediate between UAS-control and NP6333 driver (Fig 17a). Therefore, it is unclear whether the knock-down phenotype is a consequence of heterozygosity between parental controls, or the effect of *CG5989* or *CG13305* knock-down. Moreover, I am unable to determine the direction of the effect (e.g. whether or not bristle number increases or decreases).

The repressive role of both *h* and *Cpr66D* appears to be specific to the claspers as knock-down of these genes did not significantly affect posterior lobe development compared to NP6333 controls (Dunnetts test, $p > 0.05$ in both cases, Supplementary File 8b). In contrast, knock-down of both Gug (ANOVA $F(2, 34) = 97.1$, $p < 0.001$) and Mcm7 (ANOVA $F(2, 32) = 183.1$, $p < 0.001$) resulted in the development of posterior lobes significantly smaller compared to both parental controls (Tukey's test, $p < 0.001$ in both cases, Fig 18a, Supplementary File 8b); implying these genes enhance the growth of other parts

of the male genitalia also. RNAi of *Gug* and *Mcm7* resulted in the production of 48% and 76.8% smaller posterior lobes, respectively (compared to average parental phenotype, Supplementary File 8b). The severity of these phenotypes is apparent in Fig 18c' and 18d'; with *Gug* RNAi more subtly reducing lobe size by affecting the distal tip, and *Mcm7* RNAi dramatically reducing the posterior lobes to a small point (Fig 18a, 18c' and 18d') which interestingly resembles a *D. mauritiana*-like lobe morphology (Fig 1).

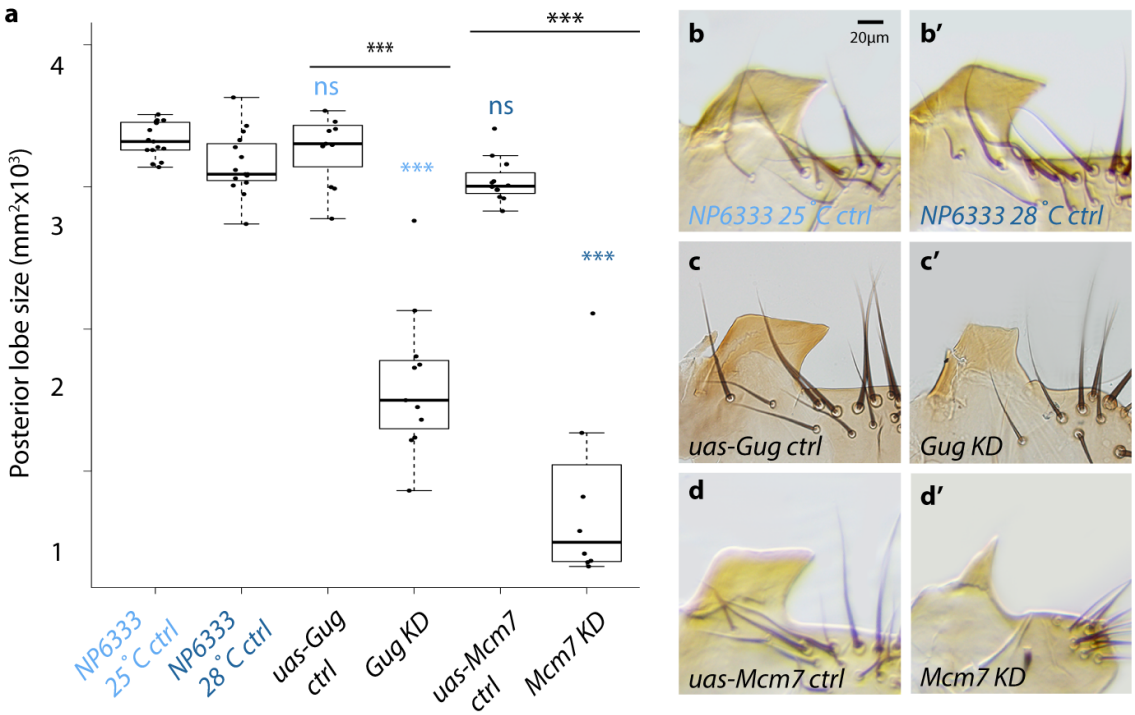


Figure 18. C1 clasper developmental candidates affect on posterior lobe morphology during RNAi knock-down. (a) Knock-down of C1 candidate genes *Mcm7* and *Gug* results in the development of significantly smaller posterior lobes compared to the NP6333 25'C control (light blue asterisks) and NP6333 28'C control (dark blue asterisks) ($p < 0.001$ in all cases). Knock-down of all three candidate genes also results in posterior lobes signficantly smaller compared to respective UAS- controls (black lines and black asterisks). Asterisks indicate significant differences detected during Tukey's test pairwise comparisons, where $p < 0.001$ *** and $p > 0.05$ = "ns" (Supplementary File 8b), for ANOVA results see main text. Colors link comparisons against NP6333 driver controls

and UAS- controls / gene knock-downs, whilst comparisons between UAS- controls and knock-downs are indicated by black lines and black asterisks. Boxes indicate the range, upper and lower quartiles and median for each sample. KD = knock-down, ctrl = control. **(b – i)** morphological affect of C1 developmental candidate gene knock-down on posterior lobe morphology.

Knock-down of *fear of intimacy (foi)* in *D. melanogaster* male genitalia resulted in extensive developmental defects; whereby the appendages of the male external genitalia were fused together, including the claspers and posterior lobes (see Fig 17i). Therefore, whilst it is clear this gene has a role in the development of the claspers and the lobes, the effect of this knock-down could not be accurately quantified.

According to my GEA, both growth-enhancing genes (*Gug* and *Mcm7*) are only differentially expressed at 30 hr APF, both being significantly up-regulated in *D. mauritiana* (the smaller posterior lobed, larger clasper species) (30APF, Supplementary File 9). In contrast, both repressive genes, *Cpr66D* and *h,* are only differentially expressed at the later pupal time point (50 hr APF, being up-regulated in the larger clasper species *D. mauritiana,* Supplementary File 9). *Foi* expression level differs only in the latter stage of pupal development between *D. simulans* and *D. mauritiana* (50 hr APF - being more highly expressed in *D. simulans,* Supplementary File 9), but also between the genital discs of *D. sechellia* and *D. mauritiana* (upregulated in *D. sechellia*) (Supplementary File 8b).

1.1.1. In situ hybridisation of Cpr66D

So far, I have only analysed the expression profile of one C1 candidate gene using *in situ* hybridisation; *Cpr66D.* During this process, as well as analysing *Cpr66D,* I observed clear differences in developmental timing of the male genitalia between *D. simulans, D. melanogaster* and *D. mauritiana*; whereby *D. simulans* and *D. melanogaster* timing appears to be comparable, but *D. mauritiana* develop ~ 4 hrs slower than the aforementioned species (Fig 19). For example, at 34 h APF, *D. mauritiana* male genital morphology appears similar to that of *D. simulans* and *D. melanogaster* 30 hr APF (with e.g. an underdeveloped anal plate (AP) primordia, and lack of ridge between the claspers and lateral plates (LP) (Fig 19a)). For this reason (as well similar observations at other stages), I started *in situ* analysis of *D. mauritiana* 4 hrs later than in *D. simulans*, and consequently conduct my final in situ 4 hrs later in this species (note 46 hr APF versus 50 hr APF final time point). This 4 hour delay may not give rise to precisely the same stages between the species, but I believe this adjustment renders the samples more comparable.

During *in situ* hybridization, no striking differences were detected during early stage pupae (30-34 hr APF) between *D. simulans*, *D. mauritiana* or *D. melanogaster*; with *Cpr66D* transcripts detected in a fairly ubiquitous pattern in the developing ventral structures, such as in the primordia of the internal genitalia (IG) and the claspers (CL) in all three species (Fig 19a). Consistently, transcripts are less abundant in the anal plate primordia (AP). In *D. mauritiana*

and *D. melanogaster*, it appears *Cpr66D* transcripts occur more dorsally than in *D. simulans*, though these differences are relatively minimal compared to the disparities detected in later stages.

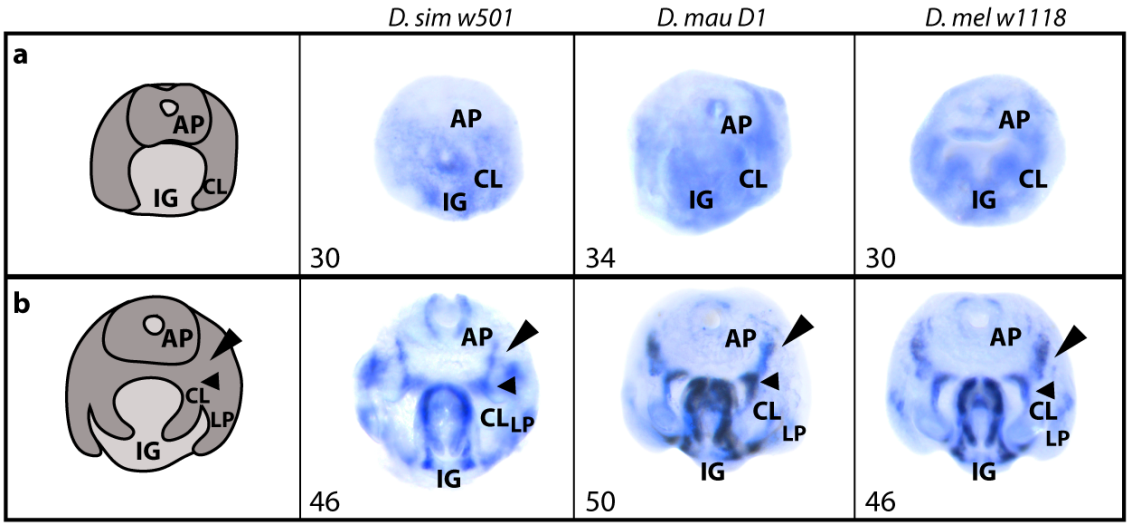


Figure 19. In situ hybridisation of Cpr66D in *D. mauritiana* , *D. simulans* and *D. melanogaster* male genitalia in early ((a) 30 - 34hrs APF) and late ((b) 46 – 50hrs APF) pupal development. Left-hand panels illustrate schematic representation of morphological stage based on DAPI staining, and posterior lobe outgrowth was omitted for simplicity. (a) At early stage, Cpr66D is expressed in a diffuse pattern over ventral region of the genitalia, excluding the region containing the anal plate primordia (AP) in all three species. (b) At late stage, Cpr66D expression becomes much more specific. Expression can be detected in the central column, as well as in the distal end of the aedeagus and in a ring around the anal plates in all three species. Cpr66D transcripts are also detected in bands extending dorsally from the base of the adeagus towards the lateral sides of the anal plates in all three species (black diagonal arrows), though this band appears to be wider in *D. mauritiana* and *D. melanogaster*. Expression is also present at the internal edge of the claspers (horizontal black arrows). In *D. simulans*, patches of Cpr66D expression could also be detected on the lateral plates, in the region where the lobes with presumably extends. AP = Anal plates primordia, IG = primordial of the internal genitalia and CL = clasper primordia.

During late pupal stages (46-50 hr APF), *Cpr66D* expression becomes much more specific in all three species; with transcripts detected throughout the internal genital organ (IG), distending from the distal tip in two wide lateral

columns down towards the base (Fig 19b). Interestingly, expression of *Cpr66D* can also be detected in bands extending from the base of the developing clasper, dorsally towards the genital arch, lateral to the anal plates (diagonal black arrows, Fig 19b). *Cpr66D* can also be detected along the inner edge of the claspers, with transcripts projecting distally, as well as towards the opposing clasper on the adjoining ridge underneath the anal plates (AP) (Fig 19b). The width of *Cpr66D* expression within the base of the claspers, and the prominence of the expression down the inner edge of the clasper, positively correlates with species that have larger claspers (*D. melanogaster* and *D. mauritiana*) (Fig 19b). Despite reaffirming expected patterns based on RNA-Seq analysis (with *Cpr66D* only being significantly up-regulated at the later pupal time point (50 hr APF) in *D. mauritiana* (Supplementary File 9) these results are also counterintuitive, since knock-down of *Cpr66D* results in larger claspers in *D. melanogaster*. If *Cpr66D* is the evolved gene in C1, we may have expected more expression of *Cpr66D* in the clasper primordia of *D. simulans* (the smaller clasper species).

As well as differing in clasper expression, *D. simulans* also differs from the two other species, in that two patches of *Cpr66D* expression could be detected in the lateral plates (just lateral to the diagonal band of expression stemming from the base of the claspers) (Fig 19b). I believe this region to be concurrent with the area where the posterior lobe will project, however (as described above), *Cpr66D* does not appear to have a role in posterior lobe development in *D. melanogaster*.

According to my GEA, the only genes which could be interesting candidates left untested by RNAi in C1 are *ergic53, sperm-Leucylaminopeptidase (s-Lap2), CG6511* (Supplementary File 9). *Ergic53* is differentially expressed between early stage *D. simulans* and *D. mauritiana* pupal terminalia (up-regulated in *D. simulans*), *s-Lap2* is consistently up-regulated in *D. mauritiana* over both time points, and *CG6511* is only up-regulated in *D. mauritiana* at late pupal stage (Supplementary File 9).

Moreover, *SrpRBeta* and *rhea* consistently yielded lethal RNAi phenotypes that rendered the clasper bristles un-measurable (Supplementary File 9). Both of these genes are up-regulated in *D. mauritiana* at the late pupal stage, and therefore would be interesting candidates to test using *in situ* hybridisation.

4.3 C2 candidate genes

C2 is currently the smallest candidate region underlying differences in clasper morphology and spans a maximum of 177 kb (Chapter Three, Table 1). This region contains variation that explains 16.5% of clasper size and 33.5% of clasper bristle number differences between the species (Chapter Three – Table One), and encompasses just nine protein-coding genes (in *D. melanogaster*).

According to my GEA, only two of these genes (*trn* and *CG11279*) are considered expressed in the developing *D. simulans* or *D. mauritiana* terminalia

(Supplementary File 9), and both are differentially expressed over both pupal time points (30 hr APF and 50 hr APF, Supplementary File 9). Whilst CG11279 is consistently up-regulated in *D. simulans*, *trn* is more dynamic; being significantly up-regulated in *D. simulans* at 30 hr APF, but at 50 hr APF is up-regulated in *D. mauritiana* (Supplementary File 9). Moreover, *trn* is the only gene in C2 that is differentially expressed between the genital discs of *D. mauritiana* and *D. sechellia* (being significantly up-regulated in the latter, Supplementary File 9).

Although C2 contains just two expressed candidate genes, I conducted RNAi manipulation on all nine candidates for completeness, since there are so few. In addition, I also included *capricious* (*caps*), because although the protein-coding region of this gene lies just outside of the C2 co-ordinate boundaries, *caps* regulatory regions may still be included. Moreover, according to the RNA-Seq data, *caps* is highly expressed in the terminalia of both species, and is expressed significantly different levels (Supplementary File 7).

Analysis of clasper bristle number knock-down phenotypes showed that the only gene that significantly affected clasper number was *trn* (Dunnetts test, $p < 0.001$, Supplementary File 8b), with two different RNAi constructs generating claspers with significantly fewer bristles (Fig 20a, see UAS-*trn* #5242 and UAS-*trn* #28525). Further analysis of *trn* #5242 knock down (ANOVA $F(2, 36) = 50.7$, $p < 0.001$) and *trn* #28525 knock down (ANOVA $F(2, 39) = 153.9$, $p < 0.001$) indicates that bristle number differed significantly from both UAS- and

NP6333 controls (Fig 20a, Tukey's test, $p < 0.001$ in all cases, Supplementary File 8b). Knock-down of *trn* using #5242 and #28525 constructs reduced clasper bristle number by 12.6% and 25.7% respectively (compared to average parental phenotype, S||upplementary File 8b, Fig 20a).

Together, these experiments strongly suggest *trn* is the most promising candidate gene in C2 underlying clasper divergence, and seemingly enhances clasper growth during development. This role for *trn* appears to be exclusive to the claspers during genital development, as *trn* knock-down had no significant effect on the development of the posterior lobes compared to NP6333 using either of the constructs (Dunnetts test, $p > 0.05$, Supplementary File 8b).

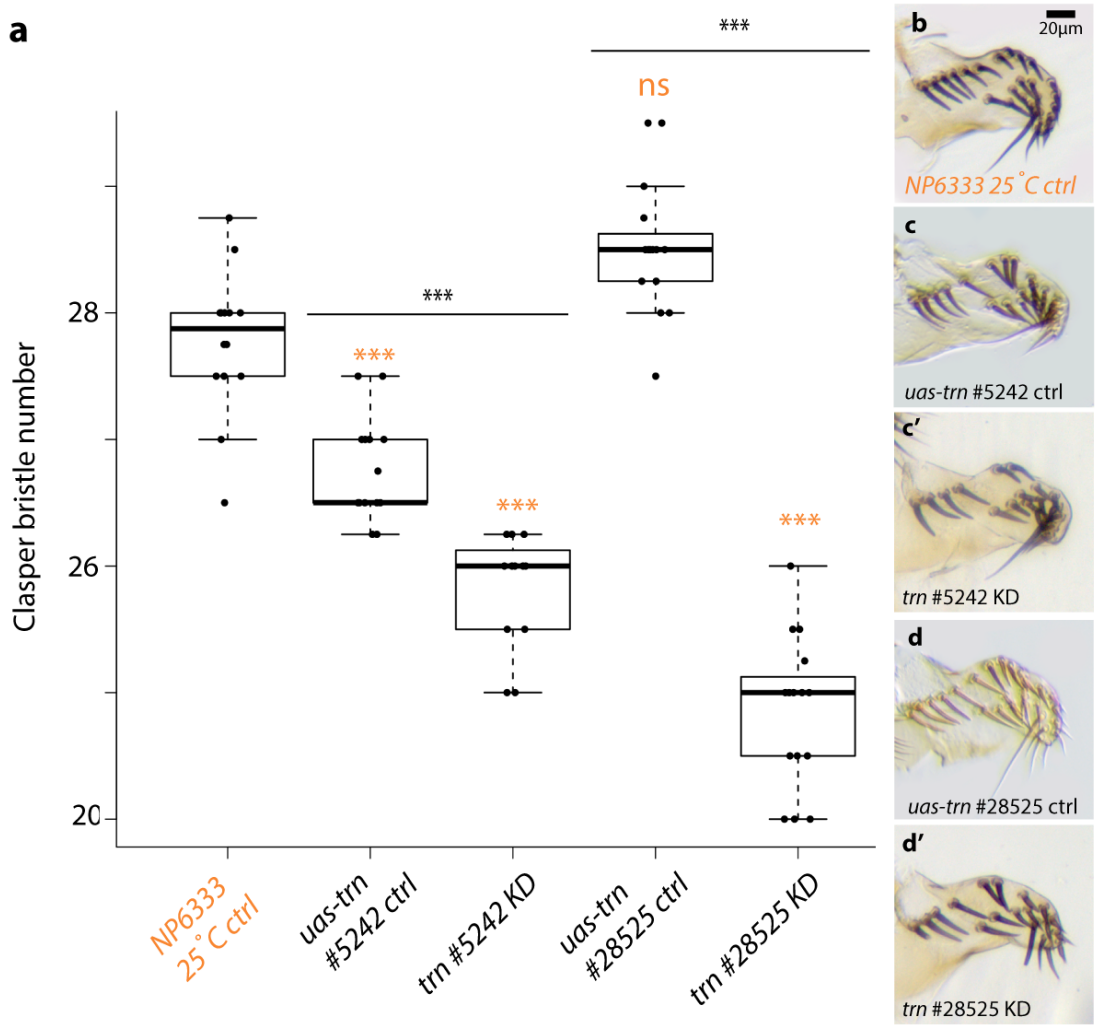


Figure 20. C2 candidate gene *trn*'s affect on clasper morphology during RNAi knock-down. (a) Knock-down of *trn* using two different RNAi contructs (#5242 and #28525) results in the development of significantly fewer clasper bristles compared to the NP6333 25'C control ($p < 0.001$ in both cases, orange asterisks), and compared to UAS- controls ($p < 0.001$ in both cases, black lines and black asterisks). Asterisks indicate significant differences detected during Tukey's test pairwise comparisons, where $p < 0.001$ *** and $p > 0.05$ = "ns" (Supplementary File 8b), for ANOVA results see main text. Colors link comparisons against NP6333 driver controls and UAS- controls / gene knock-downs, whilst comparisons between UAS- controls and knock-downs are indicated by black lines and black asterisks. Boxes indicate the range, upper and lower quartiles and median for each sample. KD = knock-down, ctrl = control. **(b – i)** morphological affect of *trn* knock-down on clasper morphology.

4.3.1 CG11279 and CG34429 in situ hybridisation in D. mauritiana and D. simulans

Although not expressed in pupal terminalia of either species (Supplementary File 9), I was unable to verify that *CG34429* does not have a role in clasper development using RNAi due to lack of an available UAS-*CG34429* line. Therefore, I conducted *in situ* hybridisation of *D. simulans* and *D. mauritiana* male genitalia to eliminate *CG34429* as a C2 candidate. Moreover, although the only other expressed gene apart from *trn*, *CG11279*, had no significant effect on clasper development during RNAi knock-down (Supplementary File 9), I also analysed *CG11279* expression to confirm this gene could also be excluded.

Unsurprisingly, I did not detect *CG11279* (Fig 21b and 21b') or *CG34429* (Fig 21c and 21c') transcripts in developing male genitalia of *D. simulans* or *D. mauritiana* at either early or late pupal stages. This result is consistent with the RNAi result for *CG11279* (no significant effect on clasper bristle number), and RNA-Seq analysis of *CG34429* in *D. simulans* and *D. mauritiana* developing terminalia (lack of expression at either 30 hr or 50 hr APF) (Supplementary File 9). I therefore exclude *CG11279* and *CG34429* as potential causative genes underlying clasper morphological differences between the species in C2.

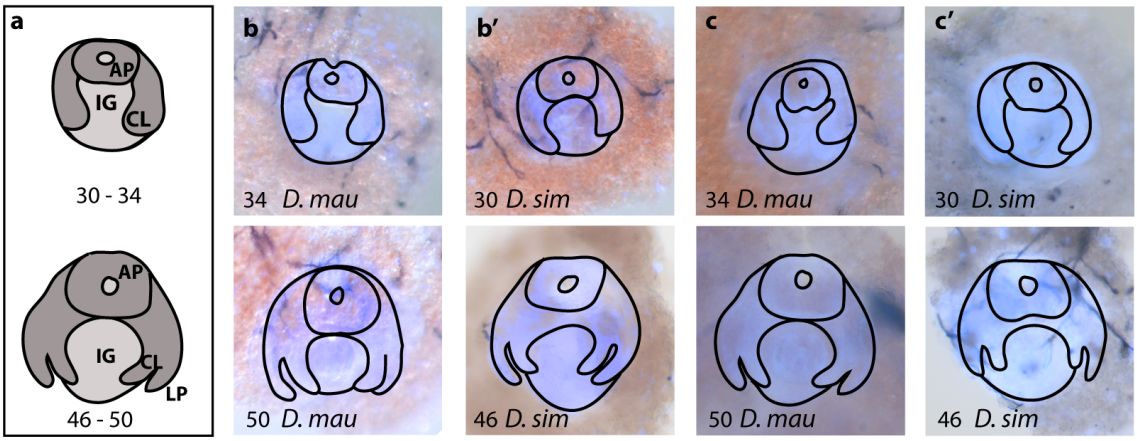


Figure 21. mRNA in situ hybridisation of CG34429 and CG11279 in *D. simulans* and *D. mauritiana* in pupal stage male genitalia. **(a)** A simplified schematic of male genital morphology at early pupal (30-34 hrs), and late pupal (46 – 50hrs) stages based on DAPI staining. Posterior lobe outgrowth was omitted for simplicity. AP = Anal plates primordia, IG = primordial of the internal genitalia and CL =clasper primordia. **(b & b')** in situ hybridisation of *CG11279* in *D. mauritiana* and *D. simulans* repectively. **(c & c')** in situ hybridisation of *CG34429* in *D. mauritiana* and *D. simulans* repectively. No transcripts were detected for either gene, in either stage / species. All panels show a frontal view, with upwards pointing dorsally and all samples have been counterstained with DAPI. Numbers indicate hours after puparium formation.

4.3.2 trn in situ hybridisation

As described above, *trn* is the only C2 candidate gene that significantly affects clasper development during RNAi. In order to confirm the presence of *trn* in the developing claspers, and to analyse expression differences between species, I conducted *in situ* hybridisation of *trn* in *D. simulans*, *D. mauritiana* and *D. melanogaster*.

While the male genitalia of all three species are still relatively under-developed (Fig 22a), a ring of *trn* expression can be detected around the anal plate primordia (AP) and in two paired patches in the tissue that will develop into the internal genitalia (IG). In *D. melanogaster*, *trn* expression could also be detected in the ventral-lateral region of the lateral plates, which are not present in the two other species at the same morphological stage (Fig 22a, see "LP").

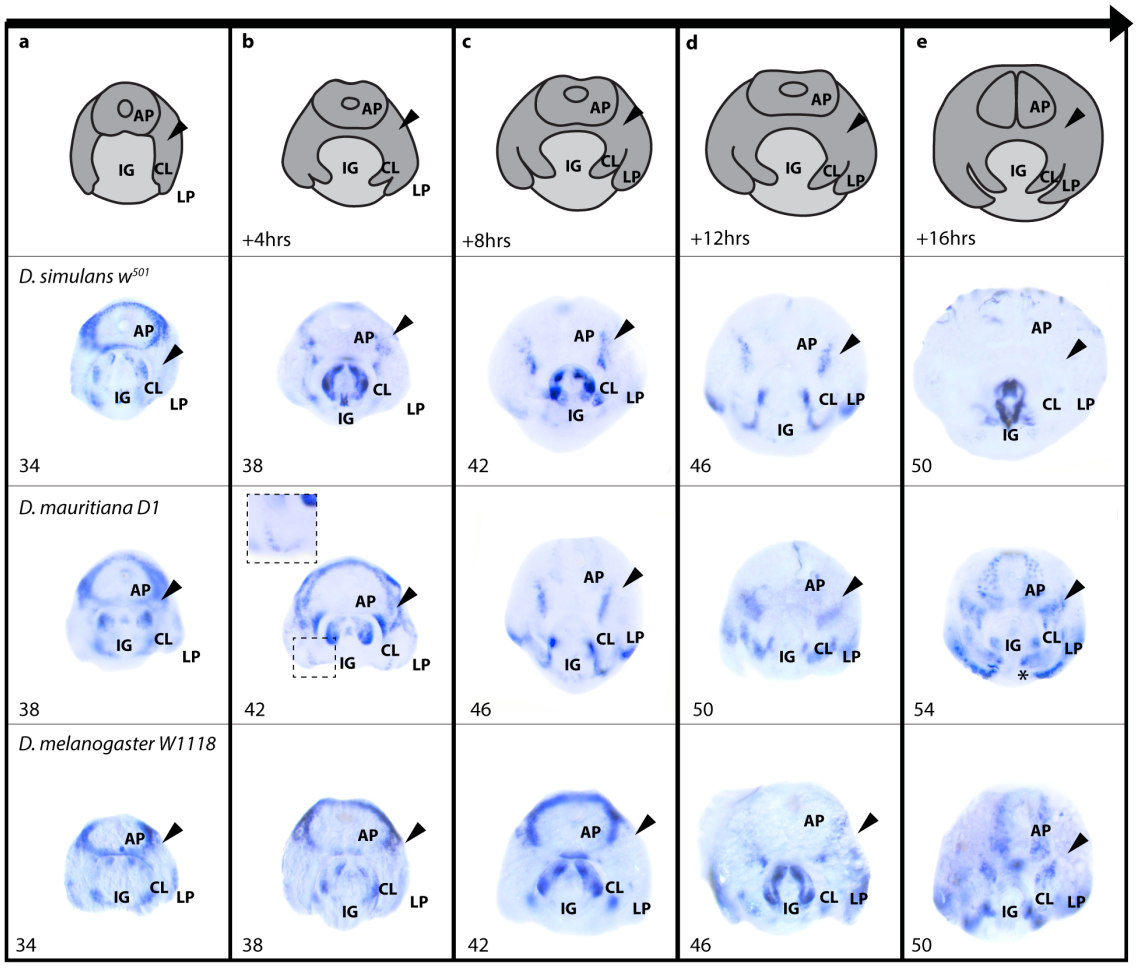


Figure 22. Time series of *trn* expression during development of male genitalia. (a – e) Illustration of the genitalia at each morphological stage based on DAPI staining (posterior lobe outgrowths were omitted for simplicity). *trn in situ* hybridisation in *D. simulans*, *D. mauritiana* and *D. melanogaster* developing male genitalia ia shown at each stage, with the hr APF indicated in each bottom left corner**.** Black arrows indicate the base of the developing clasper, which is the region with

most expression pattern divergence between the species. AP = Anal plates primordia, IG = primordial of the internal genitalia and CL =clasper primordia. Black dotted box **(b)** highlights *trn* expression at the distal edge of the clasper in *D. mauritiana* 42 hr APF, and the asterisks show clasper expression in this species as 54 hr APF **(e).**

As the claspers begin to visibly separate from the lateral plates (LP) (Fig 22b), *trn* expression retracts from around the anal plates, and begins to be expressed more ventrally towards the developing claspers in all three species (see black arrowhead, Fig 22b). However, unlike in *D. simulans*, expression could still be detected in a wide band around the edge of the anal plates in *D. melanogaster* and *D. mauritiana* (Fig 22b). In *D. mauritiana* , this wide band extends to the base of the claspers, and appears to be strongest at the inner edge (black arrows, Fig 22b). In this species, *trn* could also be detected in the distal ridge of the claspers (dashed line box, Fig 22b). *trn* expression can also be clearly detected either side of the aedeagus in all three species, which is the internal genital (IG) organ used for sperm transfer during copulation (see Introduction). However this expression appears to be slightly different in *D. mauritiana* , which contains two unilateral patches compared to the other two species in which *trn* transcripts form almost a full circle (Fig 22b).

As the claspers are almost fully separated from the surrounding lateral plate tissue (Fig 22c) *trn* is expressed as a fine band in *D. mauritiana* and less-refined in *D. simulans*, which extend from the base of the claspers towards the region of the genital arch lateral to the anal plates (AP) (black arrow, Fig 22c). In contrast, *trn* expression in *D. melanogaster* largely recapitulates expression captured at the previous stage (Fig 22b), with no clear bands detected at the

base of the clasper (Fig 22c). In *D. mauritiana* , expression at the tip of the internal genital organ is replaced by two lateral stripes of expression extending along the proximal-distal axis. In addition, *trn* transcripts can now also be detected in a patch of expression at the lateral edge of the lateral plates (LP, Fig 22c).

As the anal plate (AP) and clasper (CL) primordia becomes more defined and the genitalia as a whole grows larger (Fig 22d), these bands are finally detected in *D. melanogaster*. In *D. simulans*, these now resemble those of *D. mauritiana* in the previous stage (Fig 22c), whilst in *D. mauritiana* , they increase in width (black arrow, Fig 22d). Expression in two lateral stripes in the internal genitalia and in the lateral plates is detected in *D. simulans* at this stage.

At the final stage tested (Fig 22e), genital morphology largely resembles that of the adult structures in all three species (Fig 22e). At this relatively late stage of development, *trn* expression can no longer be detected in the developing claspers of *D. simulans* (see missing expression indicated by black arrow, Fig 22e, 50 hr APF). Expression is still detected in the internal genitalia (IG), though it is unclear whether or not this is due to background signal from the developing cuticle or is true *trn* expression (Fig 22b). In the future, additional probes can be used to determine how accessible the tissues are at this late stage in *D. simulans*. In contrast, the wide band of expression at the base of the claspers persists in *D melanogaster* and *D. mauritiana*; though is appears to be more exaggerated and wider in the latter (black arrows, Fig 22e). In addition,

transcripts can be detected at the tips of the claspers in *D. mauritiana* (asterisks in Fig 22e), which were not detected in the other species. In both *D. melanogaster* and *D. mauritiana ,* expression also persists in the lateral plates (LP), either side of the internal genital organ (IG), in the anal plates and where the anal plate bristles will develop (Fig 22e).

In conclusion, although *trn* expression at the base of the claspers appears to start later in *D. melanogaster* than that of *D. simulans* and *D. mauritiana* , *trn* expression persists in this region during the later stages of pupal development for longer, and in a wider expression domain, in the species with larger claspers (*D. mauritiana* and *D. melanogaster*, Fig 22d – 22e). This implies *trn* positively regulates clasper size in these species, which corroborates my previous analysis of *trn* whereby reducing expression levels in *D. melanogaster* significantly reduces clasper size (Fig 20). Therefore, *trn* is the likely evolved gene underlying clasper size evolution in C2, by differentially stimulating growth of the clasper between the species due to expression pattern differences (Fig 22).

4.3.3 caps in situ hybridisation

Despite my analysis indicating that *caps* has no role in clasper development (see RNAi of C2 above), I was intrigued to determine how *caps* expression differs from *trn* in the male genitalia. *Caps* and *trn* encode highly related proteins that share 67% identical extracellular domain but only 15%

identity in the intracellular domain, with the C-terminus being the most different between the proteins (Shishido et al., 1998). In some developmental contexts are known to be expressed in overlapping patterns and act redundantly to one-another (Milan et al., 2005; Milan et al., 2001; Mao et al., 2008; Sakurai et al., 2007). I therefore conducted in situ hybridisation of *caps* in *D. simulans*, *D. mauritiana* and *D. melanogaster* developing male genitalia.

Relatively early in genital development, before the claspers separate from the lateral plates (Fig 23a), *caps* expression appears to recapitulate that of *trn* at a similar morphological stage in all three species (Fig 22a). In *D. mauritiana* , *D. simulans* and *D. melanogaster*, *caps* transcripts were detected in a ring around the developing anal plates (AP), and in two paired patches within the region the internal genital primordia (IG) (Fig 23a).

As the claspers separate from the lateral plates (LP) and become defined (Fig 23b), I observed differences between *trn* and *caps* expression patterns (Fig 22b versus 23b). In all three species, *caps* expression becomes weaker in the ring around the developing anal plates, similar to our observations of *trn* (see Fig 22b). Moreover, expression in the internal genitalia between the two genes is largely indistinguishable (Fig 22b and Fig 23b). However, no expression of *caps* could be detected towards base of the developing claspers at this stage (indicated by black arrows in Fig 23b), in contrast to *trn* expression (See Fig 22b).

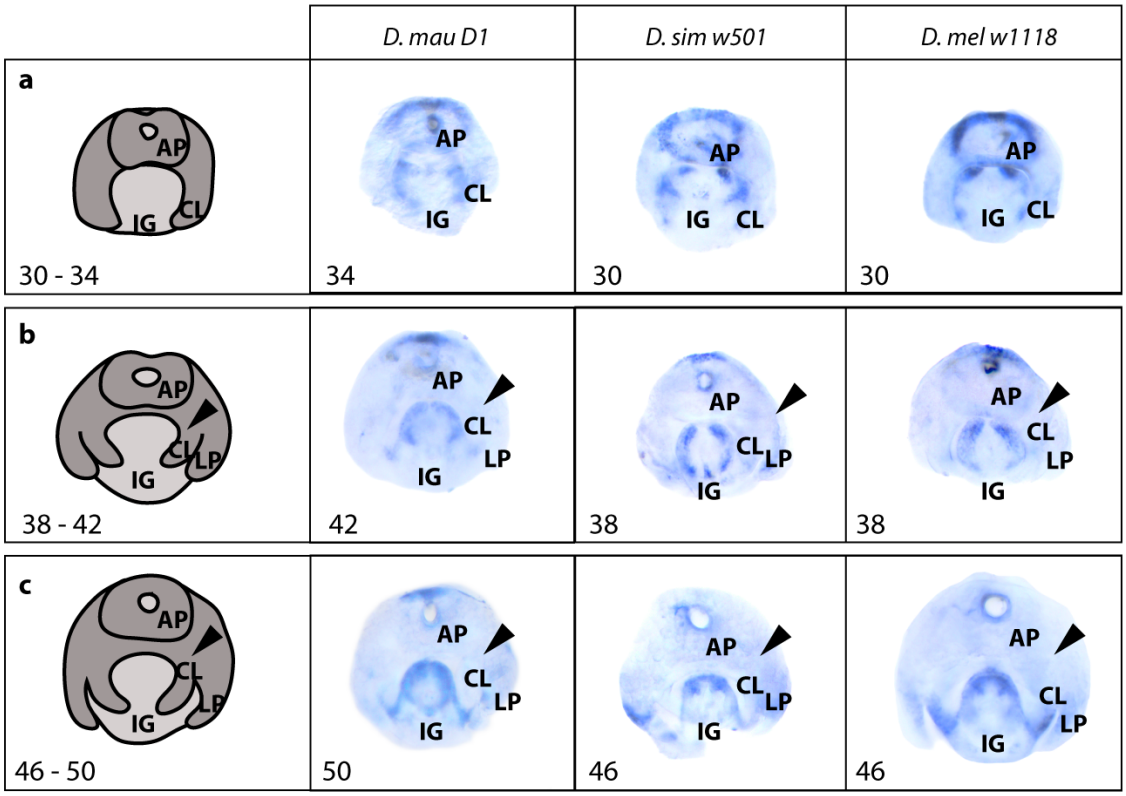


Figure 23. In situ hybridisation of *caps* in *D. mauritiana* , *D. simulans* and *D. melanogaster* over three pupal stages of male genital development. A schematic representation of morphological stage is followed by expression pattern in each species, early pupal (30-34 hrs APF) stage **(a)**, mid pupal stage (38-42hrs APF) **(b)** and late pupal (46 – 50hrs APF) stage **(c)**. Posterior lobes not illustrated for simplicity. **(a)** At early stage, *caps* transcripts could be detected in a ring of expression around the developing anal plates and within the internal genitalia in all three species. **(b)** At mid stage, *caps* transcripts can only be detected at the anterior aspect of the anal plates and internal genitalia. **(c)** *caps* expression desists in the anterior of the anal plates in *D. simulans* and *D. melanogaster*, whilst remains present in *D. mauritiana* late pupal stage. Transcripts consistently remain apparent within the internal genitalia, whilst no expression is detected at the base of the developing claspers. Black arrows indicate the base of the developing claspers, where *caps* transcript pattern differs mostly from *trn*. AP = Anal plates primordia, IG = primordial of the internal genitalia and CL =clasper primordia.

As the genitalia increases in size and the claspers appear to differentiate further (Fig 23c) *caps* expression largely resembles that of the previous stage

(Fig 23b). However, expression at the dorsal ridge of the anal plate primordia is not always present (see Fig 23c, with expression persisting in *D. mauritiana* in this region only). *caps* transcripts in the internal genitalia reproduce the pattern observed for *trn* in late-stage pupae, with stripes of expression extending down the edge of the internal genital organ (IG) (Fig 22c and 22d and Fig 23c). In contrast to *trn* expression (Fig 22d), *caps* expression was never detected at the base of the developing clasper at the stage (indicated by black arrows in Fig 23c).

From this analysis, it appears that the main difference in the expression pattern between *caps* and *trn* is the lack of expression of *caps* at the base of the developing claspers. It also appears that, based on observations between these species, *trn* expression is more dynamic within the male genitalia compared to *caps* (See Fig 23b – 22d versus Fig 23a – 23c). This suggests evolution of independent cis-regulatory regions controlling *caps* and *trn* expression in the male genitalia.

4.4 P2 candidate genes

Posterior lobe size candidate region P2 is a region of 190 kb (max), and due to overlap in the potential break points of lines used to define P2, this region contains between 0 and 7 protein-coding genes (Supplementary File 6d), and

contains variation that explains 6% of differences in posterior lobe size between the species.

Of the maximum seven protein-coding genes in candidate region P2, only *Rdl, Slc45-1* and *nwk* are expressed in *D. simulans* or *D. mauritiana* developing male terminalia (Supplementary File 9). However, it appears that whilst candidate gene *Slc-45* is significantly differentially expressed between the species throughout both pupal stage and genital disc datasets in species with larger lobes (Supplementary File 9), no significant differences in expression level could be detected for either *Rdl* or *nwk* at these stages ($p > 0.05$, Supplementary File 9). Unfortunately, however, none of these P2 candidate genes have been tested thus far in our RNAi screen.

4.5 P3 candidate genes

Region P3 contains variation that underlies 5.9% of posterior lobe size differences between *D. simulans* and *D. mauritiana* , and maps to a 394 kb (maximum) region that contains 67 protein coding genes (annotated in *D. melanogaster*) (Chapter Three – Table One). Of these 67 positional candidates, only 45 are expressed in *D. simulans* and *D. mauritiana* developing genitalia (Supplementary File 9), and only 35 of these are differentially expressed at either pupal stage (Supplementary File 9), including *SHC-adaptor protein (Shc), nbs* and *CG3552*. Six genes are differentially expressed between *D. sechellia* and *D. mauritiana* genital discs ($p < 0.001$, Supplementary File 9), but only four of

these (*astray (aay), CG16717, CG3335* and *CG3982*), are consistently differentially expressed amongst both gene data sets (Supplementary File 9).

So far, of the differentially expressed genes, we have only tested the phenotypic effect of *Shc, aay, CG3552, CG16717* and *nbs* knock-down on male genital development. None of these five genes produced significant posterior lobe size phenotype during RNAi knock-down compared to NP6333 controls (Dunnetts test, $p > 0.05$, Supplementary File 9). Interestingly however, knock-down of *CG16717* and *Shc* did significantly affect clasper bristle number phenotype compared to NP6333 controls (Dunnetts test, $p < 0.05$ in both cases, Supplementary File 8b).

Further investigation indicated *CG16717* knock-down generates significantly more bristles compared to both UAS-*CG16717* (Tukey's test, $p < 0.001$) and the NP6333 control (Tukey's test, $p < 0.05$), whilst *Shc* knock-down results in significantly fewer clasper bristles compared to UAS-*Shc* and the NP6333 control (Tukey's test, $p < 0.001$ and $p < 0.05$ respectively) (Supplementary File 2b and 3a). However, since candidate region P3 does not contain variation predicted to underlie clasper morphological divergence, *Shc* and *CG16717* are not considered as clasper candidate genes.

Based on my GEA, I suggest the next genes to be tested should be *CG3335* and *CG3982,* as these genes are consistently differentially expressed amongst both gene data sets (Supplementary File 3a). During the three stages of genital

development tested, *CG3335* is consistently upregulated in species with larger posterior lobes (*D. simulans* / *D. sechellia*, $p < 0.001$, Supplementary File 3a). *CG3982* in contrast, is more highly expressed in the smaller lobed species during pupal stages (*D. mauritiana* , $p < 0.00$), but more highly expressed in the larger lobed species at genital disc stage (*D. sechellia*, $p < 0.001$, Supplementary File 3a).

4.6 P4 candidate genes

P4 is a region of maximum 460 kb containing 52 protein-coding genes (Table One) and explains 4.7% of posterior lobe size differences between *D. simulans* and *D. mauritiana* . Only 40 of these genes are expressed in the developing genitalia according to the RNA-Seq data generated from these species (Supplementary File 9). Thirty-five of these 40 genes are differentially expressed between the species during pupal development including *ara* and *CG11279,* but only *Adenosine kinase* (*AdenoK)*, *Ribosomal protein S12 (RpS12)* and *CG10960* are also differentially expressed genital discs of *D. mauritiana* and *D. sechellia*.

So far, of positional candidates in P4 with interesting expression profiles, we have only tested the phenotypic effect of *araucan (ara)* and *CG11279* in our RNAi screen (note, CG11279 is included in both C2 and P4 as lies on the border of both regions). Both of these genes are expressed differentially between *D.*

simulans and *D. mauritiana* over both pupal stages (with ara being consistently upregulated in *D. mauritiana* and CG11279 in *D. simulans*) (Supplementary File 9). We detected no significant morphological phenotypes in *ara* or *CG11279* knock-downs for either posterior lobe size, (or moreover clasper bristle number) compared to NP6333 controls (Dunnetts test, $p > 0.05$, Supplementary File 8b).

Based on my GEA, I would next recommend testing the function of *AdenoK, RpS12* and *CG10960* in posterior lobe development. *AdenoK* appears to be consistently more highly expressed in larger lobes species ($p < 0.001$, Supplementary File 3a). *RpS12* in contrast, is more highly expressed in the larger lobes species during genital disc stage ($p < 0.01$, *D. sechellia*, Supplementary File 3a), but more highly expressed in the smaller lobed species at early pupal stage ($p < 0.05$, *D. mauritiana* (not significantly different between species at 50 hr APF, $p > 0.05$), Supplementary File 3a). *CG10960* also appears to be dynamic in expression, being significantly up-regulated in *D. mauritiana* at genital disc stage (small lobes), higher expression in *D. simulans* at early pupal stage (large lobes, 30 hr APF), and then subsequently up-regulated in the smaller lobed species later in development (*D. mauritiana* , 50 hr APF) (Supplementary File 3a).

4.7 P5 candidate genes

From analysis conducted in Chapter Three, I mapped candidate region P5 to a region of 1.14 Mb (maximum), that contains 91 – 78 candidate genes and contains variation able to explain 9% of posterior lobe size differences between species.

Of the maximum number of genes in candidate region P5, only 61 are expressed in either *D. simulans* or *D. mauritiana* male genitalia during pupal stages (Supplementary File 9). However, just 48 of these genes are differentially expressed between *D. simulans* and *D. mauritiana* pupal terminalia (Supplementary File 9), and only 15 are differentially expressed between *D. mauritiana* and *D. sechellia* genital discs (Supplementary File 9).

Unfortunately, we are yet to functionally test any of the P5 candidate genes using RNAi (Supplementary File 9). Based on my GEA, I would first test the candidate genes *Hemolectin (Hml)*, *CG3919* and *big bang (bbg),* which are consistently upregulated in the larger lobes species during the tested stages of genital development, and *CG7924* and *CG32137,* which are consistently downregulated (Supplementary File 9). *Ral guanine dissociation stimulator-like (Rgl), Hsc70Cb, CG94914, CG9384, CG9425* and *Sox21b* could also be tested, as these are consistently differentially expressed but appear to undergo dynamic expression regulation (Supplementary File 9).

4.8 Chapter Four – Summary

From the 382 positional candidate genes (Chapter Three, Table 1), only 255 had detectable expression in *D. simulans* and/or *D. mauritiana* pupal terminalia (Fig 24). I then subsequently determined that only 190 of these genes are differentially expressed between the species during pupal stages, though only 41 of these are also different in expression between *D. sechellia* and *D. mauritiana* genital discs (Fig 24).

The successful reduction of a possible 312 to 9 C2 candidate genes by introgression mapping (Fig 9), and subsequent expression analysis of these candidates inferred that *trn* is the likely evolved gene in C2. In contrast, the generation of new ILs did not improve the resolution of region C1 (Fig 15), but expression and functional analysis revealed *Gug, h, Cpr66D, Mcm7* and *foi* are strong developmental candidates (Fig 17). Although the *in situ* hybridisation expression profile of *Cpr66D* in the claspers of *D. simulans*, *D. mauritiana* and *D. melanogaster* warrants functional testing of this gene, this analysis is still required to rule out the possibility of these other C1 genes. In addition, to complete candidate analysis of this region, *in situ* hybridisation of *SrpRBeta* and *rhea* should be attempted, since RNAi of these genes produced lethality and unmeasurable phenotypes.

In the future, expression analysis of P2 candidate genes should be prioritised, as this region contains only three expressed genes (*Slc-45, Rdl, nwk,*

Supplementary File 9). None of these P2 genes have been tested in our RNAi screen, but since *Rdl* and *nwk* are expressed at a low level (< 2rpkm at any time point, in either species), and moreover neither of these genes are differentially expressed, in comparison to *Slc-45,* which is consistently upregulated in larger-lobed species in all three genital stages, Supplementary File 9), it is likely that Slc-45 is the evolved gene in P2.

In contrast, other candidate regions still contain an extensive number of candidate genes (Table 1). To date, only one C0 and one P1 candidate gene has been associated with clasper and lobe development, respectively – *sgl* and *Surf1* (Fig 16), and in some regions, such as P5, no genes have so far been tested. However, as described at the end of each section, I have identified a manageable number of genes with interesting expression profiles (e.g. that are differentially expressed between species) for future RNAi analysis (see Chapter Four - (P1) *CG10289, Best2*, *loj*, (P3) *Ribosomal protein 17 (Rps17), CG3982, CG3335* and *CG8177,* (P4) *mirr*, *CG10960, AdenoK, RpS12, mRpL20,* (P5) *Hml, CG3919, bbg, CG7924, CG32137, Rgl, Hsc70Cb, CG94914, CG9384, CG9425* and *Sox21b*), (C0) CG10289, Best2, SP1173, *loj*, (C1) *ergic53, sperm-Leucylaminopeptidase (s-Lap2), CG6511*

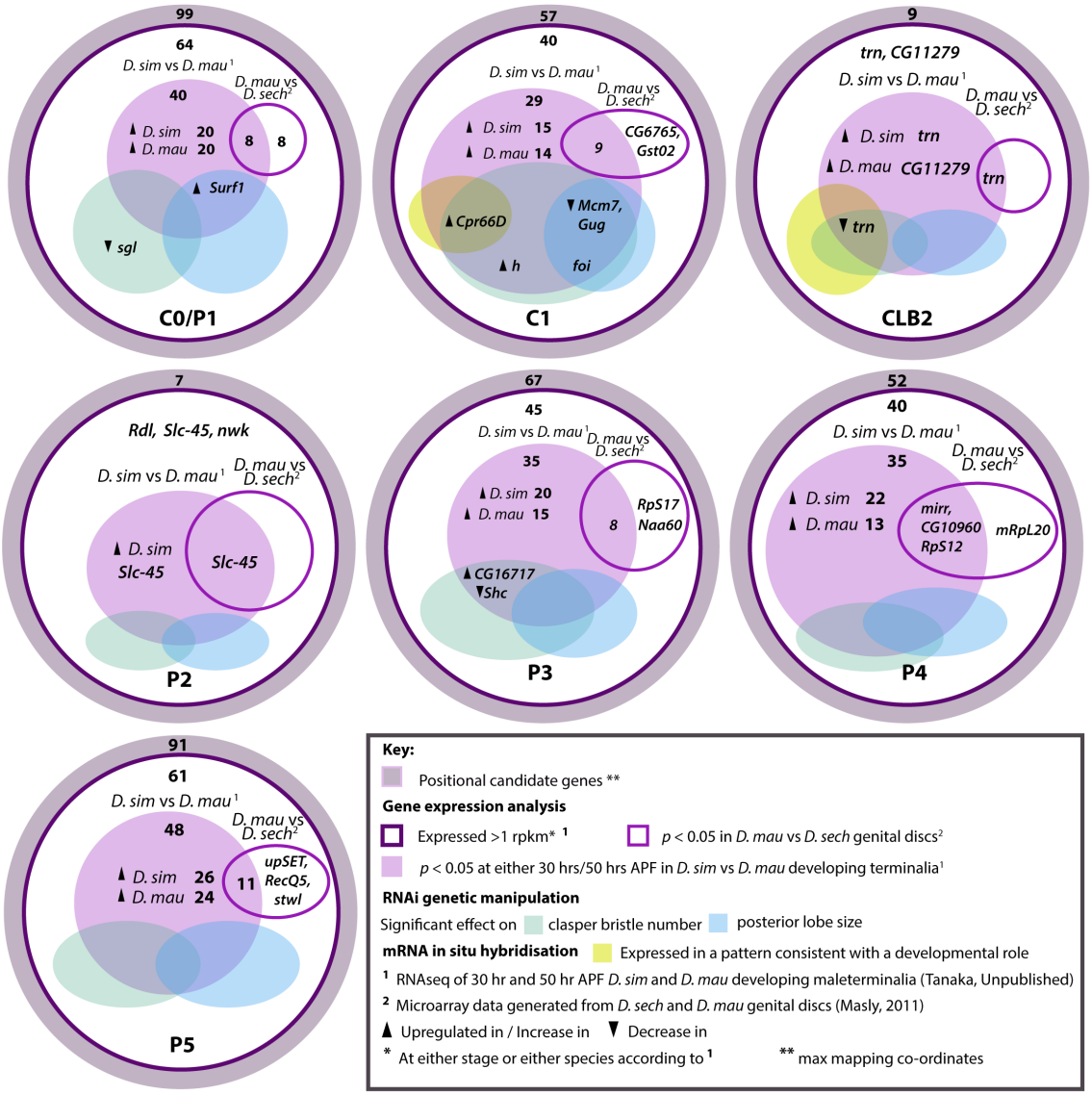


Figure 24. Summary of gene expression analysis and genetic manipulation of positional candidate genes. (a – i) Breakdown of expression analysis for each predicted region underlying clasper (CL/CLB) and posterior lobe (PL) size divergence using RNA-Seq data (Tanaka, unpublished and Masly, 2011), and RNAi knock-down. A colour key is indicated in the figure legend.

In order to better understand how *Cpr66D*, *trn* and the other genes highlighted during the RNAi screen could underlie clasper or posterior lobe evolution, their current known functions will now be described.

4.8.1 Surf1

Surf1 encodes a highly conserved protein amongst eukaryotes and prokaryotes, which is involved in the assembly if the inner mitochondrial membrane protein cytochrome c oxidase (Da-Re et al., 2014; Poyau et al., 1999). Interestingly, *Surf1* mutations are predominantly used as a disease model for Leigh Syndrome, which is a progressive mitochondrial encephalopathy in humans (Da-Re et al., 2014). In *D. melanogaster*, *Surf1* mutants exhibit a range of phenotypes; including general decrease in body size, slowed development, loss of abdominal muscles, decrease ability to phototax and lethality. These phenotypes, and presumably those observed in the RNAi knock-down of *Surf1* in the developing posterior lobes (Fig 16d – 16f'), are thought to be caused by disruption of energy supply from the mitochondrial defects caused by *Surf1* manipulation (Da-Re et al., 2014; Poyau et al., 1999).

4.8.2 sgl

sgl, also known as *kiwi*, encodes the enzyme, UDP-glucose dehydrogenase, which is necessary for the production of the factors required to biosynthesise many glycosaminoglycans and proteoglycans (Princivalle and de Agostini, 2002; Binari et al., 1997). These enable signal transduction of developmental signalling pathways such as Fibroblast Growth Factor (FGF

signalling), and are associated with the generation and regulation of their morphogen gradients (Princivalle and de Agostini, 2002; Binari et al., 1997; Haerry et al., 1997). Indirectly therefore, enzymes such as *sgl* are associated with many developmental processes, such as adhesion, motility, differentiation, mechanical support and growth (Carey, 1997; Perrimon and Bernfield, 2000). Disruption in any one of these mechanisms may explain the reduction in clasper size observed during *sgl* knock-down (Fig 16a – 16c').

4.8.3 Mcm7

Mcm7 forms part of the Cdc45-Mcm-GINS (normally referred to as CGM) complex; a helicase functioning during DNA replication. Studies have shown that mutations in *Mcm7* proteins disrupt the timing of DNA replication, which is essential for successful proliferation (Blumroder et al., 2016). Therefore, the ability of *Mcm7* to regulate clasper development (Fig 17a and 17e'), and development of the posterior lobes (Fig 18a, 18d') may be through disruption in proliferation. Considering the role of *Mcm7* in regulating this fundamental process and the observation that candidate region C1 contains variation in clasper morphology only if *Mcm7* has evolved, it is likely through cis-regulatory divergence. In situ hybridization of *Mcm7,* for example, could allow expression differences to be specifically detected in the clasper.

4.8.4 Cpr66D

Cpr66D encodes a chitin based cuticular protein, and is associated with cutical formation of the developing corneal lens (Stahl et al., 2017), trachea (Chandran et al., 2014) and wing (Ren et al., 2005). Given the role of *Cpr66D* in cuticle formation, the effect of *Cpr66D* knock-down in generating larger claspers is perhaps counterintuitive (Fig 17a and 17d').

Contradictory to this RNAi effect, but more in line with my expectations based on *Cpr66D*'s known roles, in situ analysis has shown that *Cpr66D* is consistently more highly expressed at the base and along the internal edge of the claspers in of species with larger sized organs (Chapter Four, Fig 19). These differences in expression provide a tangible mechanism for evolution of clasper size; driven by cis-regulatory evolution of *Cpr66D*.

4.8.5 foi

RNAi of *foi* generated a very severe fusion phenotype amongst all the paired appendages of the *D. melanogaster* male genitalia (Chapter Four, Fig 17i). This rendered it difficult to say whether *foi* RNAi increased or decreased the number of bristles and the size of the claspers. Since this gene is known to be involved in aiding in cell migration, or specifically, the halting of cell migration when cells reach their correct location, this severe phenotype is perhaps

unsurprising (Mathews et al., 2006; Pielage et al., 2004; Van Doren et al., 2003). *Foi* encodes a zinc transporter protein, which controls zinc influx into the cell (Carrasco-Rando et al., 2016; Gaither and Eide, 2001; Mathews et al., 2006). Many of the observed phenotypes of *foi* manipulation, including miss-specification and miss-targeting of muscle cells (Mathews et al., 2006), fusion of competent myoblasts (Van Doren et al., 2003), failure in gonad coalescence (Pielage et al., 2004), and presumably the phenotype detected during *foi* RNAi, are thought to stem from the disrupted activity of zinc-finger transcription factors which depend on correct zinc homeostasis.

4.8.6 Gug

Gug, (also known as *Atrophin*), is a nuclear co-repressor, which has been shown to regulate the expression of numerous developmental patterning genes (Zhang et al., 2013; Charroux et al., 2006; Yeung et al., 2017). Miss-regulation of these down-stream genes in the imaginal wing disc or eye disc results in the production of significantly smaller size wings, and a rough-eye phenotype. Therefore, it is likely that *Gug* contributes to clasper development (Fig 17a and 17h') and posterior lobe development (Fig 18a and 18c') by regulating the activity of downstream patterning genes in the genitalia. Therefore, similarly to *Mcm7*, if *Gug* has evolved to change clasper size between the species, it is likely due to the evolution of cis-regulatory factors, which affect expression in the claspers, without affecting expression in the lobes.

4.8.7 h

h is a pair rule gene, that acts as a long-range basic helix-loop-helix (bHLH) transcriptional repressor (Ohsako et al., 1994; Van Doren et al., 1994) by recruiting Groucho (Gro) to target promoters across the genome. Through this repressive activity, *h* regulates many developmental roles, such as patterning of the embryonic body plan (Ingham et al., 1985), but also has post-embryonic roles in determining cell fate, particularly in bristle formation. For example, *h* has been associated with sternopleural bristle number variation in *D. melanogaster* (Robin et al., 2002), the patterning of mechanosensory bristles on *D. melanogaster* T2 legs (Orenic et al., 1993), bristle patterns (or lack of) on thorax structures involved in flight (Costa et al., 2014). Therefore, it is perhaps unsurprising that knock-down of the aptly named *hairy* results in abnormal clasper bristle development (Fig 17 and 17c').

4.8.8 Trn

Trn was discovered through a P{lacW} enhancer trap screen, and subsequently named after its striking expression pattern in the developing embryo and L3 larval imaginal discs (Chang et al., 1993).

The protein-coding region of *trn* encodes a transmembrane adhesion protein, with an XC domain consisting primarily of tandemely arranged Leucine-Rich-Repeat's (LRR's) (Chang et al., 1993; Shishido et al., 1998). In both prokaryotes and eukaryotes, LRR's occur in an abudance of proteins known to regulate diverse processes, ranging from patterning, signal transduction, adhesion, cell migration, DNA repair, RNA processing and transcription (Berger-Muller et al., 2013; Hocking et al., 1998; Hong et al., 2009; Kobe and Deisenhofer, 1995; Kobe, 1994; Krantz and Zipursky, 1990; Kurusu et al., 2008; Milan et al., 2001; Shishido et al., 1998)

In the Introduction, I described the activity of patterning genes in specifying compartments of the imaginal discs. Maintenance of these boundaries is essential for successful for patterning and growth control (Dahmann and Basler, 1999; Milan and Cohen, 1999). Interestingly, *trn* is known to regulate these compartmental boundaries in the *Drosophila* wing disc and leg disc (Milan et al., 2002; Milan et al., 2001), and the mammalian homologue, *Lrrn1,* also aids in the formation of the midbrain-hindbrain boundary (Tossell et al., 2011).

As well as organizing cells in the imaginal discs, in *Drosophila*, *trn* is also known to regulate cell migration in the developing trachea and during motor-neurone axon guidance (Krause et al., 2006; Bugga et al., 2009), and this is thought to be possible through the role of *trn* in conferring "information" to migrating cells, which allows them to coordinate themselves to the correct

locations (Krause et al., 2006; Bugga et al., 2009). Moreover, it has been suggested that *trn* regulates cell organization by imposing increased mechanical tension between cells, based on the "identity" conferred by the expression of patterning genes (Michel et al., 2016).

Therefore, *trn* RNAi phenotypes in the developing claspers (Fig 20) can perhaps be explained by disruption of normal compartmental boundaries of the genital disc, or perhaps generally by miss-organising cells as the claspers evert from the disc and differentiate. Although expression of *trn* was not analysed at the genital disc stage, during pupal stages the miss-specification of cells could occur at the base of the developing clasper (Fig 22). The expression differences detected in this region may therefore explain how *trn* evolution differentially regulates clasper size between species, and implies divergence of the elements able to drive *trn* expression at the base of the claspers.

Based on my analysis of C2 in this chapter, its appears *trn* is likely to be an evolved clasper gene, underlying 16.4% of differences in clasper size, and 33.5% of differences in clasper bristle number between *D. simulans* and *D. mauritiana*. In the following chapter, I will attempt to functionally validate whether or not *trn* has evolved to alter clasper morphology between the species.

5 Chapter Five - Results

Functional validation of the Leucine-Rich-Repeat trans-membrane protein *trn* in clasper morphological divergence

From analysis conducted in Chapter Four, I was able to identify a handful of promising candidate genes underlying male genital evolution between *D. simulans* and *D. mauritiana*. In candidate region C2, *trn* is the only gene expressed in the developing claspers (Fig 22), and is the only gene involved in their development (Fig 20). Therefore, it is likely that *trn* evolution (probably cis-regulatory, giving rise to expression pattern differences detected in Fig 22), contributes to the 16.4% of clasper size and 33.5% of clasper bristle number differences between the *D. simulans* and *D. mauritiana* predicted for C2 (Table One). The aim of this chapter is to functionally validate *trn* as the evolved gene in C2, and to characterise its contribution to clasper morphological divergence.

5.1 Knock-out of *trn* in *D. simulans* and IL 43 using CRISPR

In order to test the involvement of *trn* in clasper divergence, I generated *trn* knock-outs in *D. simulans* w^{501} and in the introgression line IL 43 (i.e. the *D. mauritiana* allele of *trn*) using the CRISPR-Cas9 reagents illustrated in Fig 25 (see Methods and Supplementary File 10 for primer design). Injection of these reagents (Cambridge Fly Facility, Methods), along with an endogenous source of Cas9 from the X chromosome, generated a double-stranded cut 121 bp into the first coding exon of *trn* in both lines (Fig 25). This introduced a frame shift mutation by the insertion of a visible DsRed marker and multiple stop codons, which disrupt *trn* protein production (not yet experimentally confirmed).

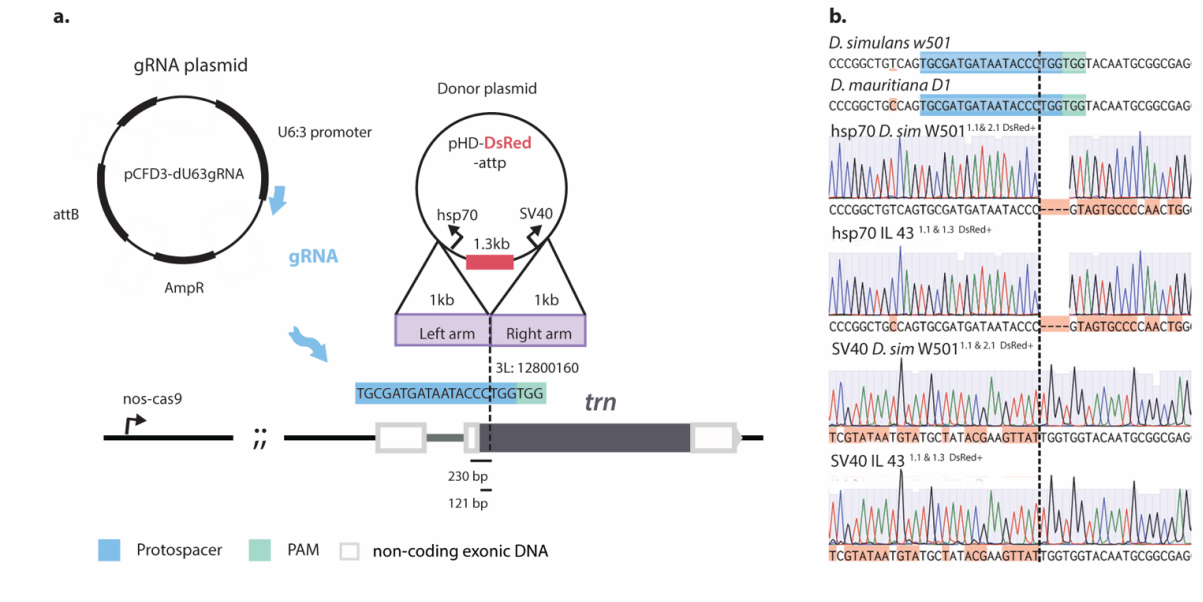


Figure 25. CRISPR strategy for generation of *trn* knock-outs in *D. simulans* w^{501} and IL 43. (a) gRNA (pCFD3-dU63gRNA) and donor plasmid (pHD-DsRed-attp) used to generate a double stranded cut 121 bp into the coding region of *trn* using CRISPR-mediated homologous recombination. hsp70 and SV40 primers are shown and a colour key is indicated in the bottom left corner. PAM =

protospacer adjacent motif **(b)** Chromatograms illustrating the disruption of the *trn* locus in *D. simulans* $w^{501\ s1.1\ \&\ s2.1}$ and IL $43^{m1.1\ \&\ m1.3}$ using hsp70 and SV40 primers.

DsRed positive G0s were identified and backcrossed to the respective lines sent for injection; since *trn* knock-outs have previously been shown to be homozygous lethal in *D. melanogaster* (Chang et al., 1993). As can be seen in Fig 25b, cut sites were validated in two randomly selected DsRed positive male G0 stocks from *D. simulans* knock-outs (*D. simulans* $w^{501\ s1.1}$ and *D. simulans* $^{s2.1}$), and two IL 43 knock-outs (IL $43^{m1.1}$ and IL $43^{m1.3}$) using hsp70 and SV40 primers (Fig 25b). I therefore confirmed the double-stranded cut occurred at an identical position in these four lines (121 bp into the first coding exon), and so *D. simulans* $w^{501\ s1.1}$, *D. simulans* $w^{501\ s2.1}$, IL $43^{m1.1}$ and IL $43^{m1.3}$ were used for all downstream analysis.

5.2 Reciprocal hemizygosity test of *trn* on clasper morphology

Using the lines described above, I conducted the reciprocal hemizygosity test (Stern, 2014). As previously described, this test allows the identification of causative genes underlying phenotypic differences between strains or species ((Stern, 2014) see Introduction). In this case, it involves the comparison of clasper size and bristle number measurements between *trn* reciprocal hemizygotes (i.e. males that are genetically identical, except for which species-specific functional allele of *trn* they contain).

In order to generate reciprocal hemizygotes of *trn,* DsRed positive males from *D. simulans* w^{501} $^{s1.1\ \&\ s2.1}$ and IL 43$^{m1.1\ \&\ m1.3}$ *trn* knock outs (which are hemizygous for *trn*) were crossed to homozygous females of the reciprocal line (e.g. *D. simulans* w^{501} or IL 43). For example, to test the effect of the *D. mauritiana trn* allele on clasper morphology, *D. simulans* $^{s1.1}$ ($trn^s trn^{s1.1}$) males and *D. simulans* $^{s2.1}$ ($trn^s trn^{s2.1}$) males were crossed to IL 43 ($trn^m trn^m$) females (Fig 26a). The resulting male F1 DsRed positive progeny are therefore hemizygous for *trn* ($trn^m trn^{s1.1}$ and $trn^m trn^{s2.1}$), with *D. mauritiana trn* being the only functioning allele.

Conversely, to test the effect of the *D. simulans trn* allele on clasper morphology, IL 43$^{m1.1}$ ($trn^m trn^{m1.1}$) males and IL 43$^{m1.3}$ ($trn^m trn^{m1.3}$) males were crossed to *D. simulans* w^{501} ($trn^s trn^s$) females (Fig 26a). Therefore, in contrast to the progeny of the previous cross, these contain a *D. simulans* functioning *trn* allele ($trn^s trn^{m1.1}$ and $trn^s trn^{m1.3}$) (Fig 26a). Since this is the only genetic difference, comparison of clasper phenotype between these F1 males allows us to directly test the effect of *trn* evolution on clasper morphology between the species.

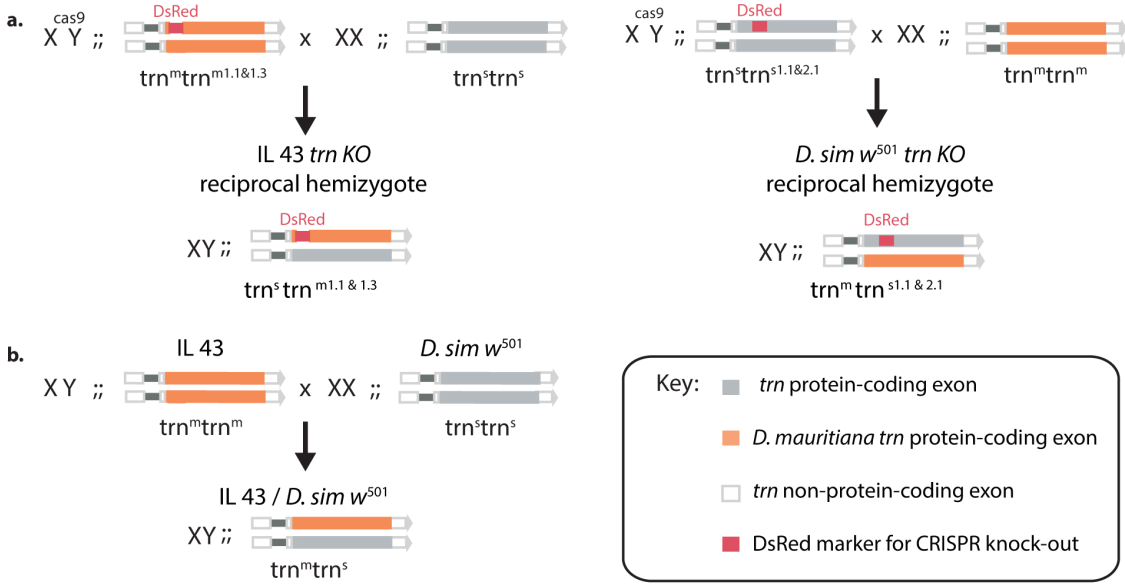


Figure 26. Crossing strategy for functionally testing *trn* alleles and characterising the contribution of this gene to clasper evolution. (a) Generation of *trn* reciprocal hemizygotes (*trn*s*trn*m1.1&1.3 and *trn*m*trn*s1.1&2.1) used to test the effect of species-specific *trn* alleles on clasper morphology. **(b)** IL 43 / *D. simulans* w^{501} heterozygous control for analyzing allelic dominance of *trn* between *D. simulans* and *D. mauritiana* (e.g. which species-specific allele contributes more to IL 43 / *D. simulans* w^{501} heterozygous phenotype). A colour key is indicated in the mid-right hand panel.

Analysis of body size (using T1 tibia length) between these four reciprocal hemizygotes ($trn^{s}trn^{m1.1}$, $trn^{s}trn^{m1.3}$, $trn^{m}trn^{s1.1}$ and $trn^{m}trn^{s2.1}$) indicated no significant differences ($F(3,93) = 0.554$, $p = 0.647$) (raw data can be found in Supplementary File 11a, and statistical analysis of reciprocal hemizygotes in Supplementary File 11b). In contrast, comparison of clasper morphology between these lines gave rise to significant differences in both clasper area ($F(3, 61) = 7$, $p < 0.001$) and clasper bristle number ($F(3, 83) = 26.3$, $p < 0.001$) (Supplementary File 11b). These differences stem from comparisons between *D. simulans* hemizygotes against *D. mauritiana* hemizygotes for clasper

size (Tukey's test, $p < 0.01$, in all cases, Fig 27a) and bristle number (Tukey's test, $p < 0.001$, in all cases, Fig 27b) (Supplementary File 11b). In contrast, hemizygote duplicate phenotypes were consistently the same as each other for both traits (Tukey's test, $p > 0.05$ in both cases, Supplementary File 11b).

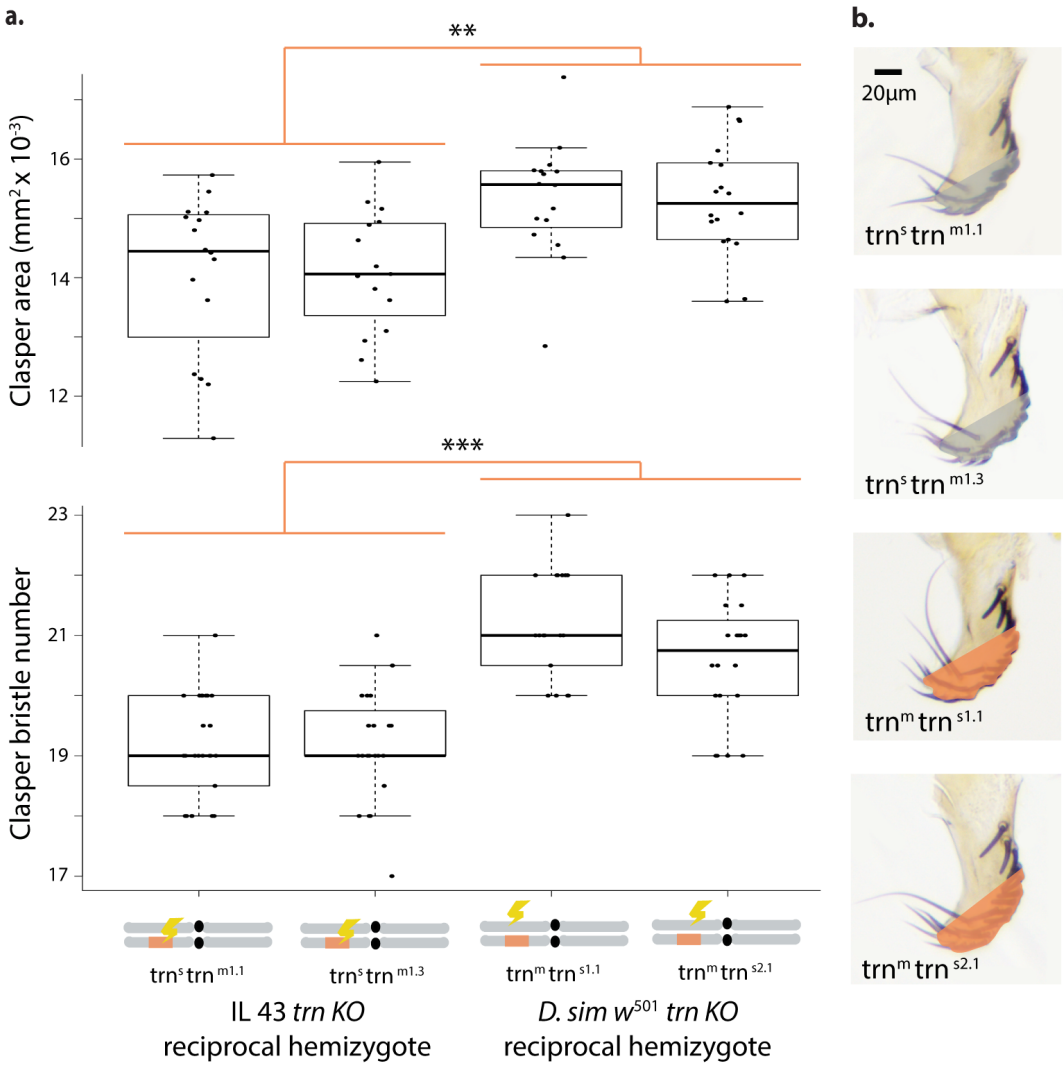


Figure 27. The phenotypic effect of *trn* evolution on clasper morphology. (a) The upper and lower plot shows the effect of *trn* evolution on clasper size and clasper bristle number respectively. The schematic below illustrates the state of (or manipulation of) *trn* in each case, with lightning bolts indicating *trn* KO by CRISPR. The orange lines within each plot show comparisons between reciprocal hemizygotes for both traits. The *D. mauritiana trn* allele confers larger claspers (Tukey's test, $p < 0.01$) with more bristles (Tukey's test, $p < 0.001$)

compared to the *D. simulans trn* allele. Asterisks indicate Tukey's test pairwise comparisons with significance value of $p < 0.01$** and $p < 0.001$***. Boxes indicate the range, upper and lower quartiles and median for each sample. Shading in the bottom panel **(b)** indicates the area measured at the distal end of the claspers in lines containing *D. simulans* (grey) or *D. mauritiana* (orange) *trn* functional alleles.

As can be seen in Fig 27a and 27b, in males where the only functioning *trn* allele is *D. mauritiana* -specific, claspers are significantly larger and contain more bristles than those with a *D. simulans*-specific *trn* allele. These results show that *trn* is the evolved gene in candidate region C2, contributing to clasper size differences between the species.

On average, the *D. mauritiana* hemizygote phenotype explains 7% of the difference in clasper size between the species, and 39% of the difference in clasper bristle number (which equates to two clasper bristles). These findings are roughly consistent with the expected effect size, as ILs homozygous for *D. mauritiana trn* contain variation explaining roughly double this effect for the quantitative trait of clasper bristle size (16.3%), and all the effect for the discrete trait of clasper bristle number (33.5% which equates to 1.7 clasper bristles) (Chapter Three – Table 1).

According to my introgression analysis, candidate region C2 contains variation that underlies clasper size differences only, with posterior lobe size being unaffected (Chapter Three). Therefore, *trn* evolution is not expected to affect posterior lobe size. In order to test this, I compared posterior lobe measurements between reciprocal hemizygotes ($trn^{s}trn^{m1.1,}$ $trn^{s}trn^{m1.3,}$

trn^{m}*trn*$^{s1.1}$ and *trn*^{m}*trn*$^{s2.1}$) (Supplementary File 11b). As expected, *trn* reciprocal hemizygotes did not differ in posterior lobes size ($F(3,84) = 0.114$, $p = 0.952$). Therefore, *trn* represents an evolved gene that has been able to drive clasper size divergence independently from posterior lobe size differences between the species.

5.3 *trn* allelic dominance

In order to improve our understanding of how *trn* alleles may have evolved in *D. simulans* and *D. mauritiana* species, I assessed *trn*^{m} and *trn*^{s} allelic dominance. To do this, I compared absolute differences in clasper size between males homozygous for *trn* (e.g. IL 43, *trn*^{m}*trn*^{m} and *D. simulans* w^{501}, *trn*^{s} *trn*^{s}) against males heterozygous for *trn* (IL 43 / *D. simulans* w^{501}, *trn*^{m} *trn*^{s}) (see Supplementary file 11a for raw data, and Methods).

Comparison of these absolute differences indicated that the heterozygous males are not a perfect intermediate in clasper size phenotype between the homozygous parental strains (Wilcox rank sum test, $p < 0.001$, $W = 59407$, Supplementary File 11c) indicating an element of dominance. Heterozygous males are skewed towards the homozygous *D. mauritiana trn* phenotype, indicating that *trn*^{m} alleles are dominant over *trn*^{s} alleles (Fig 28, Supplementary File 11c). This corroborates analysis by Tanaka et al., (2015), which determined using much larger introgression lines, that *D. mauritiana* alleles are dominant over *D. simulans* alleles in C1 and C2 (Tanaka et al., 2015).

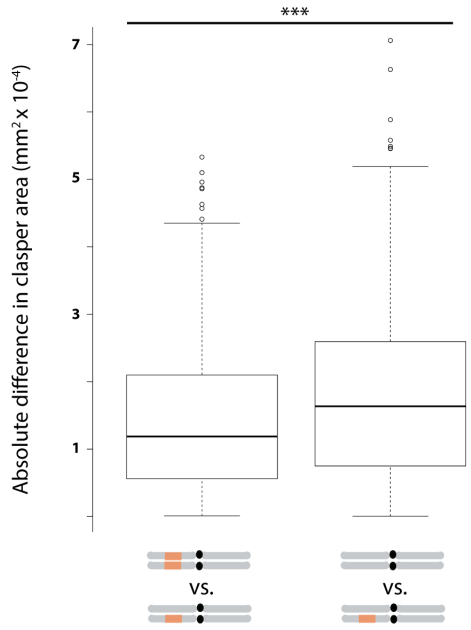


Figure 28 – *trn* allelic dominance analysis. Absolute difference between trn^{m} trn^{m} and trn^{m} trn^{s} (left-hand side) and between trn^{m} trn^{s} and trn^{s} trn^{s} (right-hand side) are not the same (Wilcox Rank Sum Test, $p < 0.001$, W = 59407). trn^{m} trn^{s} claspers are more similar in size to trn^{m} trn^{m}, than trn^{m} trn^{s}. Asterisks indicate significant level, where $p < 0.001$ *** during a Wilcox rank sum test. Boxes indicate the range, upper and lower quartiles and median for each sample.

6 Chapter Six - Results

The regulation of *trn* in the developing *Drosophila* male genitalia

In Chapter Four, I showed the effect of changing *trn* expression level on the development of the claspers in *D. melanogaster* (Fig 20), and the natural variation in *trn* expression in the male genitalia between *Drosophila* species (Fig 22). In particular, I revealed that the largest difference in expression is at the base of the developing claspers, which differs both temporally and spatially between species. This is also the main expression difference between *trn* and *caps* in situ analysis (Fig 23). Together, these results imply that cis-regulatory evolution of *trn* in the base of the claspers underlies clasper differences between species. This hypothesis is supported by previous analysis of the Trn coding region between *D. simulans* w^{501} and *D. mauritiana* D1, which identified three non-synonymous differences, but none are fixed in either species (see rows 25, 27 and 28, Supplementary File 6, Hagen et al., BioRxiv).

In this chapter, I analysed which domains of *trn* expression have a role in male genital development, and then attempt to identify cis-regulatory elements in C2 that can drive expression in these regions at the same stage. After identifying a candidate enhancer, I then performed sequence analysis to reveal variant nucleotides that differentially affect TF binding affinity between

Drosophila species, and therefore could be the causative variation underlying the role of *trn* in clasper evolution.

6.1 Analysis of *trn* expression in *Drosophila* claspers

As can be seen in Fig 22, *trn* is expressed in many places in the male genitalia as the claspers metamorphose during pupal development. Although I suggested the *trn* expression differences detected at the base of the clasper in late stage pupae are likely to affect clasper development, it is not actually clear which cells will develop into the clasper in the early pupal stage, and so it could be that *trn* expression detected earlier in e.g. the region lateral to the anal plates, is the causative expression difference. To analyse which expression domains of *trn* in the developing genitalia could be functional, I carried out *in situ* hybridisation on *trn* RNAi (#28525) male pupae (Fig 29, n.b. knock-down of *trn* using this construct resulted in a 25% reduction in clasper bristles, see Fig 20).

This analysis indicated that *trn* does not regulate clasper development during the early tested stages of clasper development (between 26 – 30 hr APF), as *trn* RNAi male genitalia exhibits comparable expression to UAS-*trn #28525* and NP6333 controls (Fig 29a and 29b) (note, NP6333 drives gene knock-down ubiquitously throughout the genital disc and pupal male genitalia, data not shown). In contrast, between 38 hr – 46 hr APF (Fig 29c – 29e), which is the window in which the claspers begin to visibly separate from the lateral plates and progressively increase in size and differentiate from the surround tissues

(see left-most panel), *trn* expression is almost completely absent in the male genitalia (Fig 1c - 1e), including lack of transcripts at the base of the developing clasper (black arrows).

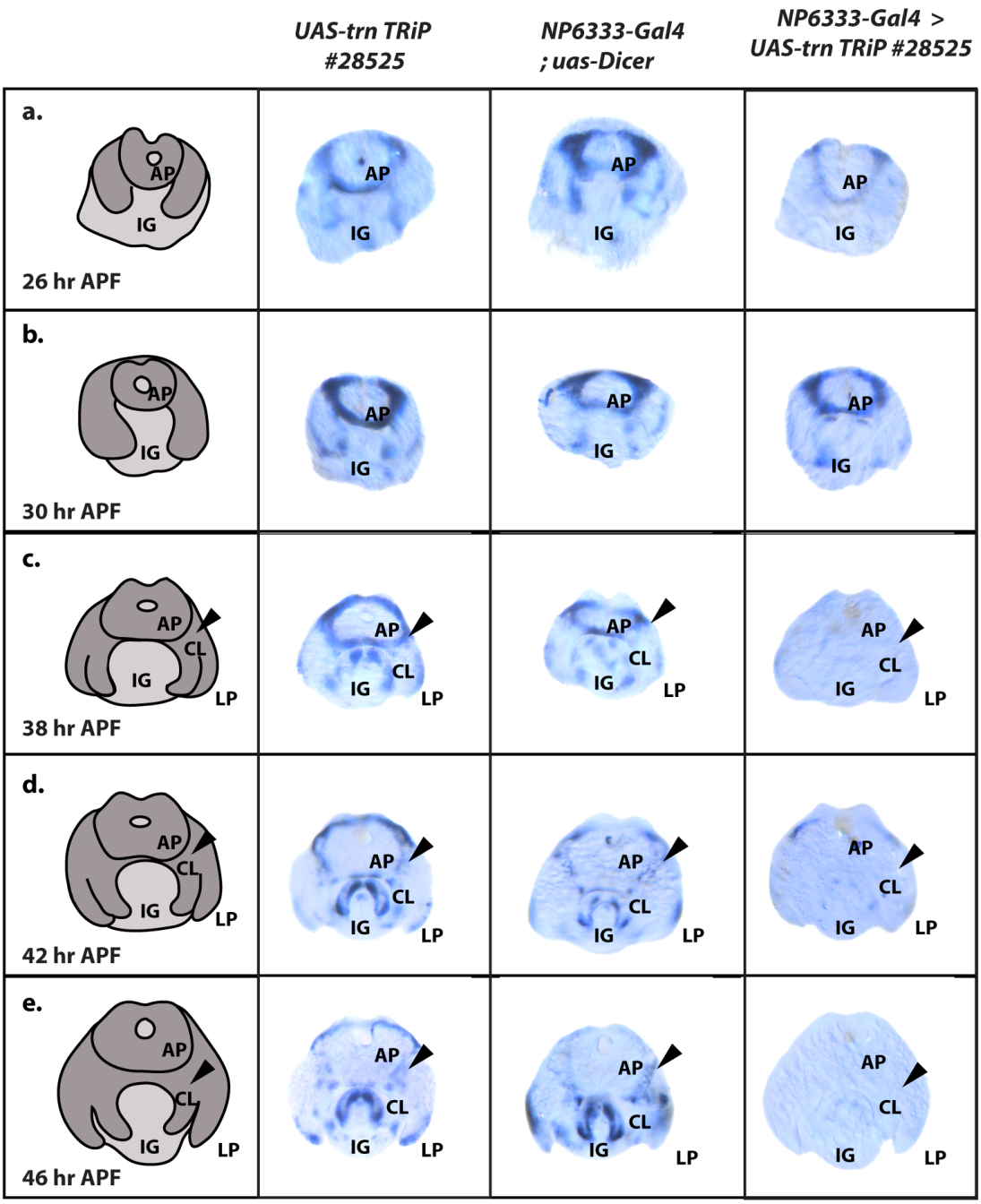


Figure 29. *in situ* hybridisation of *trn* within *trn* RNAi *D. melanogaster* male genitalia. Rows **a – e** indicate morphological stages (26 hr – 46 hr APF) (hr APF = hours after puparium formation). The first column illustrates morphological stage at each developmental time point (based on DAPI). *trn* expression in both the UAS-control (TRiP #28525) and NP6333-Gal 4 ; UAS–Dicer controls are shown in 2nd and 3rd columns from the left, respectively. The effect of *trn* RNAi on *trn* expression within the developing genitalia is shown in the right-most panel. AP = anal plates, IG = internal genitalia, LP = lateral plate and CL = claspers. Expression (or missing expression) of *trn* at the base of the claspers is indicated by the black triangle. Upwards points dorsally and all samples were counterstained with DAPI. *trn* expression in genitalia of knock-down male at the mid-to-late stage pupae (between 38 hr and 46 hr APF). Expression was lost at the base of the developing clasper in *trn* knock-downs throughout these stages (black arrows). *trn* expression was also lost in the lateral plates (LP), and was weaker in the internal genitalia (IG). N = 5 for each experiment.

Therefore, expression in the base of the claspers during late pupal stages is likely to underlie *trn*'s role in clasper development, and since this expression domain differs between species, it is also likely to underlie *trn*'s role in evolution.

6.2 ATAC-Sequencing and histone modification profiles reveals candidate regulatory elements in C2

Differences in the expression pattern of *trn* at the base of the developing claspers must be attributed to variation in *trn* cis-regulatory elements (CREs). In order to identify potential CREs in C2, I analysed existing ATAC-Seq data generated by Kittlemann et al., (2018) from *D. melanogaster* OregonR T2 legs at 20 hr - 28 hr APF (Fig 2a) (see Supplementary File 13 for a full list of peaks and their co-ordinates within C2) and histone modification profiles available on Flybase (Kharchenko et al., 2011). Although the ATAC-Seq data was not

generated from developing male genitalia, it has been described that regions of chromatin remain open even when transcription is not active (Schulz et al., 2015), and in C2, peaks are predicted over promoter regions for genes known not be be expressed in the leg (Wilson et al., 2006) (e.g. see blue peak near *sneaky* (*snky*), Fig 30a).

In total, I found 20 peaks of open chromatin in C2 in the leg ATAC-Seq data from *D. melanogaster* (Fig 30a, Supplementary File 13). Five regions cover promoters (blue), ten candidate enhancers (green), and one intronic enhancer (pink) (Fig 30a). I also found ten regions of open chromatin in C2 predicted from histone modification markers (purple shading, Fig 30b, (Kharchenko et al., 2011)), and six of these overlap with ATAC-Seq predicted peaks (indicated by black arrows in Fig 30a).

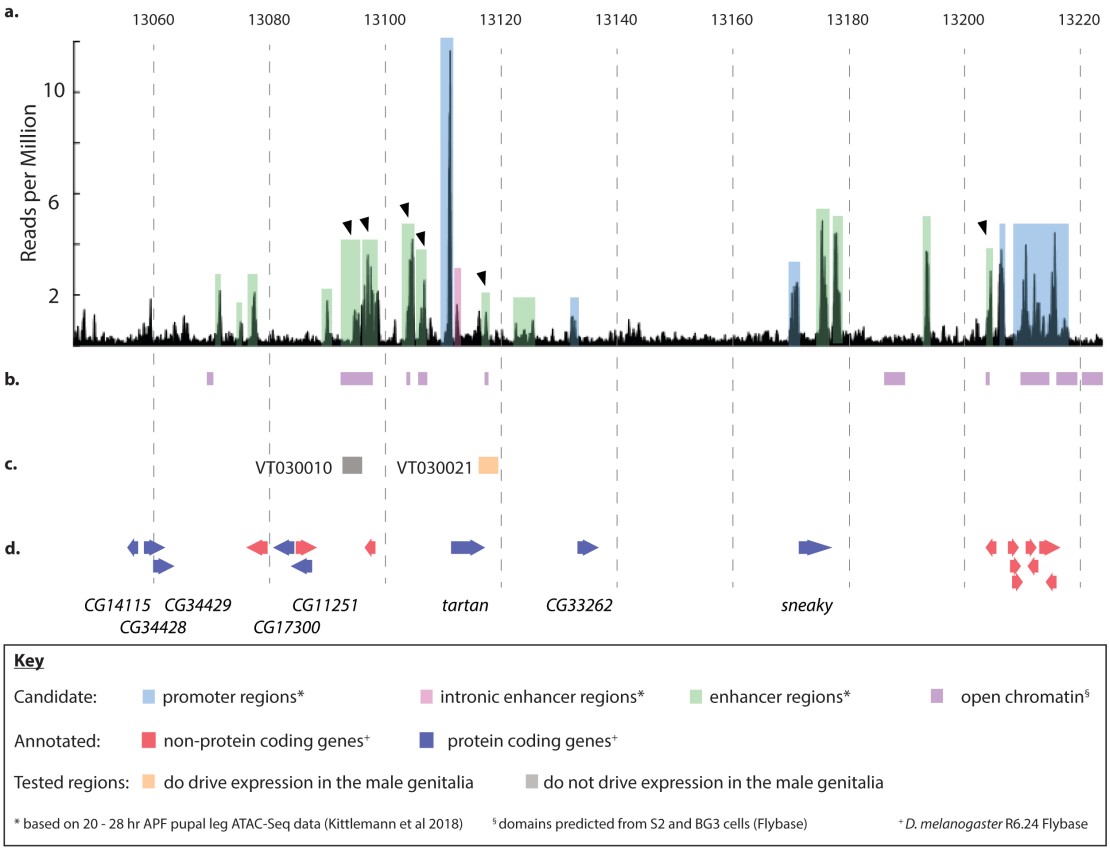


Figure 30. Analysis of regions of open chromatin in region C2 (*D. melanogaster* 3L: 13049375.. 13226520, R . A colour key is included in the black box. **(a)** ATAQ-Seq peaks in C2 based on 20 – 28 hr APF T2 legs of *D. melanogaster* (Kittlemann et al. 2018) (Supplementary File 2). In total, this data set predicts 20 peaks of open chromatin. Five regions cover promoters (blue), ten candidate enhancers (green), and one intronic enhancer (pink). **(b)** Predicted open chromatin domains in C2 gathered from demarcation of chromatin based on 18 histone modification profiles in BG3 and S2 cell lines (Flybase, (Kharchenko et al., 2011)). **(c)** Available VDRC Vienna Tile Gal-4 lines within C2; VT030010 (does not drive in anywhere in the fly) and VT30021 (used to identify *mcclaspertrn* and drives in many tissues including the male genitalia (see Fig 3) **(d)** Annotated protein coding and non-protein coding genes in C2 (*D. melanogaster*, Flybase R 6.24). Black arrows in **(a)** indicate regions of overlap between ATAC-Seq peaks and **(b).**

6.2.1 Functionally testing regions of C2 using VT-Gal 4 lines

I was able to source two VDRC Vienna Tile VT-GAL4 lines, VT030010 and VT030021 (Fig 30c), that overlap with two of the promising candidates in C2 (Fig 30a, black arrows). Each of these lines contain ~ 2.1 kb of non-coding fragments cloned upstream of GAL4 and inserted into an attP2 site. I crossed these two lines to UAS-Stinger GFP to determine if any of these predicted regions of open chromatin are able to drive expression in the developing claspers.

While VT030010 did not appear to drive detectable GFP expression in any part of the fly assayed (data not shown, whole flies were examined), VT030021 was able to drive expression in a variety of developing tissues (Fig 31). VT030021 contains a 2.1 kb cloned region between 3L: 13118090.. 13120128 (*D. melanogaster* R6.24, Flybase) just downstream of the *trn* 3' UTR (see yellow bar in Fig 30c). This line drove ubiquitous expression in the L3 larval male genital disc (Fig 31a). In the pupae, I found expression along the distal region (Fig 31b') and along the medial edge (white arrow, Fig 31b) of the 42 hr APF male wing. At 52 hr APF, VT030021 also appears to drive expression ubiquitously in the developing antennae (white arrow, Fig 31c), sporadically in ommatidia in the dorsal half of the eye, and along the medial edge of the eye (Fig 31c'). At 72 hr APF, expression in the antennae appears to become restricted to the distal region (white arrow, Fig 31d). Expression becomes speckled throughout the eye primordium (Fig 31d and 31d'). At both 30 hr APF and 52 hr APF, VT030021 drives expression in the distal regions the legs (Fig 31e – 31f) in

a gradient of expression that increases towards the distal region of each tarsal segment (Fig 31f'). At 72 hr APF expression becomes patchy throughout the tarsal segments (Fig 31g), similarly to what is observed in the eyes.

More importantly for the purposes of this thesis, this candidate enhancer also appears to be active in the male genitalia during pupal stages (Fig 31h – 31j). In early pupal development (24 hr APF), VT030021 appears to be active in cells of the clasper primordia (white arrow, Fig 31h), and the internal male genitalia (white asterisks, Fig 31h). During mid (45 hAPF) and late (72 hAPF) pupal development, VT030021 driven expression becomes refined to the base of the developing claspers (white arrows, Fig 31i and 31j) in a pattern that recapitulates *trn in situ* hybridization in *D. melanogaster* (Fig 22c). Expression also persists in the adeagus of the internal genitalia (asterisks, Fig 31i and 31j). Based on the ability of VT030021 to drive expression in the developing claspers, we named this promising *trn* enhancer candidate *mcclaspertrn*.

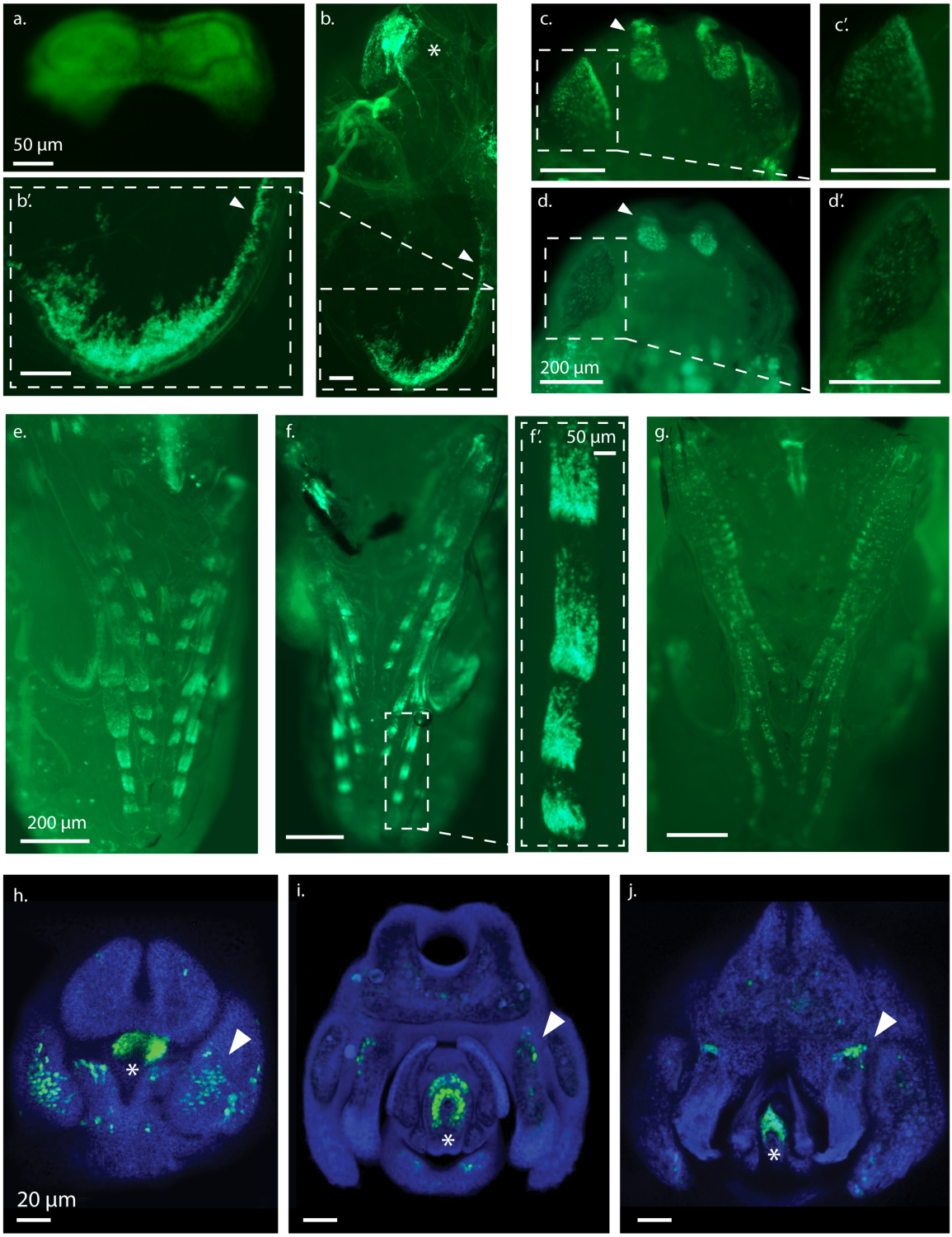


Figure 31. Expression analysis of candidate enhancer VT030021. VT-Gal4 VT030021 #214261 crossed to UAS-Stinger GFP in a male **(a)** L3 genital disc, **(b)** 42 hr APF wing, **(b')** 42 hr APF wing distal tip, **(c)** 52 hr APF head expression, **(c')** 52 hr APF eye, **(d)** 72 hr APF head, **(d')** 72 hr APF eye, **(e)** 30hr APF legs, **(f)** 52 hr APF legs, **(f')** 52 APF tarsal

expression, **(g)** 72 hr APF legs, **(h)** 24 hr APF genitalia, **(i)** 45 hr APF genitalia, **(j)** 60 hr APF genitalia. In 2 h – 2j, samples have also been counter stained with DAPI. Scale bars indicate a distance of 50 μm **(a – b')**, 200 μm **(c – g)**, 20 μm **(h – j)**, unless otherwise stated. **(b' – g)** – anterior / proximal points upwards, and distal points downwards. **(a, h – j)** - dorsal points upwards and ventral points downwards.

6.3 Sequence variation analysis of *mcclaspertrn*

Genetic variation in *mcclaspertrn* between *D. simulans* and *D. mauritiana may* explain the temporal and spatial *trn* expression pattern differences that we observe at the base of the clasper between species (Fig 22). Sequence analysis between *D. simulans* w^{501} and *D. mauritiana* D1 lab strains (See Supplementary File 1 for sequencing primers, and Supplementary File 12 for VT030021 sequence of lab strains) led to the detection of 26 nucleotide differences (Supplementary File 14, see blue, green and purple text). Comparison of these sites against reference genomes (two *D. simulans* and two *D. mauritiana* genomes) and Popoolation database (Pandey et al., 2011)(see Methods), revealed that only five are likely to be fixed (in that they are consistently different between reference genomes, lab strains and absent from the polymorphism database) (see blue "x's", Fig 32a and blue text, Supplementary File 3). An additional 16 detected nucleotide changes were only different between *D. simulans* w^{501} and *D. mauritiana* D1 lab strains (and not found in either the reference genomes, or the Popoolation polymorphism data set (green text, Supplementary File 14)), and five sites that differ between *D. simulans* w^{501} and *D. mauritiana* D1 lab strains are segregating in either or both of the species

(using Popoolation DB, see purple text, Supplementary File 14 and red x's Fig 32).

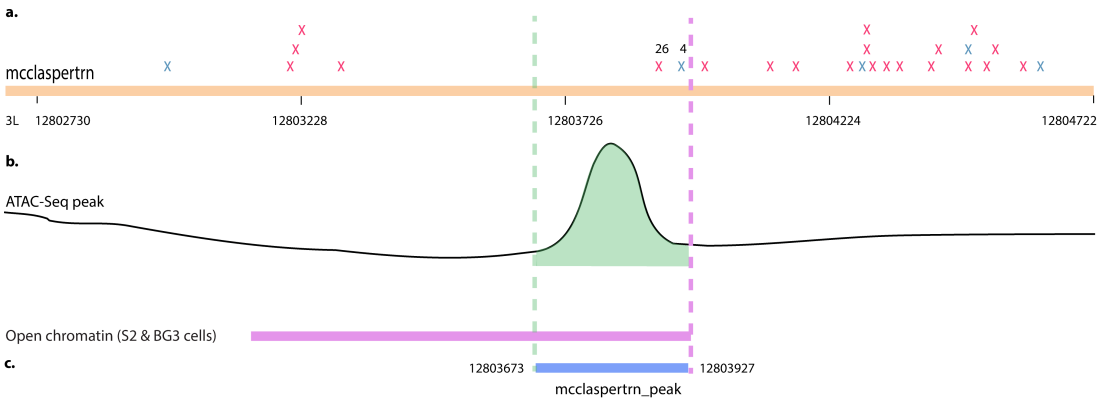


Figure 32– Variant nucleotide analysis and refinement of VT30021 (*mcclaspertrn*). **(a)** The distribution of variant nucleotides throughout the entire VT30021 (*mcclaspertrn*) region. Each "x" marks a nucleotide which differs between *D. simulans* and *D. mauritiana* , with blue "x's" indicated fixed differences, and red "x's" indicating polymorphic sites (in either of the species). **(b)** open chromatin described by ATAQ-Seq peaks (based on 20 – 28 hr APF T2 legs of *D. melanogaster* (green peak) (Kittlemann et al. 2018) (Supplementary File 13) and open regions gathered from demarcation of chromatin based on 18 histone modification profiles within BG3 and S2 cell lines (pink bar)(Kharchenko et al., 2011). **(c)** refined predicted *mcclaspertrn*_peak region defined by the boundaries of the aforementioned datasets (in **(b)**). *mcclaspertrn*_peak now lies between 3L: 12803673.. 12803927 (*D. simulans* R2.02, Flybase).

In order to make predictions about which of the fixed nucleotide variants between *D. simulans* and *D. mauritiana* are ancestral or derived, I also compared these sites against *D. melanogaster* (Flybase R6.24), *D. melanogaster* ^{1118} and *D. sechellia* (Flybase R1.03). From this analysis, I predict that two of the five fixed nucleotide changes are derived in both *D. mauritiana and D. sechellia* (ID 4 and ID 11, Supplementary File 14), one site (ID 5) is derived in *D. mauritiana only* and one site is derived in *D. simulans* only (ID 9). The evolutionary origin of the fifth fixed site (ID 12) is unclear, as the deletion / insertion of "T" appears to be

polymorphic in *D. melanogaster* (Supplementary File 14). Any one of these substitutions, or a combination of any of them, could be causative nucleotide changes for clasper morphological evolution between the species.

6.4 Refinement of *mcclaspertrn*

I attempted to resolve the number of candidate variant nucleotides by searching for a genomic region that overlaps between the boundaries of *mcclaspertrn* (Fig 32a, 3L: 13118090.. 13120128 in *D. melanogaster* R6.24, and 3L: 12802730.. 12804781 in *D. simulans* R2.02, Flybase), the boundaries of the ATAC-Seq peak mapped within *mcclaspertrn* (Fig 32b, 3L: 13119044 ..13119350 in *D. melanogaster*, Flybase R6.24 and 3L: 12803673.. 12803978 in *D. simulans* R2.02, Flybase), and of the region annotated as open according to histone modification analysis (Kharchenko et al., 2011) (3L: 13118500.. 13119299 in *D. melanogaster* R6.24 and 3L: 12803137.. 12803927 in *D. simulans* R2.02, Flybase). This overlap is only 256 bp (Fig 32c, located between 3L: 13119044.. 13119299 in *D. melanogaster* R6.24 and 3L: 12803672.. 12803927 in *D. simulans* , R2.02, Flybase), and will be referred to as *mcclaspertrn_peak* for all downstream analysis.

6.5 Sequence variation analysis of mcclasper*trn*_peak

Of the 26 variant nucleotides between *D. simulans* w^{501} and *D. mauritiana* D1 lab strains identified throughout *mcclaspertrn*, only two, #4 and #26 are

included in *mcclaspertrn_peak* (see Fig 32a and 32c, Fig 33 and see pink shaded loci in Supplementary File 14).

Variant nucleotide #4 represents a fixed difference (Fig 33a, Supplementary File 14); with the *D. simulans* w^{501} lab strain and reference genomes consistently contains an "A" at this locus, *D. mauritiana D1* lab strain and reference genomes contain a "G". As previously mentioned, *D. simulans* appears to share the ancestral allele, whilst *D. mauritiana* and *D. sechellia* appear to be derived (Fig 33a, Supplementary File 14).

The second variant nucleotide between *D. simulans* w^{501} and *D. mauritiana* lab strain is #26 (Fig 33b), and is a polymorphic site; segregating in *D. simulans*. All *D. mauritiana, D. melanogaster* and *D. sechellia* sequences examined have a "C" at this site, and two reference genomes of *D. simulans* have a "C" (Fig 33b). However, the *D. simulans* w^{501} lab strain contains an "A" rather than a "C".

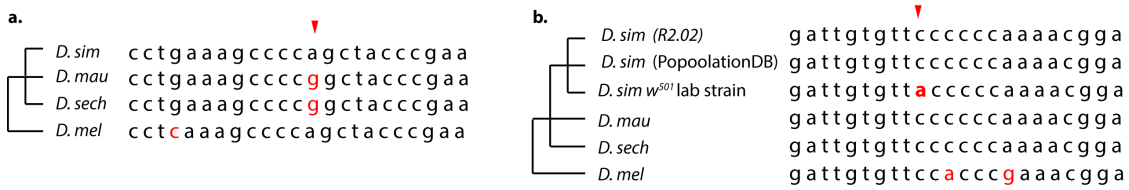


Figure 33. **Variant loci #4 (a) and #26 (b) in *mcclaspertrn_peak*.** Note, the species label (e.g. "*D. mau*") includes the lab strain *D. mauritiana* D1 and *D. mauritiana* reference genomes (as the site is not polymorphic between strains). For polymorphic sites, (e.g. *D. simulans* in **(b)**) the site for the lab strain and reference genome shown given separately. The red arrow indicates the variant site, and the nucleotide change is shown as red font. Additional relevant variant nucleotides are also shown in red. **(a)** Loci #4 represents a fixed difference between species, with *D. simulans* and *D. melanogaster* containing a "A" at this site, and *D. mauritiana* and *D. sechellia* containing a "G". *D. melanogaster* contains an additional variant nucleotide further

upstream of nucleotide #4 (see red "C" where other species have "G"). **(b)** All species and strains tested consistently had a "C" at nucleotide #26, except for lab strain *D. simulans* w^{501}, which contains an "A". Variant sites exclusively found in *D. melanogaster* downstream of nucleotide #26 are also shown (see red "A" and "G" where other species contain a "C" and "A", respectively).

6.5.1 Transcription factor binding site analysis

In order to determine whether variant nucleotide 4 and/or 26 differentially affects transcription factor binding activity between *Drosophila* species, I utilised the open access online resource Jasper (Khan et al., 2018). Jasper predicts transcription factor (TF) binding affinity profiles of 140 transcription factors, (for which the predicted binding sites are annotated), in a given DNA sequence. Though sites were only considered at a sequence match threshold of > 70% (Methods), it is worth noting that Jaspar is inefficient at detecting low affinity binding sites (e.g. that require a match of just 4 nucleotides). Nonetheless, comparison of TF binding affinity sites in *mcclaspertrn_peak* between *D. simulans, D. mauritiana* and *D. melanogaster* and *D. sechellia*, has led to the identification of candidate TF's that may differentially regulate *trn* at the base of the claspers due to variation at nucleotides #4 and #26 between the species (Supplementary File 15).

Variant nucleotide #4

Variant nucleotide #4 (which is derived in *D. mauritiana* and *D. sechellia* (Fig 33a), results in loss of binding sites (< 70%) for Bgb::Run (Fig 34a), CTCF

(Fig 34d), Ecdysone receptor*::* Ultraspiracle (EcR::Usp) (Fig 34g) in these species compared to *D. simulans* and *D. melanogaster* (Supplementary File 15a). Interestingly, the latter TF, EcR::Usp, is also affected by an additional nucleotide difference exclusive to *D. melanogaster* upstream of nucleotide #4 (see red "C" in Fig 34g whilst all other species contain a "G"). This additional site in *D. melanogaster* is predicted to increase EcR::Usp binding in this species (Fig 34g); thereby generating three different binding affinities for this TF in the *D. melanogaster* subgroup (Supplementary File 15a). Similarly, but in the opposite direction, Dl binding affinity is rendered < 70% in *D. mauritiana* and *D. sechellia* due to variation in nucleotide #4, and binding affinity is also diminished to < 70% in *D. melanogaster* by the additional variant nucleotide in this species (see red "C" in Fig 34f). Therefore, in this case, *D. simulans* contains the only 70 % affinity Dl site (Supplementary File 15a).

Instead of losing affinity sites (< 70%), some TF binding sites are more subtly affected by nucleotide 4. For example, the introduction of a "G" in *D. mauritiana* and *D. simulans* decreased binding affinity of a Brk binding site (Fig 34b) and a Gcm2 binding site (Fig 34i) (Supplementary File 15a). In contrast, other TFs, such as Odd (Fig 34j) and a second Dl site (Fig 34e) contain higher binding affinity in *D. mauritiana* and *D. sechellia* due to variant site #4. Interestingly, in the case of the latter, this Dl site is also affected by the additional nucleotide difference in *D. melanogaster* (see red c, Fig 34e), which serves to decrease Dl binding below that of *D. simulans* (Supplementary File 15a). Therefore, similarly to EcR::Usp (Fig 34g), Dl contains three different binding

affinities due to sequence variation between the species (Fig 34e). In other cases, such as that shown an additional Brk site (Fig 34c) and an Ets21C site (Fig 34h), variant nucleotide #4 actually generates novel binding sites (> 70 %) in *D. mauritiana* and *D. simulans*, not found in the other two species (Supplementary File 15a).

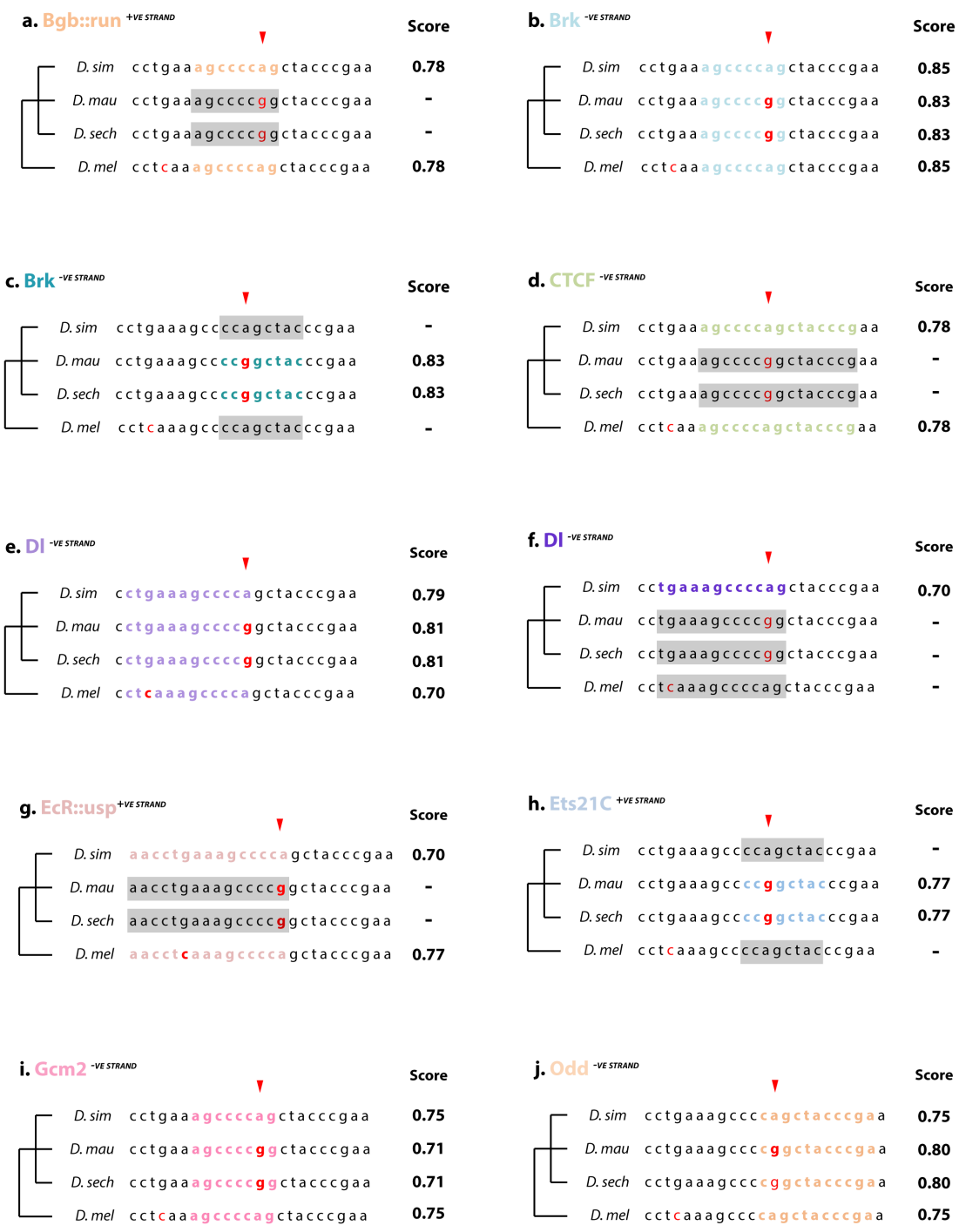


Figure 34. Analysis of TF binding affinity affected by variant nucleotide #4 in the *D. melanogaster* species subgroup. Analysis of **(a)** Bgb::run, **(b)** Brk, **(c)** Brk, **(d)** CTCF, **(e)** Dl, **(f)** Dl, **(g)** EcR::usp, **(h)** Ets21C, **(i)** Gcm2 and **(j)** Odd binding affinity affected by variant nucleotide 4. Red arrows and red text indicate variant nucleotide #4. Coloured sequences

indicate predicted TF binding sites (> 70% sequence match), whilst grey shading indicates absence of TF binding site (< 70% sequence match). In total, one Bgb::run, CTCF, EcR::usp, Ets21C, Gcm2, Odd binding affinity sites, and two Brk and Dl sites are perturbed due to variation nucleotide #4.

Variant nucleotide #26

In the case of Caup, Mirr, Ara, and Cad an "A" in the polymorphic site of lab strain *D. simulans* w^{501} increased binding affinity by > 5% compared to the "C" in *D. simulans* reference genomes and by the other *D. melanogaster* subgroup species (Supplementary File 15b). Interestingly, the Cad and Ara sites are also affected in *D. melanogaster* due to two additional variant nucleotides exclusive to this species (see red "A" and "G" in Fig 33b). In the case of Cad, binding affinity is rendered < 70 % as a result of these additional sites, whilst for Ara, binding affinity is increased in this species (>~ 5%) (Supplementary File 15b). As well as subtly increasing affinity of these TFs in the *D. simulans* w^{501} lab strain, there are 20 other TFs where affinity sites > 70% are created (Supplementary File 15b). Conversely, variate nucleotide #26 disrupts Dl and Slp1 binding affinity to < 70%, compared to other *D. simulans* strains and *D. mauritiana* and *D. sechellia* sequences, and the additional nucleotide changes exclusive to *D. melanogaster* reduces Slp1 binding affinity (by > 5%), and completely disrupts the Dl binding site (<70%) in this species (Supplementary File 15b). Therefore, although these TF binding differences are not fixed in *D. simulans*, since the lab strain of *D. simulans* w^{501} used for mapping contains these differences, they must be considered.

6.6 Testing the role of *hairy* in *trn* regulation in the developing male genitalia

After analysing in vitro the possibility that sequence variation could affect the ability of elements to activate or repress *trn* at the base of the claspers, I then functionally tested one known *trn* repressor; *hairy (h)*.

H is a long-range transcriptional co-repressor, which has been previously been shown to repress *trn* expression in the *D. melanogaster* embryo (Kok et al., 2015; Chang et al., 1993). Interestingly, *h* is also a candidate gene of region C1, and is expressed in the developing terminalia, but only differentially expressed between *D. simulans* and *D. mauritiana* at 50 hr APF (being significantly upregulated in *D. mauritiana* , see Supplementary File 9). However, knockdown of *h* results in the generation of significantly larger claspers in *D. melanogaster* (Chapter Four); implying *h* represses clasper growth in this species. Therefore, I performed an hybridisation of *trn* on *h* RNAi knock-down in *D. melanogaster* to test whether or not *h* is also able to repress *trn* in the context of the developing male genitalia.

At 30 hr - 42 hr APF, *trn* expression was not noticeably different from UAS-*h* #27738 and NP6333 driver controls (data not shown). However, at 46 hr APF, I detected ectopic expression of *trn* in *h* knock-down compared to the UAS-*h* control (see black arrow, NP6333-Gal4 x UAS-*h* #27738, Fig 35 compared to

the UAS-*h* control). In the UAS-*h* control, *trn* transcripts are detected as bands extending across the base of the developing claspers (as was seen in D. Fig 35). In *h* RNAi flies, however, these bands appear to be "messier", and extend in wisps dorsally towards the lateral edges of the anal plate primordial (see "AP" in Fig 35). These whisps were never detected in NP6333 *trn* in situ (see Fig 29) or *trn* in situ in other *D. melanogaster* strains (e.g. ^{1118}, see Fig 22). This ectopic expression indicates that the increase in clasper bristle number detected in *h* knockdown is likely due to increased *trn* expression at the base of the claspers, and that *h* normally acts upstream of *trn* in the male genitalia GRN, to represses and possibly refine its expression.

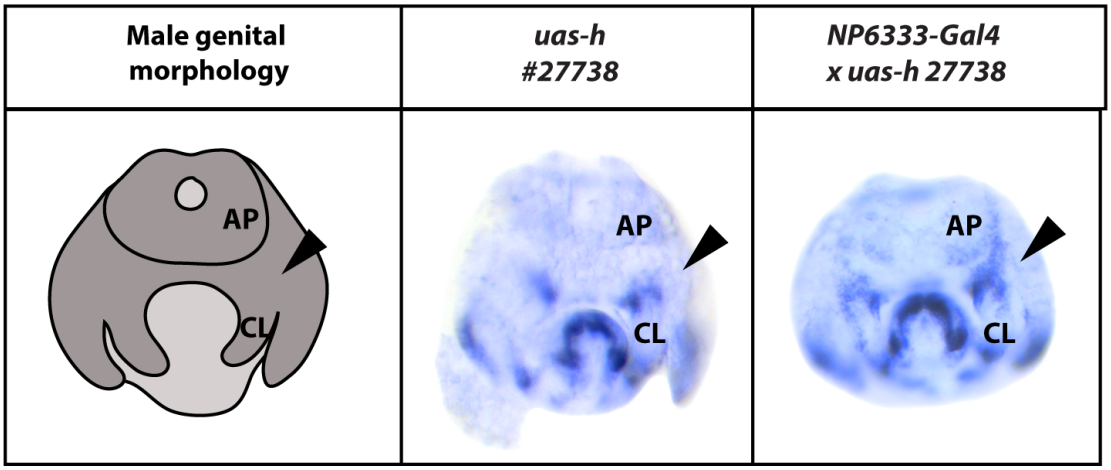


Figure 35. *trn* mRNA *in situ* hybridisation on *h* RNAi genitalia at 46 hr APF *D. melanogaster* male genitalia. The left-most column represents a schematic of morphological development based on DAPI at 46 hr APF (all samples were counterstained with DAPI). The middle panel shows *trn* in situ hybridisation on UAS-*h* parental control, whilst the right most panel for *h* RNAi knockdown. At 46 hr APF, *h* RNAi results in a distortion of *trn* expression compared to the UAS-*h* control. The band of *trn* expression at the base of the developing clasper appears to extend dorsally in a wisp towards the lateral sides of the anal plate primordia (black arrows). AP = Anal plates and CL = claspers. N = 5 for each experiment.

Since *h* appears to affect *trn* expression in the region where *mcclaspertrn* has been shown to drive (Fig 31i and 31j), I next checked whether *mcclaspertrn* contains any of the annotated *h* binding site sequences (Ohsako et al., 1994). Interestingly, I found that all species of the *D. melanogaster* subgroup (including both *D. simulans* w^{501} and *D. mauritiana* D1 lab strains) contain the preferred non-canonical *h* binding site (CACGCG, (Ohsako et al., 1994)). This binding site appears to have the same affinity between the species, since according to my sequence analysis, it does not contain any nucleotide differences (Supplementary File 12). Although *mcclaspertrn* may contain other, low affinity *h* sites that deviate between species, these were not detected in this analysis. Despite containing the same affinity, it could be that the different levels of *h* expression (with *h* being differentially expressed at 50 hr APF between the species, Supplementary File 9), could differentially repress *trn* at the base of the claspers.

6.7 Conclusion

In this chapter, I investigated the hypothesis that *trn* expression changes at the base of the developing clasper affect the development and therefore evolution of this structure (Fig 29). Using a combination of open chromatin profiles from other tissues (Kittelmann et al., 2018; Kharchenko et al., 2011), I identified a candidate CRMs in C2 (Fig 30). I was able to functionally validate that one of these regions, downstream of the *trn* 3' UTR, is able to drive expression in the male genitalia (including at the base of the developing clasper during pupal stages). This region, *mcclaspertrn,* contains a total of 26 variant nucleotide changes between *D. simulans* w^{501} and *D. mauritiana D1* lab strains (Supplementary File 3), though only two of these (#4 and #26, Fig 33) are in the

only region consistently annotated as open chromatin throughout the analysed datasets (mcclasper*trn*_peak)(Kittelmann et al., 2018; Kharchenko et al., 2011) (Fig 32). Sequence variation at fixed variant nucleotide #4 differentially affects transcription factor binding between the species (Supplementary File 15 and Fig 34); most significantly, Bgb::Run, CTCF, EcR::Usp, Brk and Ets21C (#4, Fig 34), however it is not yet clear whether or not these may affect *trn* expression at the base of the developing clasper. Conversely, *h* appears to negatively regulate *trn* expression in this region, and mcclasper*trn* does contain a *h* binding site, but the affinity of this site does not differ between species (as it does not contain a nucleotide differences between *D. simulans* and *D. mauritiana*). Although differences in *h* expression level and not binding affinity could differentially affect *trn* expression at the base of the clasper, the genetic variation that must exist in order to map candidate region C2 is yet to be identified.

7 Chapter Seven - General discussion

The aim of my PhD work was to identify genes underlying clasper and posterior lobe divergence in morphology between *D. simulans* and *D. mauritiana* . To do this, I started by improving the mapping resolution of several candidate regions on the left arm of the third chromosome, which allowed me to narrow down one of these regions (C2) to only 9 genes. To determine which of these genes was the evolved locus I investigated their role during genitalia development using RNA-Seq from developing genitalia of *D. simulans* and *D. mauritiana* (Hagen et al., BioRxiv), RNAi in *D. melanogaster* and *in situ* hybridisation in these three species. Based on these analyses, *trn* was the only remaining candidate. The reciprocal hemizigosity test (Stern, 2014) allowed me to confirm that *trn* is the evolved locus and by analysing open chromatin in C2 I was also able to find a candidate *trn* enhancer, *mcclaspertrn*. Below I discuss these findings in more detail, suggest a mechanism for *trn* evolution, and propose future directions for investigating the significance of *trn* evolution in developmental mechanisms and reproductive isolation between species. Moreover, I also discuss, based on other genes identified in this study, a possible GRN underlying clasper development.

1.1. Mapping posterior lobe and clasper size differences between *D. simulans* and *D. mauritiana*

The generation of new ILs allowed me to reduce P1 from 1.83 Mb to 949 kb (eliminating 136 candidate genes) and C2 from 3.49 Mb to 177 kb (eliminating 303 candidate genes) (Tanaka et al., 2015). In addition, I validated the previous genomic mapping of C1, remapped candidate regions P2 and P3 to different locations, and discovered regions P4, P5 and C0, which were not detected during lower resolution mapping conducted previously (Tanaka et al., 2015). The discovery of novel candidate regions reiterates the polygenic nature of these traits; consisting of multiple evolved loci of small effect size. Without fine-scale mapping, closely linked loci of small effect can sometimes be mistaken for single locus of large effect, or loci which do not interact additively can be missed (as was the case with C0; wherein lines containing both C1 and C0 were previously thought to contain just C1).

So far, I have only detected loci that affect posterior lobe or clasper morphology in the expected direction of the species difference (with all IL generating a more *D. mauritiana* -like phenotype compared to *D. simulans* w^{501}). This implies genes underlying clasper morphology and lobe morphology may have evolved under directional selection in *D. mauritiana* (Zeng et al., 2000). However, it is possible that large introgressed regions harbour more than one gene with opposite effects on genital phenotype, which might have caused them to be missed.

Consistent with previous mapping studies (Tanaka et al., 2015), I found most regions underlying clasper morphological differences do not overlap with those underlying posterior lobe differences (Fig 15). C0 and P1 are the only regions predicted to contain variation underlying both clasper and posterior lobe differences (Chapter Three, Table 1), which could indicate the presence of one locus that is able to generally affect the size of the male genital appendages. This is unlikely since variation in this region affects the size of these traits in opposite directions (see Fig 7 and 11), but perhaps the evolved gene could regulate a "trade-off" in clasper and posterior lobe size during development. However, since C0/P1 is still relatively large (949 kb), the generation of novel ILs could ultimately separate C0/P1 into separate clasper and posterior lobe loci.

In contrast, as was also shown previously by Tanaka et al (2015), clasper area and clasper bristle number consistently map to the same genomic locations; implying a shared genetic bases for the evolution of these traits. This could at least in part be explained by the process of bristle formation through lateral inhibition (Heitzler and Simpson, 1991), whereby genetic variation giving rise to larger claspers also causes the formation of more bristles. It is not clear, therefore, that if selection did drive the fixation of genetic variation in *D. mauritiana*, it was caused by their effect on clasper size or bristle morphology.

Interestingly, it could be that some of the candidate genes identified in this study may not only underlie genital differences between species; but also within species. To date, there have been two mapping studies that attempted to identify genetic variation underlying differences in posterior lobe morphology between *D. melanogaster* strains, and these studies successfully identified several QTL (Hackett et al., 2016; McNeil et al., 2011). A peak at a similar position on 3L was found in both studies, which overlaps with those predicted for inter-species variation between species of the *D. simulans* species clade (Liu et al., 1996; Macdonald and Goldstein, 1999; Masly et al., 2011; Zeng et al., 2000). The peak on 3L overlaps with the P1 region, including the only posterior lobe developmental candidate identified in this study - *Surf1*. Many other studies have also found cases where intraspecific variation maps to the same genomic region as interspecific variation (Gleason et al., 2002; Gleason and Ritchie, 2004; Nuzhdin et al., 1995; Tatsuta and Takano-Shimizu, 2006; True et al., 1997), and in some cases, such as in *Drosophila* pigmentation, alleles underlying within-species differences that also contribute to differences between species have been identified (Wittkopp et al., 2009). Therefore, *Surf1*, is an excellent positional and developmental candidate for posterior lobe variation both within and between species.

7.1 Identifying *trn*

Introgression mapping left only a possible 9 candidate genes in region C2, and subsequent expression analysis of these candidates inferred that *trn* is the likely evolved gene. The use of CRISPR-Cas9 to generate reciprocal hemizygotes of *trn* (Fig 25 – 27), allowed me to show *trn* is the evolved gene in C2, which underlies 16.3% of differences in clasper size and 33.5% differences in clasper bristle number between the species. The *D. mauritiana* allele of *trn* specifies larger claspers, with more sensory bristles compared to that of *D. simulans* (Fig 27). Whilst many examples of phenotypic evolution are known to be caused by changes in the expression of signaling molecules and transcription factors (Martin and Orgogozo, 2013; Nagy et al., 2018), *trn* is an Leucine Rich Repeat (LRR) protein which has never before been associated with the regulation or natural variation of organ size. In order to better understand how *trn* evolution affects clasper development, the known biological roles of *trn* will now be discussed.

1.1.1. Trn's role in development

Trn is related to Caps, and historically they have been functionally analysed alongside one-another in most studies. Located just 115 kb apart in the genome, *caps* and *trn* are highly related proteins (Shishido et al., 1998) that are thought to represent a gene duplication event (Mao et al., 2008). Many previous experiments suggest *trn* and *caps* confer "information" to cells to, for example,

facilitate the correct pattern of tracheal branching, motor-neuron axon guidance, and precise specification of cell location between compartments of the imaginal wing disc and leg disc (Milan et al., 2002; Milan et al., 2001; Sakurai et al., 2007; Krause et al., 2006; Mao et al., 2008; Bugga et al., 2009).

Experiments have shown that these proteins confer some of these roles by "informing" cells that they are positioned in the right location (Milan et al., 2002; Bugga et al., 2009). For example, if cell clones of the ventral wing disc compartment are ectopically generated in the dorsal compartment, they normally recognize they are miss-positioned and undergo apoptosis (Milan et al., 2002). However, if *trn* and *caps*, which are normally only expressed in cells with a dorsal identity, are expressed in these clones; then apoptosis does not occur (Milan et al., 2002). Therefore, Trn and Caps appear to allow the cell to "read" their environment, and recognize when they are positioned correctly. Interestingly, the mammalian homologue of *trn*, *Lrrn1*, is known to confer positional information during mammalian brain development (Tossell et al., 2011). Therefore, Trn may be involved in the regulation of organ size by specifying the correct positional information to cells more generally among metazoans.

In *Drosophila*, the positional identity information conferred by these proteins appears to be functional over large distances. Clones ectopically expressing *trn* and *caps* in the ventral compartment preferentially "sort-out" towards the dorsal compartment (where *trn* and *caps* are endogenously

expressed (Milan et al., 2001)). This information and movement appears to be achieved through "filopodia-like" extensions projecting towards the dorsal compartment from the surface of the ectopic clones which contain Trn and Caps protein (Milan et al., 2001). Once at the DV boundary, these projections have been shown to extend over the boundary, contacting the dorsal cells (Milan et al., 2001). Not only does this imply that Trn and Caps confer a "dorsal" identity to cells, but that these proteins are able to direct their movement towards the correct location.

Currently, it is not known whether or not Trn and Caps have higher affinity for themselves i.e. drawing clones towards the dorsal compartment, or to some unknown "Factor X" also expressed in this region. Moreover, the ability of Trn and Caps in specifying direction of movement does not seem to be conferred simply through the level of adhesion between cells, since related LRR adhesion proteins Connectin and Fasciclin II are not able to recapitulate the properties of Trn and Caps in wing disc organization (Milan et al., 2001).

The ability of Trn and Caps to provide positional information has also been implicated in developmental processes involving cell migration, in order to allow cells to make informed behavioral decisions. In the case of motor neuron axon guidance, Bugga et al., (2009) implied the mechanism through which *trn* is able to provide this positional information to migratory cells.

RPTP's (Receptor-linked Protein Tryrosine Phosphotases) are enzymes,

which are key regulators of axon guidance and synaptogenesis in the *Drosophila* CNS (Bugga et al., 2009). However, these enzymes, such as Ptp52F, are expressed throughout most motor neurons. Therefore, in order for motor neurons to achieve specificity and find the correct muscle to innervate, RPTP substrates, such as Trn, are selectively expressed on specific growth cones (Bugga et al., 2009). Ptp52F is able to dephosphorylate Trn in specific motor neurons, and this is thought to provide a "recognition que" for migrating neurons to stop migration and form a synapse. Some have suggested that this recognition cue comes in the form of endocytosis of the Trn protein after dephosphorylation; a process known to occur with other RPTP substrates (Keleman et al., 2002; Bugga et al., 2009).

Interestingly, dephosphorlyation of Trn by Ptp52F is dependent on the presence of another enzyme (an 'RTK' = receptor tyrosine kinase), which is able to add the phosphate to Trn in the first place (Bugga et al., 2009). Although this RTK has not been identified, the only RTK involved in the development of the male genital organs is Breathless (Btl) (an FGF receptor, that is known to interact with it's ligand Branchless (Bnl), in order to attract mesodermal cells to the A9 segment of the male genital disc (Ahmad and Baker, 2002)). Although the spatial expression of Btl and Ptp52F in the genital disc or during pupal stages is unknown, according to our RNA-Seq data of *D. simulans* and *D. mauritiana* terminalia, both of these genes are expressed (Supplementary File 7). Interestingly, *btl* is significantly differentially expressed between *D. mauritiana* and *D. simulans* terminalia during pupal stages (being significantly upregulated

in the latter (Supplementary File 7)), and *Ptp52F* is also differentially expressed, though only at the later time point (also more highly expressed in *D. simulans*, Supplementary File 7).

Perhaps then, these known and hypothesized interactions could explain how Trn regulates clasper size during male genital development; either through dictating the migration of cells into the male genital disc (Ahmad and Baker, 2002), regulating the organisation of cells and the size of compartments in the disc, or by orchestrating cell movements and rearrangements that might occur to generate the claspers during pupal stages, though developmental analysis is required to test these ideas.

1.1.2. The evolution of trn in clasper development

In light of the overlapping roles of *caps* and *trn*, comparison of these genes could reveal how and why *trn* evolved in the context of the claspers, and *caps* did not. In the case of the eye disc, *caps* and *trn* expression starts off overlapping (e.g. in the morphogenetic furrow), but later in eye development, their expression becomes distinct; with *Caps* expression being restricted to R8 cells of the ommatidia, and *trn* to R1, R6 and R7 photoreceptor cells in the apical membrane (Mao et al., 2008). These findings, which suggest cis-regulatory divergence of these genes, recapitulate my observations in the male genitalia, where *caps* and *trn* expression during early pupal stages is indistinguishable, but at later stages clear differences can be detected, such as lack of *caps* at the

base of the developing clasper (Fig 22 and 23). Therefore, cis-regulatory evolution in enhancers such as mcclasper*trn* could explain why *caps*, despite being functionally equivalent to *trn* in other tissues, does not underlie differences in clasper size between *Drosophila* species.

Moreover, protein swapping experiments (Milan et al., 2005) and mutant clonal analysis (Mao et al., 2008) between Caps and Trn in the wing disc and morphogenetic furrow of the eye disc implied these proteins are equivalent, as they display functional redundancy in cell organization. In contrast, studies in the developing trachea have showed that protein-coding differences, specifically in the intracellular domain of these proteins, are enough to functionally diverge them (Krause et al., 2006). Combining the extracellular domain of Caps with the intracellular domain of Trn rescues abnormal tracheal branching in *trn* mutants, whilst the opposite combination does not (Krause et al., 2006). These findings suggest evolution in the Trn intracellular domain could underlie functional divergence of Trn from Caps in the male genitalia, and the ability of *trn* to differentially regulate clasper size between the species.

However, given the pleiotropic developmental roles of Trn (see above), it is unlikely the protein-coding region of this gene has evolved to change development of the claspers between *Drosophila* species. Moreover, as previously described, the Trn coding region of *D. simulans* w^{501} and *D. mauritiana* D1 contains no fixed non-synonymous changes (Hagen et al., 2018), and phenotypic evolution is thought to be caused predominantly by regulatory

changes (Carroll, 2008). With this in mind, and considering the temporal and spatial expression differences observed at the base of the developing claspers between *Drosophila* species, I conclude *trn* evolution is likely caused by cis-regulatory divergence; possibly in *mcclaspertrn*.

As can be seen in Fig 31, *mcclaspertrn* drives in the L3 genital disc, in the cells of the clasper primordia during early pupal stage, and subsequently at the base of the developing claspers (Fig 31a, 31h – 31j). *Mcclaspertrn* is also able to drive expression in the pupal eye, leg, antennae and wing, where *trn* is also known to be expressed (Milan et al., 2002; Milan et al., 2001; Sakurai et al., 2007; Krause et al., 2006; Mao et al., 2008; Bugga et al., 2009; Immonen and Ritchie, 2012).

I showed *mcclaspertrn* contains a *h* binding site in all *D. melanogaster* subgroup species, and that knock-down of *h* in *D. melanogaster* results in ectopic expression of *trn* at the base of the claspers (Fig 35). Therefore, I propose *h* represses *trn* at the base of the developing clasper via *mcclaspertrn*. However, since this site contains no nucleotide differences between species, I have been unable to link differential *h* repression to the *trn* expression variation at the base of the claspers between *Drosophila* species. This being said, since *h* is upregulated in *D. mauritiana* terminalia during late pupal development (Supplementary File 9), it could be that the amount of *h* expression, not the binding affinity of *h*, is able to alter *trn* activity during clasper development.

I have identified many candidate nucleotide differences (Fig 32a) that could affect binding of other TF to differentially regulate *trn* in the clasper, and only five of these are fixed. Based on open chromatin profiling, (Kharchenko et al., 2011; Kittelmann et al., 2018), I analysed the significance of two of these sites in depth (nucleotide #4 and # 26, Supplementary File 15). This generated a list of candidate TFs whose activity are affected by these variant nucleotides, though to my knowledge none of these are known to interact with *trn*. Moreover, neither of these nucleotide differences are completely convincing as the causative difference underlying clasper size differences between the species.

Fixed variant #4, for example, contains the same nucleotide change in *D. mauritiana* as in *D. sechellia* (Fig 33). This is counterintuitive, since as previously mentioned, *D. sechellia* contain similar sized claspers to *D. simulans*, which implies this genetic variation does not underlie differences between the mapped species. However, it could be that another variant nucleotide, functioning in combination with #4, is able to generate smaller claspers in D. sechellia, or perhaps *trn*'s role in clasper evolution is not conserved between species (though based on the dynamic expression of *trn* in *D. melanogaster* (Fig 22), I hypothesize it is unlikely).

Moreover, it seems questionable that a polymorphic site, which is only detected in the w^{501} lab strain of *D. simulans*, underlies 16% of clasper size and 33% of clasper bristle number differences between this strain and *D. mauritiana* D1. *D. simulans* w^{501} was selected for mapping based on the observation that

these males contain intermediate genital phenotypes compared to other *D. simulans* strains (data not shown), and so is unlikely to contain any novel mutations significantly decreasing clasper size by such an extent. Therefore, although functional testing of the highlighted TF could yield interesting results, generating open chromatin profiles specific to the male genitalia tissue in these species could also allow more accurate detection of open chromatin and subsequent analysis of more likely genetic variation in *mcclaspertrn* (Supplementary File 15).

1.2. The gene regulatory network of clasper development

As well as identifying a gene involved in clasper evolution, this study has found additional genes involved in clasper development (Fig 16, 17, 20). Interestingly, *h* appears to act upstream of several other factors that regulate clasper formation identified in this study including *trn, Gug* and *sgl* (Fig 36). As previously mentioned, repression of *trn* by H has been shown in *Drosophila* embryos (Kok et al., 2015; Chang et al., 1993), and my analysis suggests that this also occurs at the base of the developing claspers during late stages of male pupal development (46 hr APF, Fig 35). In addition to the repression of *trn*, H is also known to repress C1 candidate *Gug* (in embryos (Kok et al., 2015)), and since Gug is predicted to repress C0 candidate gene *sgl* (as this gene contains a Gug binding site in its intron (Yeung et al., 2017)), H appears to indirectly regulate *sgl* expression also (Fig 35).

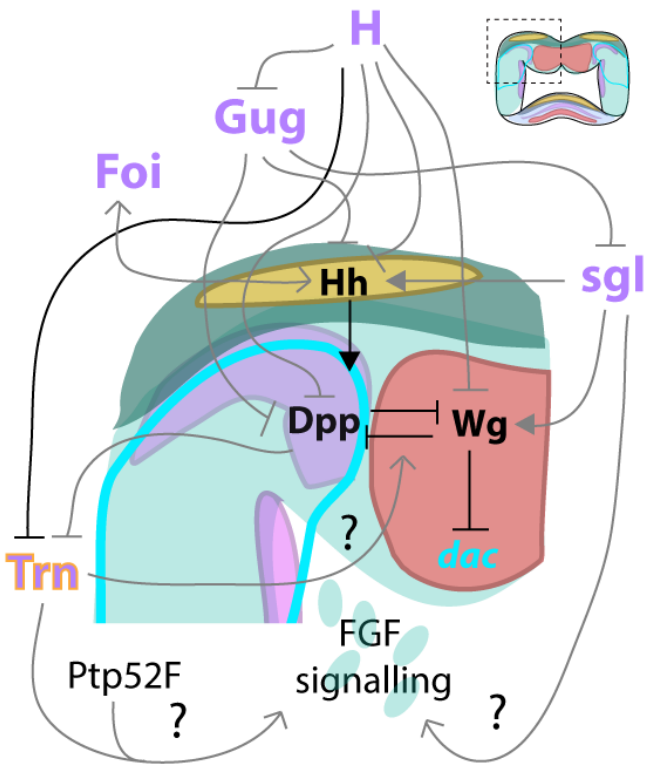


Figure 36 - Outline of possible candidate gene regulatory network underlying clasper development. Purple genes and those outlined with orange indicate genes which have been shown in this study to have a direct role in clasper development and evolution, respectively. A section of the A9 segment of the male genital disc (indicated in top right corner) is illustrated to show the known interactions occurring in the male genitalia at this developmental stage (black lines). Grey arrows indicate interactions shown in other tissues, but not in the disc or any other male genital developmental stage. Question marks indicate hypothesized interactions that have not been proven. H negatively regulates both Gug and *trn* (with the repression of *trn* by H shown in other tissues, but also in the claspers (Fig 35) (Kok et al., 2015; Chang et al., 1993)), and Gug is predicted to repress sgl (Yeung et al., 2017). These factors, as well as Foi, have been shown to interact with genes known to pattern the genital disc (at compartmental boundaries) (Hh, Dpp, wg, (Casares et al., 1997; Chen and Baker, 1997; Freeland and Kuhn, 1996; Sanchez et al., 1997) and regulate clasper identity (*dac* (Keisman et al., 2001). For example, Gug and H are known to regulate expression of *dpp* and *hh* (Yeung et al., 2017; Kok et al., 2015)), and Sgl is also thought to regulate Hh signaling (Binari et al., 1997; Haerry et al., 1997; Princivalle and de Agostini, 2002). H and Sgl also appear to interact with *wg* in other tissues (with *h* having a repressive function (Kok et al., 2015), and Sgl possibly facilitating Wg signaling (Binari et al., 1997; Princivalle and de Agostini, 2002). These

interactions with known regulators of compartmental boundaries, as well as the negative regulation of *trn* by Dpp (Chang et al., 1993) (which is known to regulate boundaries in other tissues (Milan et al., 2002; Milan et al., 2001)), could affect clasper development by regulating the separation between cells throughout male genital development. Moreover, these interactions could also affect expression of downstream factor *dac*, which is known to directly regulate clasper size and bristle number in *D. melanogaster* (Keisman et al., 2001). Trn and Sgl may also affect clasper development by affecting cell number at the genital disc stage, though FGF signaling (see question marks).

Interestingly, as well as regulating each-other, these newly identified clasper developmental genes are known to regulate the factors which pattern the compartmental boundaries of the genital disc during male genital development (in other developmental contexts) (Eaton and Kornberg, 1990; Kornberg et al., 1985; Garcia-Bellido, 1973; Morata and Lawrence, 1975; Diaz-Benjumea and Cohen, 1995) (Fig 36). For example, many of these factors are known (such as H), or predicted (such as Gug, Sgl and Foi) to regulate *Hedgehog* (*Hh*) signalling in the embryo and during tracheal morphogenesis (Yeung et al., 2017; Kok et al., 2015). Therefore, since Hh initiates the expression of *dpp* and *wg* in a complementary pattern to define compartmental boundaries of the genital disc (see Fig 36), these genes' role in clasper development could be in the regulation of genital disc organisation.

Evidence for this hypothesis is also present downstream of Hh signalling, as H and Sgl are thought to regulate *wg* (Kok et al., 2015) (Binari et al., 1997; Haerry et al., 1997), and both H and Gug are predicted to negatively regulate *dpp* expression (in the embryo) (Yeung et al., 2017; Kok et al., 2015) (Fig 36). All of these interactions are through regulating gene transcription, except for Sgl,

which facilitates the production of co-factors in Hh signalling (Binari et al., 1997; Princivalle and de Agostini, 2002). Moreover, Dpp is known to negatively regulate *trn* expression (in the embryo) (Chang et al., 1993), and considering Trn's known roles in the wing and leg disc (see above), it is plausible that Trn directly regulates compartmental boundaries of the genital disc (Fig 36). Functional validation of these interactions in the genital disc, and during the metamorphosis of male genitalia during pupal stages is required to test these interactions.

As well as potentially affecting the organisation of the disc (or the segments of the disc during metamorphosis of the disc during pupal stages), these genes could specifically affect clasper development through their indirect regulation of *dac* (Fig 36). As previously mentioned, *dac* is known to directly regulate the size of the claspers and the number of clasper bristles in *D. melanogaster* (Keisman et al., 2001), and functions downstream of the *wg*, *dpp* interaction in the genital disc (Fig 36). Therefore, the interactions between these genes and upstream patterning factors (e.g. Hh, Wg and Dpp) could affect clasper development by indirectly regulating the activity of the downstream clasper differentiation factor, *dac*.

However, Trn and Sgl could also affect clasper development through other means. As previously mentioned, Sgl facilitates the production of co-factors in Hh signalling, but these co-factors are also known to function during FGF signalling (Binari et al., 1997; Princivalle and de Agostini, 2002). Therefore,

Sgl could mediate the number of cells attracted to the clasper primordial cells of the genital disc via the FGF signalling known to result in incorporation of mesodermal cells (Ahmad and Baker, 2002). Moreover, as speculated in the section above, FGF receptors may facilitate the interaction between Trn and Ptp52-F, which could affect guidance cues of cells during genital development. Expression and functional analysis of *sgl*, *trn*, *Ptp52F* and *FGF* factors are required to test these hypotheses.

1.3. *Trn, sneaky* and the mechanisms driving rapid male genital evolution

Sneaky (snky) is a gene in C2, located 57 kb downstream of the *trn* 3'UTR (in *D. simulans Flybase* R2.02). It is expressed exclusively in the testes and is an integral membrane protein at the apical tip of the acrosome of sperm (Wilson et al., 2006). In *Drosophila*, Snky is required for successful sperm plasma membrane break down following the sperm entering the egg (Wilson et al., 2006).

GEA of *snky*, and the identification of *trn* as the evolved gene in C2, suggests that *snky* has no direct role in clasper evolution. However, given Snky's known role in male fertility, it could be that females are cryptically choosing which males will fertilize her eggs, based on clasper morphology (using clasper size / bristles as an indication of male fitness, see Introduction). Indirectly therefore, cryptic female choice could be driving the evolution of clasper

morphology. Both genes will presumably be under joint strong sexual selection, which, due to their relatively close association on 3L, could lead to linkage disequilibrium of beneficial haplotypes that include both genes.

1.4. Future directions

Identification of *trn* as an evolved gene underlying clasper divergence, and the generation of flies which only differ in the species-specific functioning *trn* allele (see reciprocal hemizygotes, Chapter Five), opens up many possibilities for future experiments, such as investigating how genetic variation changes developmental mechanisms between species, and the consequence of differences in male genital morphology on mating behaviour.

1.4.1. Investigating the developmental impact of gene evolution

At this stage, it is not clear whether or not differential regulation of *trn* leads to differences in overall clasper cell number, arrangement or size. Comparison of these parameters between reciprocal hemizygotes (using quantitative image analysis techniques), would allow me to answer these questions. Using image analysis software, myself and Pedro Gaspar (Oxford Brookes University) have already gathered preliminary data that suggests cells undergo apical constriction in the region where *trn* is expressed in *D. melanogaster* species claspers (Fig 37), implying *trn* may result in changes in

cell shape due to cell rearrangements.

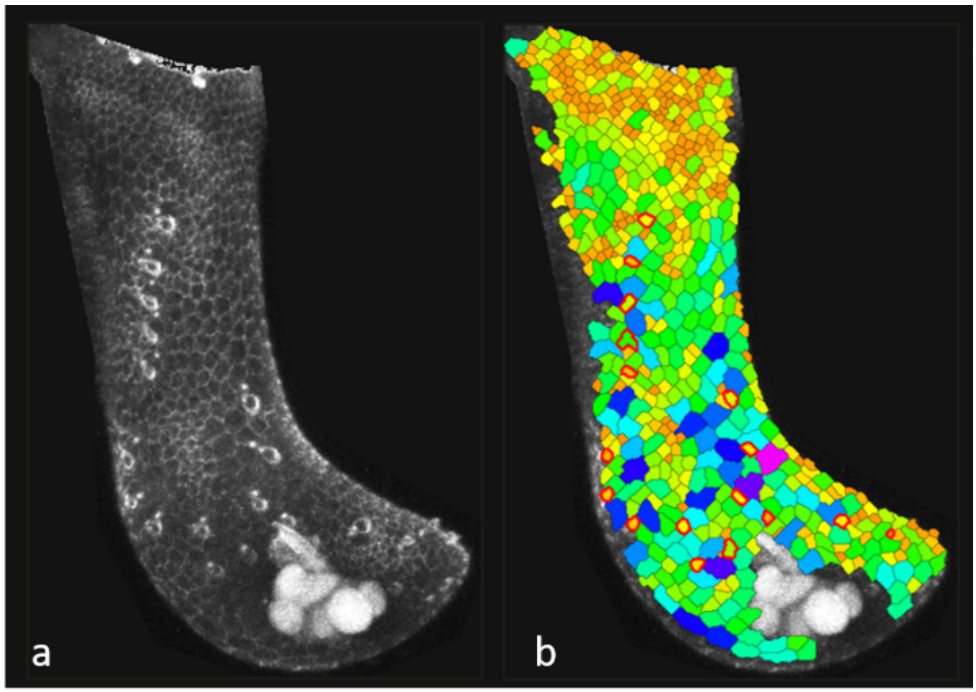


Figure 37. Preliminary insights into clasper development (*D. melanogaster*, ~45 hr APF). **(a)** E-cadherin GFP *D. melanogaster* clasper. **(b)** Cell apical area analysis of E-cadherin GFP clasper, with cell apical area labelled by colour; from orange (smallest), yellow, green, light blue and dark-blue (largest). Cells outlined in red are those from with the bristles will develop. Cells at the base of the clasper appear to be the most apically constricted.

1.4.2. Investigating the behavioural impact of genital evolution

Comparison of the reciprocal hemizygotes would also allow us to address the age-old question of "does size matter" in mating. These reagents allow the direct comparison of flies that only differ in clasper morphology, and not in other species-specific confounding factors, which could also affect copulation. For example, we could assess differences in pre-copulatory success of males in mounting, but also mechanisms that infer the role of clasper size and bristle

number in post-copulatory sexual selection mechanisms such as cryptic female choice (e.g. by comparing sperm transfer, number of progeny, sperm storage and selective fertilisation between males with different sized claspers). This could ultimately provide clues as to which evolutionary mechanisms dictate the rapid evolution of male genital morphology (e.g. the lock and key hypothesis or the sexual selection hypothesis).

8 Closing remarks

In conclusion, this PhD has successfully identified the first evolved gene underlying male genital size evolution, *trn*. Moreover, the role of *trn* in clasper development may represent a conserved, newly identified mechanism of organ size regulation. Based on my analysis, I have also inferred how this regulation has evolved between species, and implicated a role for cis-regulatory evolution. Therefore, this PhD has increased our understanding of the ways in which the amazing phenotypic diversity in animals evolves.

9 Bibliography

Acebes, A., Cobb, M. & Ferveur, J. F. 2003. Species-specific effects of single sensillum ablation on mating position in Drosophila. *J Exp Biol,* 206(17), pp 3095-3100.

Ahmad, S. M. & Baker, B. S. 2002. Sex-specific deployment of FGF signaling in Drosophila recruits mesodermal cells into the male genital imaginal disc. *Cell,* 109(5), pp 651-61.

Alonso, C. R. & Wilkins, A. S. 2005. The molecular elements that underlie developmental evolution. *Nature Reviews,* (6), pp 709-715.

Arnoult, L., Su, K. F., Manoel, D., Minervino, C., Magrina, J., Gompel, N. & Prud'homme, B. 2013. Emergence and diversification of fly pigmentation through evolution of a gene regulatory module. *Science,* 339(6126), pp 1423-1426.

Arnqvist, G. 1998. Comparative evidence for the evolution of genitalia by sexual selection. *Nature,* 393(6687), pp 784-786.

Ashburner, M. 1989. *Drosophila. A laboratory handbook.*, Cold Spring Harbor, NY: Cold Spring Harbor Laboratory Press.

Averof, M. 1997. Arthropod evolution: same Hox genes, different body plans. *Curr Biol,* 7(10), pp 634-636.

Baker, B. S. & Ridge, K. A. 1980. Sex and the single cell. I. On the action of major loci affecting sex determination in Drosophila melanogaster. *Genetics,* 94(2), pp 383-423.

Berger-Muller, S., Sugie, A., Takahashi, F., Tavosanis, G., Hakeda-Suzuki, S. & Suzuki, T. 2013. Assessing the role of cell-surface molecules in central synaptogenesis in the Drosophila visual system. *PLoS One,* 8(12), pp 1-14.

Bertin, A. & Fairbairn, D. J. 2007. The form of sexual selection on male genitalia cannot be inferred from within-population variance and allometry - a case study in Aquarius remigis. *Evolution,* 61(4), pp 825-837.

Binari, R. C., Staveley, B. E., Johnson, W. A., Godavarti, R., Sasisekharan, R. & Manoukian, A. S. 1997. Genetic evidence that heparin-like glycosaminoglycans are involved in wingless signaling. *Development,* 124(13), pp 2623-2632.

Blackman, R. K., Sanicola, M., Raftery, L. A., Gillevet, T. & Gelbart, W. M. 1991. An extensive 3' cis-regulatory region directs the imaginal disk expression of decapentaplegic, a member of the TGF-beta family in Drosophila. *Development,* 111(3), pp 657-666.

Blumroder, R., Glunz, A., Dunkelberger, B. S., Serway, C. N., Berger, C., Mentzel, B., de Belle, J. S. & Raabe, T. 2016. Mcm3 replicative helicase mutation impairs neuroblast proliferation and memory in Drosophila. *Genes Brain Behav,* 15(7), pp 647-659.

Bugga, L., Ratnaparkhi, A. & Zinn, K. 2009. The Cell Surface Receptor Tartan Is a Potential In Vivo Substrate for the Receptor Tyrosine Phosphatase Ptp52F. *Molecular and Cellular Biology,* 29(12), pp 3390-3400.

Burtis, K. C. & Baker, B. S. 1989. Drosophila doublesex gene controls somatic sexual differentiation by producing alternatively spliced mRNAs encoding related sex-specific polypeptides. *Cell,* 56(6), pp 997-1010.

Carey, D. J. 1997. Syndecans: multifunctional cell-surface co-receptors. *Biochem J,* 327 (1), pp 1-16.

Carrasco-Rando, M., Atienza-Manuel, A., Martin, P., Burke, R. & Ruiz-Gomez, M. 2016. Fear-of-intimacy-mediated zinc transport controls the function of zinc-finger transcription factors involved in myogenesis. *Development,* 143(11), pp 1948-1957.

Carroll, S. B. 2008. Evo-devo and an expanding evolutionary synthesis: a genetic theory of morphological evolution. *Cell,* 134(1), pp 25-36.

Casares, F., Sanchez, L., Guerrero, I. & Sanchez-Herrero, E. 1997. The genital disc of Drosophila melanogaster. : I. Segmental and compartmental organization. *Dev Genes Evol,* 207(4), pp 216-228.

Chandran, R. R., Iordanou, E., Ajja, C., Wille, M. & Jiang, L. 2014. Gene expression profiling of Drosophila tracheal fusion cells. *Gene Expr Patterns,* 15(2), pp 112-123.

Chang, Z., Price, B. D., Bockheim, S., Boedigheimer, M. J., Smith, R. & Laughon, A. 1993. Molecular and genetic characterization of the Drosophila tartan gene. *Dev Biol,* 160(2), pp 315-332.

Charroux, B., Freeman, M., Kerridge, S. & Baonza, A. 2006. Atrophin contributes to the negative regulation of epidermal growth factor receptor signaling in Drosophila. *Dev Biol,* 291(2), pp 278-290.

Chatterjee, S. S., Uppendahl, L. D., Chowdhury, M. A., Ip, P. L. & Siegal, M. L. 2011. The female-specific doublesex isoform regulates pleiotropic

transcription factors to pattern genital development in Drosophila. *Development,* 138(6), pp 1099-1109.

Chen, E. H. & Baker, B. S. 1997. Compartmental organization of the Drosophila genital imaginal discs. *Development (Cambridge, England),* 124(1), pp 205-218.

Christiansen, A. E., Keisman, E. L., Ahmad, S. M. & Baker, B. S. 2002. Sex comes in from the cold: the integration of sex and pattern. *Trends Genet,* 18(10), pp 510-516.

Cobb, M., Burnet, B. & Connolly, K. 1988. Sexual isolation and courtship behavior in *D. simulans*, D mauritiana, and their interspecific hybrids. *Behavior Genetics,* 18(2), pp 211-225.

Costa, M., Calleja, M., Alonso, C. R. & Simpson, P. 2014. The bristle patterning genes hairy and extramacrochaetae regulate the development of structures required for flight in Diptera. *Dev Biol,* 388(2), pp 205-215.

Cowling, D., E., Burnet, B. 1981. Courtship songs and genetic control of their acoustic characteristics in sibling species of the Drosophila melanogaster subgroup. *Animal Behaviour,* 29(3), pp 924-935.

Coyne, J., A. 1989. Genetics of sexual isolation between two sibling species, Drosophila simulans and Drosophila mauritiana. *Proceedings of the National Academy of Sciences of the United States of America,* 86(14), pp 5464-5468.

Coyne, J. A. 1983. Genetic basis of differences in genital morphology among three sibling species of Drosophila. *Evolution,* 37(6), pp 1101-1118.

Coyne, J. A., Rux, J. & David, J. R. 1991. Genetics of Morphological Differences and Hybrid Sterility between Drosophila-Sechellia and Its Relatives. *Genet Res,* 57(2), pp 113-122.

Crudgington, H. S. & Siva-Jothy, M. T. 2000. Genital damage, kicking and early death. *Nature,* 407(6806), pp 855-856.

Da-Re, C., von Stockum, S., Biscontin, A., Millino, C., Cisotto, P., Zordan, M. A., Zeviani, M., Bernardi, P., De Pitta, C. & Costa, R. 2014. Leigh syndrome in Drosophila melanogaster: morphological and biochemical characterization of Surf1 post-transcriptional silencing. *J Biol Chem,* 289(42), pp 29235-29246.

Dahl, E., Koseki, H. & Balling, R. 1997. Pax genes and organogenesis. *Bioessays,* 19(9), pp 755-765.

Dahmann, C. & Basler, K. 1999. Compartment boundaries: at the edge of development. *Trends Genet,* 15(8), pp 320-326.

De Wilde, J. 1964. Reproduction. *In:* Rockstein, M. (ed.) *Physiology of Insecta.* New York, USA: Academic Press.

Diaz-Benjumea, F. J. & Cohen, S. M. 1995. Serrate signals through Notch to establish a Wingless-dependent organizer at the dorsal/ventral compartment boundary of the Drosophila wing. *Development,* 121(12), pp 4215-4225.

Ding, Y., Berrocal, A., Morita, T., Longden, K. D. & Stern, D. L. 2016. Natural courtship song variation caused by an intronic retroelement in an ion channel gene. *Nature,* 536(7616), pp 329-332.

Dufour, L. 1844. Anatomie générale des diptères. *Ann. Sci. Nat,* pp 244–264.

Eaton, S. & Kornberg, T. B. 1990. Repression of ci-D in posterior compartments of Drosophila by engrailed. *Genes Dev,* 4(6), pp 1068-1077.

Eberhard, W. G. 1985. *Sexual selection and animal genitalia*, Cambridge, Mass.: Harvard University Press.

Eberhard, W. G. 1992. Species Isolation, Genital Mechanics, and the Evolution of Species-Specific Genitalia in Three Species of Macrodactylus Beetles (Coleoptera, Scarabeidae, Melolonthinae). *Evolution,* 46(6), pp 1774-1783.

Eberhard, W. G. 2004a. Male-female conflict and genitalia: failure to confirm predictions in insects and spiders. *Biol Rev Camb Philos Soc,* 79(1), pp 121-186.

Eberhard, W. G. 2004b. Rapid divergent evolution of sexual morphology: comparative tests of antagonistic coevolution and traditional female choice. *Evolution,* 58(9), pp 1947-1970.

Eberhard, W. G. 2010. Evolution of genitalia: theories, evidence, and new directions. *Genetica,* 138(1), pp 5-18.

Eberhard, W. G. & Ramirez, N. 2004. Functional Morphology of the Male Genitalia of Four Species of Drosophila: Failure to Confirm Both Lock and Key and MaleFemale Conflict Predictions. *Annals of the Entomological Society of America,* 95(5), pp 1007-1017.

Epper, F. 1981. Morphological analysis and fate map of the intersexual genital disc of the mutant doublesex-dominant in Drosophila melanogaster. *Dev Biol,* 88(1), pp 104-14.

Epper, F. 1983. Three-dimensional fate map of the female genital disc of Drosophila melanogaster. *Wilehm Roux Arch Dev Biol,* 192(5), pp 270-274.

Estrada, B., Casares, F. & Sánchez-Herrero, E. 2003. Development of the genitalia in Drosophila melanogaster. *Differentiation,* 71(6), pp 299-310.

Estrada, B. & Sanchez-Herrero, E. 2001. The Hox gene Abdominal-B antagonizes appendage development in the genital disc of Drosophila. *Development,* 128(3), pp 331-339.

Frankel, N., Erezyilmaz, D. F., McGregor, A. P., Wang, S., Payre, F. & Stern, D. L. 2011. Morphological evolution caused by many subtle-effect substitutions in regulatory DNA. *Nature,* 474(7353), pp 598-603.

Frazee, S. R. & Masly, J. P. 2015. Multiple sexual selection pressures drive the rapid evolution of complex morphology in a male secondary genital structure. *Ecol Evol,* 5(19), pp 4437-4450.

Freeland, D. E. & Kuhn, D. T. 1996. Expression patterns of developmental genes reveal segment and parasegment organization of *D. melanogaster* genital discs. *Mech Dev,* 56(1-2), pp 61-72.

Gaither, L. A. & Eide, D. J. 2001. Eukaryotic zinc transporters and their regulation. *Biometals,* 14(4), pp 251-270.

Garcia-Bellido, A., Ripoll, P. and Morata, G. 1973. Developmental Compartmentalisation of the Wing Disk of Drosophila. *Nat New Biol,* 244(147), pp 351-253.

Garrigan, D., Kingan, S. B., Geneva, A. J., Andolfatto, P., Clark, A. G., Thornton, K. R. & Presgraves, D. C. 2012. Genome sequencing reveals complex speciation in the Drosophila simulans clade. *Genome Res,* 22(8), pp 1499-1511.

Gehring, W. J. 1985. Homeotic genes, the homeo box, and the genetic control of development. 50(

Glassford, W. J., Johnson, W. C., Dall, N. R., Smith, S. J., Liu, Y., Boll, W., Noll, M. & Rebeiz, M. 2015. Co-option of an Ancestral Hox-Regulated Network Underlies a Recently Evolved Morphological Novelty. *Dev Cell,* 34(5), pp 520-531.

Gleason, J. M., Nuzhdin, S. V. & Ritchie, M. G. 2002. Quantitative trait loci affecting a courtship signal in Drosophila melanogaster. *Heredity (Edinb),* 89(1), pp 1-6.

Gleason, J. M. & Ritchie, M. G. 2004. Do quantitative trait loci (QTL) for a courtship song difference between Drosophila simulans and D. sechellia coincide with candidate genes and intraspecific QTL? *Genetics,* 166(3), pp 1303-1311.

Gompel, N., Prud'homme, B., Wittkopp, P. J., Kassner, V. A. & Carroll, S. B. 2005. Chance caught on the wing: cis-regulatory evolution and the origin of pigment patterns in Drosophila. *Nature,* 433(7025), pp 481-487.

Gorfinkiel, N., Sanchez, L. & Guerrero, I. 2003. Development of the Drosophila genital disc requires interactions between its segmental primordia. *Development,* 130(2), pp 295-305.

Greenspan, R. J. & Ferveur, J. F. 2000. Courtship in Drosophila. *Annu Rev Genet,* 34, pp 205-232.

Grenier, J. K., Garber, T. L., Warren, R., Whitington, P. M. & Carroll, S. 1997. Evolution of the entire arthropod Hox gene set predated the origin and radiation of the onychophoran/arthropod clade. *Curr Biol,* 7(8), pp 547-553.

Guerreiro, I., Nunes, A., Woltering, J. M., Casaca, A., Novoa, A., Vinagre, T., Hunter, M. E., Duboule, D. & Mallo, M. 2013. Role of a polymorphism in a Hox/Pax-responsive enhancer in the evolution of the vertebrate spine. *Proc Natl Acad Sci U S A,* 110(26), pp 10682-10686.

Hackett, J. L., Wang, X., Smith, B. R. & Macdonald, S. J. 2016. Mapping QTL Contributing to Variation in Posterior Lobe Morphology between Strains of Drosophila melanogaster. *PLoS One,* 11(9), pp 1-20.

Haerry, T. E., Heslip, T. R., Marsh, J. L. & O'Connor, M. B. 1997. Defects in glucuronate biosynthesis disrupt Wingless signaling in Drosophila. *Development,* 124(16), pp 3055-3064.

Hagen, J. F. D., Mendes, C., C., Kittelmann, M., McGregor, A., P. & Nunes, M., D, S. 2018. tartan underlies the evolution of male genital morphology. bioRxiv

Heitzler, P. & Simpson, P. 1991. The choice of cell fate in the epidermis of Drosophila. *Cell,* 64(6), pp 1083-1092.

Hocking, A. M., Shinomura, T. & McQuillan, D. J. 1998. Leucine-rich repeat glycoproteins of the extracellular matrix. *Matrix Biol,* 17(1), pp 1-19.

Hoekstra, H. E. & Coyne, J, A. 2007. The locus of evolution: evo devo and the genetics of adaptation. *Evolution,* (6), pp 995-1016.

Holland, P. W., Marletaz, F., Maeso, I., Dunwell, T. L. & Paps, J. 2017. New genes from old: asymmetric divergence of gene duplicates and the evolution of development. *Philos Trans R Soc Lond B Biol Sci,* 372(1713), pp 1-11.

Hong, W., Zhu, H., Potter, C. J., Barsh, G., Kurusu, M., Zinn, K. & Luo, L. 2009. Leucine-rich repeat transmembrane proteins instruct discrete dendrite targeting in an olfactory map. *Nat Neurosci,* 12(12), pp 1542-1550.

House, C. M., Lewis, Z., Hodgson, D. J., Wedell, N., Sharma, M. D., Hunt, J. & Hosken, D. J. 2013. Sexual and natural selection both influence male genital evolution. *PLoS One,* 8(5).

Immonen, E. & Ritchie, M. G. 2012. The genomic response to courtship song stimulation in female Drosophila melanogaster. *Proc Biol Sci,* 279(1732), pp 1359-1365.

Indjeian, V. B., Kingman, G. A., Jones, F. C., Guenther, C. A., Grimwood, J., Schmutz, J., Myers, R. M. & Kingsley, D. M. 2016. Evolving New Skeletal Traits by cis-Regulatory Changes in Bone Morphogenetic Proteins. *Cell,* 164(1-2), pp 45-56.

Ingham, P. W., Pinchin, S. M., Howard, K. R. & Ish-Horowicz, D. 1985. Genetic Analysis of the Hairy Locus in DROSOPHILA MELANOGASTER. *Genetics,* 111(3), pp 463-486.

Jacob, F. 1977. Evolution and tinkering. *Science,* 196(4295), pp 1161-1166.

Jacob, F. & Monod, Jacques. 1961. Genetic regulatory mechanisms in the synthesis of proteins. *J. Mol. Biol,* (3), pp 318-356.

Jagadeeshan, S. & Singh, R. S. 2006. A time-sequence functional analysis of mating behaviour and genital coupling in Drosophila: role of cryptic female choice and male sex-drive in the evolution of male genitalia. *J Evol Biol,* 19(4), pp 1058-1070.

Jiggins, C. D., Wallbank, R. W. & Hanly, J. J. 2017. Waiting in the wings: what can we learn about gene co-option from the diversification of butterfly wing patterns? *Philos Trans R Soc Lond B Biol Sci,* 372(1713), pp 1-10.

Johnstone, R. A. & Keller, L. 2000. How Males Can Gain by Harming Their Mates: Sexual Conflict, Seminal Toxins, and the Cost of Mating. *Am Nat,* 156(4), pp 368-377.

Kamimura, Y. 2007. Twin intromittent organs of Drosophila for traumatic insemination. *Biol Lett,* 3(4), pp 401-404.

Kamimura, Y. & Mitsumoto, H. 2011. Comparative copulation anatomy of the Drosophila melanogaster species complex (Diptera: Drosophilidae). *Entomological Science,* 14(4)**,** pp 399-410.

Keisman, E. L. & Baker, B. S. 2001. The Drosophila sex determination hierarchy modulates wingless and decapentaplegic signaling to deploy dachshund sex-specifically in the genital imaginal disc. *Development,* 128(9)**,** pp 1643-1656.

Keisman, E. L., Christiansen, a. E. & Baker, B. S. 2001. The sex determination gene doublesex regulates the A/P organizer to direct sex-specific patterns of growth in the Drosophila genital imaginal disc. *Developmental cell,* 1(2)**,** pp 215-225.

Keleman, K., Rajagopalan, S., Cleppien, D., Teis, D., Paiha, K., Huber, L. A., Technau, G. M. & Dickson, B. J. 2002. Comm sorts robo to control axon guidance at the Drosophila midline. *Cell,* 110(4)**,** pp 415-427.

Khan, A., Fornes, O., Stigliani, A., Gheorghe, M., Castro-Mondragon, J. A., van der Lee, R., Bessy, A., Cheneby, J., Kulkarni, S. R., Tan, G., Baranasic, D., Arenillas, D. J., Sandelin, A., Vandepoele, K., Lenhard, B., Ballester, B., Wasserman, W. W., Parcy, F. & Mathelier, A. 2018. JASPAR 2018: update of the open-access database of transcription factor binding profiles and its web framework. *Nucleic Acids Res,* 4(46(D1))**,** pp 260-266.

Kharchenko, P. V., Alekseyenko, A. A., Schwartz, Y. B., Minoda, A., Riddle, N. C., Ernst, J., Sabo, P. J., Larschan, E., Gorchakov, A. A., Gu, T., Linder-Basso, D., Plachetka, A., Shanower, G., Tolstorukov, M. Y., Luquette, L. J., Xi, R., Jung, Y. L., Park, R. W., Bishop, E. P., Canfield, T. K., Sandstrom, R., Thurman, R. E., MacAlpine, D. M., Stamatoyannopoulos, J. A., Kellis, M., Elgin, S. C., Kuroda, M. I., Pirrotta, V., Karpen, G. H. & Park, P. J. 2011. Comprehensive analysis of the chromatin landscape in Drosophila melanogaster. *Nature,* 471(7339)**,** pp 480-485.

King, M. & Wilson, A. C. 1975. Evolution at two levels in humans and chimpanzees. *Science*, 188(4184), pp 107-116.

Kittelmann, S., Buffry, A. D., Franke, F. A., Almudi, I., Yoth, M., Sabaris, G., Couso, J. P., Nunes, M. D. S., Frankel, N., Gomez-Skarmeta, J. L., Pueyo-Marques, J., Arif, S. & McGregor, A. P. 2018. Gene regulatory network architecture in different developmental contexts influences the genetic basis of morphological evolution. *PLoS Genet,* 14(5)**,** pp 1-21.

Kobe, B. & Deisenhofer, J. 1995. Proteins with leucine-rich repeats. *Curr Opin Struct Biol,* 5(3)**,** pp 409-416.

Kobe, B. D., J. 1994. The leucine-rich repeat: a versatile binding motif. *Trends Biochem Sci,* 19(10), pp 415-421.

Kok, K., Ay, A., Li, L. M. & Arnosti, D. N. 2015. Genome-wide errant targeting by Hairy. *Elife,* 35(4), pp 1-21.

Kornberg, T., Siden, I., O'Farrell, P. & Simon, M. 1985. The engrailed locus of Drosophila: in situ localization of transcripts reveals compartment-specific expression. *Cell,* 40(1), pp 45-53.

Krantz, D. E. & Zipursky, S. L. 1990. Drosophila chaoptin, a member of the leucine-rich repeat family, is a photoreceptor cell-specific adhesion molecule. *EMBO J,* 9(6), pp 1969-1977.

Krause, C., Wolf, C., Hemphala, J., Samakovlis, C. & Schuh, R. 2006. Distinct functions of the leucine-rich repeat transmembrane proteins capricious and tartan in the Drosophila tracheal morphogenesis. *Dev Biol,* 296(1), pp 253-264.

Kuhn, D. T., Mack, J. A., Duan, C. & Packert, G. 1993. Tumorous-head (tuh-1; tuh-3) modulates Abd-B bithorax-complex functions in Drosophila melanogaster. *Genetics,* 133(3), pp 593-604.

Kurusu, M., Cording, A., Taniguchi, M., Menon, K., Suzuki, E. & Zinn, K. 2008. A screen of cell-surface molecules identifies leucine-rich repeat proteins as key mediators of synaptic target selection. *Neuron,* 59(6), pp 972-985.

Lachaise, D. D., J . R.; Lemeunier, F.; Tsacas, L.; Ashburner, M. 1986. The Reproductive Relationships of Drosophila sechellia with *D. mauritiana* , *D. simulans*, and *D. melanogaster* from the Afrotropical Region. *Evolution,* 40(2), pp 262-271.

Laurie, C. C., True, J. R., Liu, J. & Mercer, J. M. 1997. An introgression analysis of quantitative trait loci that contribute to a morphological difference between Drosophila simulans and *D. mauritiana* . *Genetics,* 145(2), pp 339-348.

LeVasseur-Viens, H., Polak, M. & Moehring, A. J. 2015. No evidence for external genital morphology affecting cryptic female choice and reproductive isolation in Drosophila. *Evolution,* 69(7), pp 1797-1807.

Lewis, E. B. 1978. A gene complex controlling segmentation in Drosophila. *Nature,* 276(5688), pp 565-570.

Liu, J., Mercer, J. M., Stam, L. F., Gibson, G. C., Zeng, Z. B. & Laurie, C. C. 1996. Genetic analysis of a morphological shape difference in the male genitalia

of Drosophila simulans and *D. mauritiana* . *Genetics,* 142(4), pp 1129-1145.

Lynch, V. J. & Wagner, G. P. 2008. Resurrecting the role of transcription factor change in developmental evolution. *Evolution,* 62(9), pp 2131-2154.

Macdonald, S. J. & Goldstein, D. B. 1999. A quantitative genetic analysis of male sexual traits distinguishing the sibling species Drosophila simulans and D. sechellia. *Genetics,* 153(4), pp 1683-1699.

Manning, A. 1959. The sexual isolation between Drosophila melanogaster and Drosophila simulans. *Anim. Behav.,* 7(1-2), pp 60-65.

Mao, Y., Kerr, M. & Freeman, M. 2008. Modulation of Drosophila retinal epithelial integrity by the adhesion proteins capricious and tartan. *PLoS One,* 3(3), pp 1-9.

Martin, A. & Orgogozo, V. 2013. The Loci of repeated evolution: a catalog of genetic hotspots of phenotypic variation. *Evolution,* 67(5), pp 1235-1250.

Masly, J. P., Dalton, J. E., Srivastava, S., Chen, L. & Arbeitman, M. N. 2011. The genetic basis of rapidly evolving male genital morphology in Drosophila. *Genetics,* 189(1), pp 357-374.

Mathews, W. R., Ong, D., Milutinovich, A. B. & Van Doren, M. 2006. Zinc transport activity of Fear of Intimacy is essential for proper gonad morphogenesis and DE-cadherin expression. *Development,* 133(6), pp 1143-1153.

Mattei, A. L., Riccio, M. L., Avila, F. W. & Wolfner, M. F. 2015. Integrated 3D view of postmating responses by the Drosophila melanogaster female reproductive tract, obtained by micro-computed tomography scanning. *Proc Natl Acad Sci U S A,* 112(27), pp 8475-8480.

Mayr, E. 1966. Animal species and evoluton. Cambridge, MA: The Belknap Press of Harvard University Press

McGregor, A. P., Orgogozo, V., Delon, I., Zanet, J., Srinivasan, D. G., Payre, F. & Stern, D. L. 2007. Morphological evolution through multiple cis-regulatory mutations at a single gene. *Nature,* 448(7153), pp 587-590.

McNeil, C. L., Bain, C. L. & Macdonald, S. J. 2011. Multiple Quantitative Trait Loci Influence the Shape of a Male-Specific Genital Structure in Drosophila melanogaster. *G3 (Bethesda),* 1(5), pp 343-351.

Michel, M., Aliee, M., Rudolf, K., Bialas, L., Julicher, F. & Dahmann, C. 2016. The Selector Gene apterous and Notch Are Required to Locally Increase

Mechanical Cell Bond Tension at the Drosophila Dorsoventral Compartment Boundary. *PLoS One,* 11(8), pp 1-18.

Milan, M. & Cohen, S. M. 1999. Notch signaling is not sufficient to define the affinity boundary between dorsal and ventral compartments. *Mol Cell,* 4(6), pp 1073-1078.

Milan, M., Perez, L. & Cohen, S. M. 2002. Short-range cell interactions and cell survival in the Drosophila wing. *Dev Cell,* 2(6), pp 797-805.

Milan, M., Perez, L. & Cohen, S. M. 2005. Boundary formation in the Drosophila wing: functional dissection of Capricious and Tartan. *Dev Dyn,* 233(3), pp 804-810.

Milan, M., Weihe, U., Perez, L. & Cohen, S. M. 2001. The LRR proteins capricious and Tartan mediate cell interactions during DV boundary formation in the Drosophila wing. *Cell,* 106(6), pp 785-794.

Mirth, C. & Akam, M. 2002. Joint development in the Drosophila leg: cell movements and cell populations. *Dev Biol,* 246(2), pp 391-406.

Morata, G. & Lawrence, P. A. 1975. Control of compartment development by the engrailed gene in Drosophila. *Nature,* 255(5510), pp 614-617.

Nagy, O., Nuez, I., Savisaar, R., Peluffo, A. E., Yassin, A., Lang, M., Stern, D. L., Matute, D., David, J. R. & Courtier-Orgogozo, V. 2018. Correlated Evolution of two Sensory Organs via a Single Cis-Regulatory Nucleotide Change. *Curr Biol,* 28(21), pp 3450-3457.

Nothiger, R. & Steinmann-Zwicky, M. 1987. Genetics of sex determination: what can we learn from Drosophila? *Development,* 101( ), pp 17-24.

Nöthiger, R. D., A; Epper, F. 1977. Gynandromorphs reveal two separate primordia for male and female genitalia in Drosophila melanogaster. *Wilhelm Roux's archives of developmental biology,* 181(4), pp 367-373.

Nunes, M. D., Arif, S., Schlotterer, C. & McGregor, A. P. 2013. A perspective on micro-evo-devo: progress and potential. *Genetics,* 195(3), pp 625-34.

Nunes, M. D., Wengel, P. O., Kreissl, M. & Schlotterer, C. 2010. Multiple hybridization events between Drosophila simulans and Drosophila mauritiana are supported by mtDNA introgression. *Mol Ecol,* 19(21), pp 4695-4707.

Nusslein-Volhard, C. & Wieschaus, E. 1980. Mutations affecting segment number and polarity in Drosophila. *Nature,* 287(5785), pp 795-801.

Nuzhdin, S. V., Fry, J. D. & Mackay, T. F. 1995. Polygenic mutation in Drosophila melanogaster: the causal relationship of bristle number to fitness. *Genetics,* 139(2), pp 861-872.

O'Brown, N. M., Summers, B. R., Jones, F. C., Brady, S. D. & Kingsley, D. M. 2015. A recurrent regulatory change underlying altered expression and Wnt response of the stickleback armor plates gene EDA. *Elife,* 4( ), pp 1-17.

Ohsako, S., Hyer, J., Panganiban, G., Oliver, I. & Caudy, M. 1994. Hairy function as a DNA-binding helix-loop-helix repressor of Drosophila sensory organ formation. *Genes Dev,* 8(22), pp 2743-2755.

Orenic, T. V., Held, L. I., Jr., Paddock, S. W. & Carroll, S. B. 1993. The spatial organization of epidermal structures: hairy establishes the geometrical pattern of Drosophila leg bristles by delimiting the domains of achaete expression. *Development,* 118(1), pp 9-20.

Pandey, R., Kofler, R., Orozco-terWengel, P., Nolte, V. & Schlötterer, C. 2011. PoPoolation DB: a user-friendly web-based database for the retrieval of natural polymorphisms in Drosophila. *BMC Genetics,* 12(27), pp 1-8.

Perrimon, N. & Bernfield, M. 2000. Specificities of heparan sulphate proteoglycans in developmental processes. *Nature,* 404(6779), pp 725-728.

Pielage, J., Kippert, A., Zhu, M. & Klambt, C. 2004. The Drosophila transmembrane protein Fear-of-intimacy controls glial cell migration. *Dev Biol,* 275(1), pp 245-257.

Poiani, A. 2005. Complexity of seminal fluid: a review. *Behav Ecol Sociobiol,* 60(3), pp 298-310.

Postlethwait, J. H., Bryant, P. J. & Schubiger, G. 1972. The homoeotic effect of "tumorous head" in Drosophila melanogaster. *Dev Biol,* 29(3), pp 337-342.

Poyau, A., Buchet, K. & Godinot, C. 1999. Sequence conservation from human to prokaryotes of Surf1, a protein involved in cytochrome c oxidase assembly, deficient in Leigh syndrome. *FEBS Lett,* 462(3), pp 416-420.

Price, C. S., Kim, C. H., Gronlund, C. J. & Coyne, J. A. 2001. Cryptic reproductive isolation in the Drosophila simulans species complex. *Evolution,* 55(1), pp 81-92.

Princivalle, M. & de Agostini, A. 2002. Developmental roles of heparan sulfate proteoglycans: a comparative review in Drosophila, mouse and human. *Int J Dev Biol,* 46(3), pp 267-278.

Prud'homme, B., Gompel, N., Rokas, A., Kassner, V. A., Williams, T. M., Yeh, S. D., True, J. R. & Carroll, S. B. 2006. Repeated morphological evolution through cis-regulatory changes in a pleiotropic gene. *Nature,* 440(7087), pp 1050-1053.

Ren, N., Zhu, C., Lee, H. & Adler, P. N. 2005. Gene expression during Drosophila wing morphogenesis and differentiation. *Genetics,* 171(2), pp 625-638.

Robertson, H. M. 1983. Mating Behavior and the Evolution of Drosophila mauritiana. *Evolution,* 37(6), pp 1283-1293.

Robertson, H. M. 1988. Mating Asymmetries and Phylogeny in the *Drosophila melanogaster* Species Complex. *Pacific Science,* 42(1-2), pp 72-80.

Robertson, H. M. 2013. Mating Behavior and the Evolution of Drosophila mauritiana. *Society for the Study of Evolution,* 37, pp 1283-1293.

Robin, C., Lyman, R. F., Long, A. D., Langley, C. H. & Mackay, T. F. 2002. hairy: A quantitative trait locus for drosophila sensory bristle number. *Genetics,* 162(1), pp 155-164.

Routtu, J., Mazzi, D., Van der Linde, K., Mirol, P., Butlin, R. K. & Hoikkala, A. 2007. The extent of variation in male song, wing and genital characters among allopatric Drosophila montana populations. *J Evol Biol,* 20(4), pp 1591-1601.

Sakurai, K. T., Kojima, T., Aigaki, T. & Hayashi, S. 2007. Differential control of cell affinity required for progression and refinement of cell boundary during Drosophila leg segmentation. *Dev Biol,* 309(1), pp 126-136.

Sanchez, L., Casares, F., Gorfinkiel, N. & Guerrero, I. 1997. The genital disc of Drosophila melanogaster : II. Role of the genes hedgehog, decapentaplegic and wingless. *Dev Genes Evol,* 207(4), pp 229-241.

Sanchez, L. & Guerrero, I. 2001. The development of the Drosophila genital disc. *Bioessays,* 23(8), pp 698-707.

Schneider, C. A., Rasband, W. S. & Eliceiri, K. W. 2012. NIH Image to ImageJ: 25 years of image analysis. *Nat Methods,* 9(7), pp 671-675.

Schulz, K. N., Bondra, E. R., Moshe, A., Villalta, J. E., Lieb, J. D., Kaplan, T., McKay, D. J. & Harrison, M. M. 2015. Zelda is differentially required for chromatin accessibility, transcription factor binding, and gene expression in the early Drosophila embryo. *Genome Res,* 25(11), pp 1715-1726.

Schupbach, T., Wieschaus, E. & Nothiger, R. 1978. The embryonic organization of the genital disc studied in genetic mosaics ofDrosophila melanogaster. *Wilehm Roux Arch Dev Biol,* 185(3), pp 249-270.

Schutt, C. & Nothiger, R. 2000. Structure, function and evolution of sex-determining systems in Dipteran insects. *Development,* 127(4), pp 667-677.

Shishido, E., Takeichi, M. & Nose, A. 1998. Drosophila synapse formation: regulation by transmembrane protein with Leu-rich repeats, CAPRICIOUS. *Science,* 280(5372), pp 2118-2121.

Shubin, N., Tabin, C. & Carroll, S. 2009. Deep homology and the origins of evolutionary novelty. *Nature,* 457(7231), pp 818-823.

Song, H. 2009. Species-specificity of male genitalia is characterized by shape, size, and complexity. *Insect Systematics & Evolution,* 40(2), pp 159 - 170.

Stahl, A. L., Charlton-Perkins, M., Buschbeck, E. K. & Cook, T. A. 2017. The cuticular nature of corneal lenses in Drosophila melanogaster. *Dev Genes Evol,* 227(4), pp 271-278.

Stern, D. L. Perspective: evolutionary developmental biology and the problem of variation. *Evolution*, 54(4), pp 1079-1091.

Stern, D. L. 2014. Identification of loci that cause phenotypic variation in diverse species with the reciprocal hemizygosity test. *Trends Genet,* 30(12), pp 547-554.

Stern, D. L., Crocker, J., Ding, Y., Frankel, N., Kappes, G., Kim, E., Kuzmickas, R., Lemire, A., Mast, J. D. & Picard, S. 2017. Genetic and Transgenic Reagents for Drosophila simulans, *D. mauritiana* , D. yakuba, D. santomea, and D. virilis. *G3 (Bethesda),* 7(4), pp 1339-1347.

Stern, D. L. & Frankel, N. 2013. The structure and evolution of cis-regulatory regions: the shavenbaby story. *Philos Trans R Soc Lond B Biol Sci,* 368(1632), pp 1-10.

Stern, D. L. & Orgogonzo, V. 2008. The loci of evolution: how predictable. is genetic evolution? *Evolution*, 62(9), pp 2155-2177.

Stieper, B. C., Kupershtok, M., Driscoll, M. V. & Shingleton, A. W. 2008. Imaginal discs regulate developmental timing in Drosophila melanogaster. *Dev Biol,* 321(1), pp 18-26.

Sucena, E. & Stern, D. L. 2000. Divergence of larval morphology between Drosophila sechellia and its sibling species caused by cis-regulatory

evolution of ovo/shaven-baby. *Proc Natl Acad Sci U S A,* 97(9), pp 4530-4534.

Suga, H., Tschopp, P., Graziussi, D. F., Stierwald, M., Schmid, V. & Gehring, W. J. 2010. Flexibly deployed Pax genes in eye development at the early evolution of animals demonstrated by studies on a hydrozoan jellyfish. *Proc Natl Acad Sci U S A,* 107(32), pp 14263-14268.

Tanaka, K. M., Hopfen, C., Herbert, M. R., Schlotterer, C., Stern, D. L., Masly, J. P., McGregor, A. P. & Nunes, M. D. 2015. Genetic architecture and functional characterization of genes underlying the rapid diversification of male external genitalia between Drosophila simulans and Drosophila mauritiana. *Genetics,* 200(1), pp 357-369.

Tatsuta, H. & Takano-Shimizu, T. 2006. Genetic architecture of variation in sex-comb tooth number in Drosophila simulans. *Genet Res,* 87(2), pp 93-107.

Team, R. 2015. RStudio: Integrated Development for R. Boston, MA: RStudio, Inc.

Tokita, M., Yano, W., James, H. F. & Abzhanov, A. 2017. Cranial shape evolution in adaptive radiations of birds: comparative morphometrics of Darwin's finches and Hawaiian honeycreepers. *Philos Trans R Soc Lond B Biol Sci,* 372(1713), pp 1-17.

Tossell, K., Andreae, L. C., Cudmore, C., Lang, E., Muthukrishnan, U., Lumsden, A., Gilthorpe, J. D. & Irving, C. 2011. Lrrn1 is required for formation of the midbrain-hindbrain boundary and organiser through regulation of affinity differences between midbrain and hindbrain cells in chick. *Dev Biol,* 352(2), pp 341-352.

True, J., Liu, J., Stam, L., Zeng, Z. & Laurie, C. 1997. Quantitative genetic analysis of divergence in male secondary sexual traits between Drosophila simulans and *D. mauritiana* . *Evolution; International Journal of Organic Evolution,* 51(3), pp 816-832.

True, J. R., Mercer, J. M. & Laurie, C. C. 1996. Differences in crossover frequency and distribution among three sibling species of Drosophila. *Genetics,* 142(2), pp 507-523.

Tsacas, L. & David, J. 1974. *Drosophila mauritiana* n. sp. du groupe melanogaster de I'lle Maurice. *Bulletin de la Societe entomologique de France,* 79, pp 42-46.

Tucker, A. S. 2017. Major evolutionary transitions and innovations: the tympanic middle ear. *Philos Trans R Soc Lond B Biol Sci,* 372(1713), pp 1-11.

Van Doren, M., Bailey, A. M., Esnayra, J., Ede, K. & Posakony, J. W. 1994. Negative regulation of proneural gene activity: hairy is a direct transcriptional repressor of achaete. *Genes Dev,* 8(22), pp 2729-2742.

Van Doren, M., Mathews, W. R., Samuels, M., Moore, L. A., Broihier, H. T. & Lehmann, R. 2003. fear of intimacy encodes a novel transmembrane protein required for gonad morphogenesis in Drosophila. *Development,* 130(11), pp 2355-2364.

Wilson, K. L., Fitch, K. R., Bafus, B. T. & Wakimoto, B. T. 2006. Sperm plasma membrane breakdown during Drosophila fertilization requires sneaky, an acrosomal membrane protein. *Development (Cambridge, England),* 133(24), pp 4871-4879.

Wittkopp, P. J., Stewart, E. E., Arnold, L. L., Neidert, A. H., Haerum, B. K., Thompson, E. M., Akhras, S., Smith-Winberry, G. & Shefner, L. 2009. Intraspecific polymorphism to interspecific divergence: genetics of pigmentation in Drosophila. *Science,* 326(5952), pp 540-544.

Yassin, A. & Orgogozo, V. 2013. Coevolution between Male and Female Genitalia in the Drosophila melanogaster Species Subgroup. *PLoS One,* 8(2), pp 1-12.

Yeung, K., Boija, A., Karlsson, E., Holmqvist, P. H., Tsatskis, Y., Nisoli, I., Yap, D., Lorzadeh, A., Moksa, M., Hirst, M., Aparicio, S., Fanto, M., Stenberg, P., Mannervik, M. & McNeill, H. 2017. Atrophin controls developmental signaling pathways via interactions with Trithorax-like. *Elife,* 6, pp 1-24.

Zeng, Z. B., Liu, J., Stam, L. F., Kao, C. H., Mercer, J. M. & Laurie, C. C. 2000. Genetic architecture of a morphological shape difference between two Drosophila species. *Genetics,* 154(1), pp 299-310.

Zhang, Z., Feng, J., Pan, C., Lv, X., Wu, W., Zhou, Z., Liu, F., Zhang, L. & Zhao, Y. 2013. Atrophin-Rpd3 complex represses Hedgehog signaling by acting as a corepressor of CiR. *J Cell Biol,* 203(4), pp 575-583.